AN APPROACH FOR THE CHARACTERIZATION OF SPATIAL VARIABILITY OF PERMEABILITY IN THE SIERRA LADRONES FORMATION, ALBUQUERQUE BASIN, CENTRAL NEW MEXICO

by

J. Matthew Davis

Submitted in Partial Fulfillment
of the Requirements for the Degree of
Master of Science in Hydrology

New Mexico Institute of Mining and Technology
Socorro, New Mexico
May, 1990

This thesis is accepted on behalf of the faculty of the Institute by the following committee:

Fred W. Phillips 8 May 90

Adviser

John L. Wilson 5/7/90

David W. Love 5/8/90

Allan Kirkpatrick 5/8/90

Date

ACKNOWLEDGMENTS

This research was funded by the New Mexico Water Resources Research Institute (Grant #1345681) and the U.S. Department of Energy (#DE–FG04–89ER60843). I am indebted to Drs. Fred M. Phillips and John L. Wilson for establishing this research and laying the initial groundwork. I am also grateful to Fred Phillips for taking me on as a research assistant and serving as my advisor. My other committee members Drs. John Wilson, Allan Gutjahr, and Dave Love have all added a great deal of insight and support throughout my work on this project. It has been a true pleasure to work with such a diverse group on a project that involves such a wide range of disciplines.

I would like to extend a special thanks to Dave Love for his guidance in the field. The long hours Dave has spent in the field have made a profound contribution to the project as a whole. When I was out with knee surgery, Dave Love along with Ruth Lohmann and Susan Colarullo completed much of the mapping that is presented in this thesis for which I am very grateful. I would also like to thank Chris Koltermann for sharing her wisdom and acting as a sounding board throughout the later stages of this research.

Most of all I would like to thank my family and friends for their unending support throughout my stay at New Mexico Tech.

ABSTRACT

Spatial variation of hydraulic conductivity has been generally recognized as the dominant medium–dependent control on the transport and dispersion of contaminants in groundwater. The characterization of such spatial variability requires the incorporation of both geologic and permeability data. An empirical study of the relationship between patterns of sedimentology and patterns of permeability is being conducted at an outcrop of the Pliocene/Pleistocene Sierra Ladrones Formation, central New Mexico.

Methods of geostatistics and sedimentary basin analysis are employed to study the problem. Mapping of litofacies provide a basis for defining architectural elements. Development of an air permeameter provides a means to obain extensive field measurements of air–flow–rate. Both the geologic information and the air–flow–rate data provide the basis for analysis. Preliminary geologic mapping indicates that the sediments in the study area are the products of an arid fluvial/interfluvial depositional environment. Distribution analysis of the air–flow–rate data indicate that permeability is log–normally distributed. The air permeability data are used to estimate variograms and correlation lengths at several spatial scales in both the horizontal and vertical direction. At the scale of 10's of centimeters, the horizontal variograms exhibit both exponential and bell–shaped variogram behavior. Variogram models are fit to the variogram estimates. At the scale of 10's of meters, a lithofacies map was used to estimate the spatial distribution of the mean permeability. Variogram analysis of the mean data indicate a nested structure in the horizontal direction and a periodic

correlation structure in the vertical direction. The horizontal nested structure is believed to be the result of subtle changes in bed thickness while the vertical periodic structure corresponds to the layering of the system. The air–flow–rate data can be broken into separate populations based on grain size. The distribution of air–flow–rate (permeability) for each grain class exhibits distinctly different means across classes and similar statistics when comped to similar classes.

Results of the current study indicate that there is a direct connection between observable geologic structures and permeability statistics. Further work will need to be conducted to develop methods by which mappable features can be efficiently wisely and efficiently in the estimation of permeability statistics.

TABLE OF CONTENTS

List of Figures

Figure Page

Figure Page

List of Tables

List of Plates

Plate (all plates in pocket)

CHAPTER 1: Introduction

In recent decades the problem of groundwater contamination has emerged as the most serious threat to the nation's supply of potable groundwater. Historically, groundwater hydrology has been concerned with the problem of water supply. Mathematical formulations have been derived to solve these problems. As with any engineering problem, simplifying assumptions with regard to the physical parameters are necessary when deriving the governing equations and subsequently solving the equations. At the physical scale of the water supply problem, it has been customary to assume that the aquifer consists of one or more effectively homogeneous layers. Virtually all water supply problems are solved in two dimensions, averaging over the vertical. This method has been fairly successful. Usually, it is of little concern which parcel of water arrives at the well first. As long as a certain number of parcels arrive in a given time interval, the water supply problem can be considered solved.

The major challenge facing hydrogeology today occurs not only at a smaller spatial scale but also must be able to distinguish between parcels of water. The problem is that of groundwater contamination. Generally, groundwater contamination occurs at spatial scales orders of magnitude smaller than those of water supply problems. Where it was once reasonable to solve a problem in two dimensions averaging the hydraulic properties over the vertical, the third dimension and its control on flow must now be taken into account. To study a groundwater system at the scale at which groundwater contamination occurs it is necessary to look in detail at the geology. Geologically, water supply problems

occur at the formation and stratigraphic group level; groundwater contamination occurs at the formation and lithologic facies scale. With problems of water supply in alluvial aquifers, hydrogeologists deal with basin fill stratigraphy and in some case the subsequent structural deformation of that stratigraphy [Meinzer, 1923]. With groundwater contamination we, as hydrogeologists, must begin to study how flow and transport are controlled by facies relationships within stratigraphic units. The geologic problem has changed from one of stratigraphy and general basin fill to a problem of sedimentology.

When dealing with groundwater contamination and the transport of solutes through the subsurface, it has been observed since the earliest studies of groundwater flow [Sclichter, 1899] that dispersion of the solute occurs when the tracer is transported through the subsurface. The dispersion process can be broken down into three contributing processes: 1)molecular diffusion, 2) advective flux, and 3) mechanical mixing. Molecular diffusion is often insignificant and can be neglected. The advective flux is represented by a mean velocity, and the mechanical mixing component is modeled with a coefficient of dispersivity. The coefficient of dispersivity is assumed to be a property of the medium, and though it may be represented by a tensor, it is most often assumed to be spatially invariant.

Figure 1 illustrates dispersion with three examples. The first (Figure 1a) shows dispersion of a solute in a homogeneous media. In the second example (Figure 1b), lenses of two different hydraulic conductivities result in a fingering type of mixing. The third example (Figure 1c) is a result from Skibitzke and Robertson [1963] in which a box was packed with fine sand and long sinuous lenses of coarse sand. The dispersion of the injected tracer plume is strongly dependent on the location and interconnection of the coarse sand lenses.

More recent studies [e.g. Pickens and Grisak, 1981a,b] have suggested that the coefficient of dispersivity depends on the distance that solutes are trans-

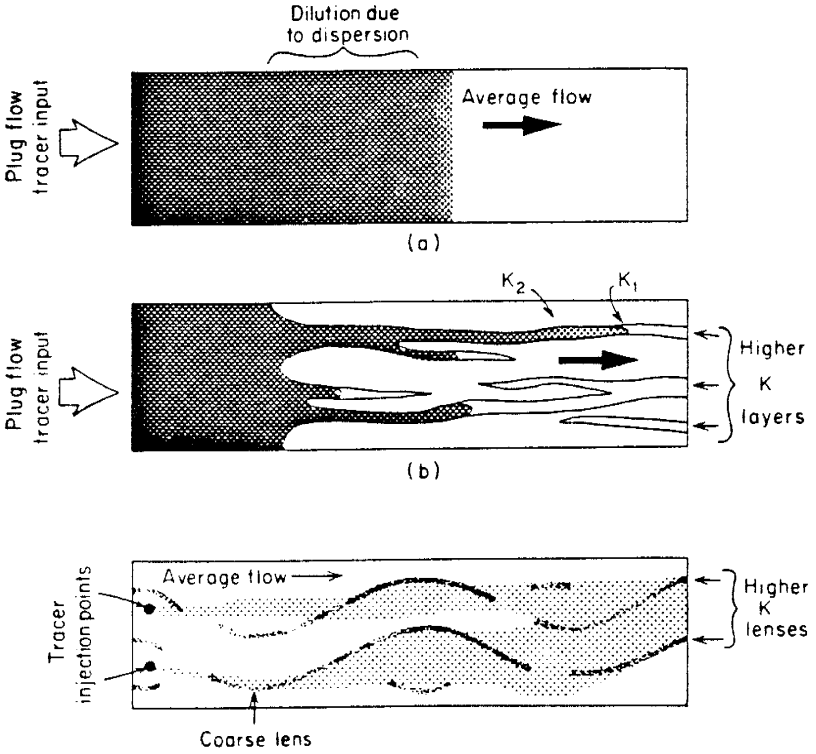

Figure 1. Illustration of the effects of hydrodynamic dispersion in: (a) Homogeneous medium; (b) fingering caused by layered beds and lenses; (c) spreading caused irregular lenses. (from Freeze and Cherry, 1979)

ported through the subsurface. This phenomenon is commonly referred to as scale dependent dispersion. When considering the geologic heterogeneity of most aquifers, scale dependence is not surprising. As the groundwater moves through the aquifer, different water parcels move at different velocities depending on the local gradient and conductivity. If there exists a broad range of geologic material (for example, from clays to gravel), then the corresponding velocities will also be highly variable [Schwartz, 1977; Smith and Schwartz, 1980; and Silliman and Simpson, 1987]. The further the contaminant plume travels, the more heterogeneities are encountered, and the more dispersed the plume becomes.

The classical advection–dispersion equation is not capable of handling such a phenomenon. The degree of heterogeneity is represented by the coefficient of dispersivity. As the scale of the contaminant migration increases, additional levels of heterogeneity are encountered. To lump all the information regarding the heterogeneity of a complex geologic system into one coefficient which is assumed to be spatially invariant is inadequate.

The need for quantitative studies of dispersion through heterogeneous porous media and the inability to determine the heterogeneity completely has led researchers to a probabalistic interpretation of the spatial variability of hydraulic conductivity. Studies over the past two decades have interpreted geologic heterogeneity as being a spatially correlated random process. These studies in stochastic hydrology have yielded a great deal of insight into how a hydrologic system would respond if K is a spatially correlated random process. Works of Gutjahr et al. [1978], Bakr et al. [1978], Gelhar et al. [1979], and Gelhar and Axness [1983] have addressed some of the more theoretical aspects of the stochastic approach. The papers by Bakr et al. [1978], Gutjahr et al. [1978], and Dagan [1986] primarily address the problems of solving the flow equation with a continuum represen-

tation of the random hydraulic conductivity field. Gelhar et al. [1979] and Gelhar and Axness [1983] focus on solving the equations of flow and transport in stratified and statistically anisotropic porous media, respectfully. Dagan [1986] addresses the conceptual relationship between the flow domain scales (pore scale, laboratory scale, formation scale) and the scales of spatial correlation. Many works have followed [e.g. Naff and Vecchia, 1987; Neumann et al. 1987, Shapiro and Cvetkovic, 1988] which have focused on various theoretical aspects of the stochastic interpretation of fluid flow and solute transport through porous media. These theoretical investigations have been important in determining the statistical parameters that are most crucial for the prediction of subsurface flow and contaminant transport.

Some studies have focused on estimating the proper statistical representation of natural geologic material. For example, MacMillan and Gutjahr [1986] studied porosity and permeability in vertical cores of quartzose sandstone and suggest that the average thickness of geologic layering exerts a dominant control on the length over which measurements are correlated statistically. Another study performed by Goggin et al. [1988a] reports that permeability patterns in eolian deposits are strongly dependent on sedimentary structure. Their study was conducted on the scale of lithologic facies.

Determination of the necessary statistical parameters requires hundreds to hundreds of thousands of measurements. This is obviously unrealistic in any groundwater system. The economical constraints on obtaining a data base of this extent has resulted in a serious situation of insufficient data.

An alternative to this "hard" data approach is to incorporate geologic information which, while more abundant, is subjective and contains a higher degree of uncertainty [e.g. see Journel and Alabert, 1986; Phillips and Wilson, 1989; Phillips et al., 1989; Anderson, 1989]. This type of information has been referred

to in the literature as "soft" information [e.g. see Journel and Alabert, 1988; Gelhar, 1986]. The question then becomes: "How can soft geologic information help in supplementing the available data?"

The field of sedimentology offers us an analytical framework for the study of soft geologic information. Lithologic types, their spatial extent, degree of interconnection, and characteristic sedimentary structures are examples of soft information. These characteristics of sedimentary deposits vary according to the depositional processes that dominated deposition [Galloway and Hobday, 1983; Reading, 1986]. Sedimentology is the study of how depositional processes are related to depositional products and how one can be inferred from the other. It is this process/product relationship that may allow us to estimate the hydrologic character of an aquifer based on an understanding of the depositional processes.

The ability of geologists to predict the spatial geometric relationships and assemblages of lithologic facies has in the past been limited. This is not due to an intractable nature of the problem but rather to the lack of spatially located sedimentological data and an appropriate mathematical framework in which to work.

If there exists a quantifiable correlation between permeability patterns and geology, one may be able to predict the permeability patterns of an aquifer based on limited well bore and other "soft" geologic information. It is then the duty of geologists and mathematicians to collaborate and examine the validity of this hypothesis. Refinement and modification of this hypothesis will result in methodologies by which the hydraulic conductivity field can be characterized geologically and quantitatively.

To arrive at such methodologies it will be necessary to conduct numerous field investigations which focus on 1) the relation between the geology and the permeability, 2) how that relation can be described mathematically, and 3) how

the mathematical description can be paramaterized based on available information. Appropriate studies would consist of a geologically/mathematically based investigation of spatial relationships of lithologic "flow" units with emphasis on how different depositional processes affect these spatial patterns.

This thesis describes and evaluates a field methodology that will address the issue of incorporating geologic information into the quantitative description of hydraulic conductivity. Background material on geostatistics and basin analysis are reviewed. This material then serves as a basis for the field methodology presented. Finally, some preliminary results of the current field investigation are presented and discussed.

Sedimentary basin analysis and geostatistics are here adopted as the methods of analysis. The basin analysis techniques presented are dominantly those of fluvial process/product relationships. The concepts however should be amenable to other types of deposits. The field site, located in the Albuquerque Basin of central New Mexico, has been chosen to study both sedimentology and permeability in an extensively outcropped formation. The Sierra Ladrones Formation crops out in badlands topography for approximately 15 miles. The sediments are largely undisturbed as far as diagenesis and structural deformation. This field site offers us an excellent opportunity to investigate the three dimensional–character of a fluvial deposit.

The scope of this thesis is restricted to the presentation and analysis of methods that may be used to obtain a consistent geological/statistical description of outcrop heterogeneities. Once such a description of heterogeneity is obtained, further work will be required to study how that description can be used to quantitatively characterize and analyze problems of fluid flow and solute transport. It is not the intent of this thesis to present the methods by which that characterization is to be done.

CHAPTER 2: Background

2.0 Introduction

This chapter introduces and reviews some of the basic concepts of the two methods of analysis that we wish to combine: geostatistics and sedimentary basin analysis. Each of these methods of analysis will be reviewed in the context of this study. This is not intended to provide a thorough explanation of these advanced topics; the goal however is to introduce the key concepts and how they are related to the problem of aquifer characterization.

In order to realistically address the problem of quantifying the spatial distribution of hydraulic conductivity in aquifers, we must have an understanding of the current state of the analytical tools available. Geostatistics and basin analysis not only provide us with methods of analysis but also a with set of constraints that must be acknowledged. These constraints need not prohibit advancement toward the goal; but ignorance of them will prevent prudent use of the analytical tools available.

Geostatistics provides us with a mathematical desciptor to quantitatively describe heterogeneity. Heterogeneity is in fact a deterministic system. That is, at a given time the permeability at every location in an aquifer is fixed and theoretically could be described exactly with a deterministic function. The probabalistic interpretation is adopted to account for both the uncertainty associated with measured values and uncertainty associated with values at unsampled locations. An implicit assumption in the probabalistic interpretation of heterogeneity is that the spatial distribution of permeability can be modeled mathematically as a ran-

dom function. Matheron's definition of geostatistics, "the application of the formalism of random functions to the reconnaissance and estimation of natural phenomena" [Journel and Huijbregts; 1978], will be retained here.

The statistical approach is based on a probabalistic interpretation of regionalized variables. A regionalized variable is a variable distributed in space. It is simply a function f(x) which takes on a value at every point x in three–dimensional space. The regionalized variables we are concerned with are permeability and hydraulic conductivity.

We are not restricted to permeability and hydraulic conductivity as the variables of study. Issues of facies distributions and the connectivity of the facies could also be handled using the theory of regionalized variables, as will be discussed later.

Geology and the techniques of basin analysis serve as a guide to the statistical approach. The main purpose of sedimentary basin analysis is to assimilate a wide variety of geologic information into models of the depositional processes and sedimentary products. These models are all manifestations of the concept of process/product relationship. The concept asserts that depositional environments can be delineated according to particular characteristics of the preserved sediments.

Sedimentary models and basin analysis are useful in the characterization of aquifer properties in that they allow the estimation of the geologic characteristics of an aquifer based on knowledge of the depositional environment. These characteristics focus on lithologic types, spatial relationships of the lithologies, and dimensions of the elements that compose the formation. In the case of both geostatistics and basin analysis, we see an emphasis toward general structural characteristics.

2.1 Geostatistics

The most fundamental concept in the application of probabalistic regionalized variables in the description of geologic heterogeneity is that of spatial correlation. Spatial correlation simply states that values of a function taken at two points located near one another, with respect to a length of correlation, are more similar than values at points far apart.

2.1.1 Estimation of statistical moments

In actual systems, the correlation structure is approximated graphically by use of a variogram. Essentially, the variogram is a plot of the dissimilarity between values at points plotted against the distance that separates them (Figure 2). On the order of a hundred measurements are required for estimating the variogram at a given scale.

The variogram allows one to assess the statistical properties of a random field. Figure 3 illustrates a hypothetical variogram of a field containing horizontally oriented lenses of higher conductivity. The preferred orientation of the lenses results in a larger length of correlation in the horizontal direction as reflected by the variograms. This type of situation is referred to as being statistically anisotropic. It should be noted that this is an example of how statistical anisotropy may occur. The correlation lengths a_1 and a_2 may or may not be mappable quantities.

The variogram is an essential element in the use of geostatistics. In general the representation of the hydraulic conductivity field as a continuum requires the joint probability density function of the hydraulic conductivity. This differs from a single random variable which can be described completely by its probabil-

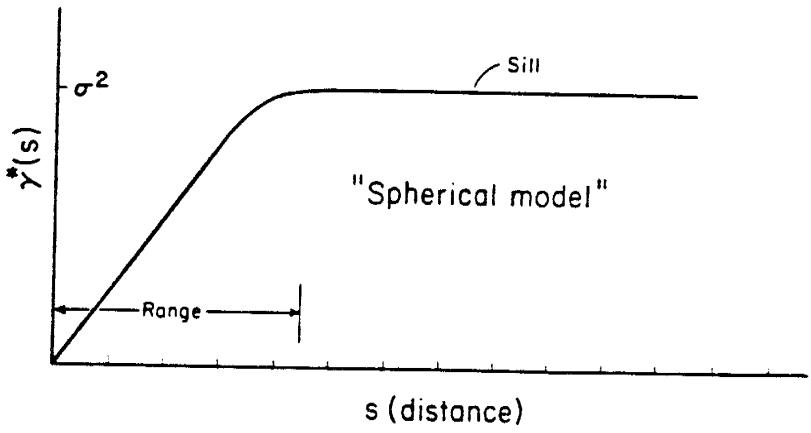

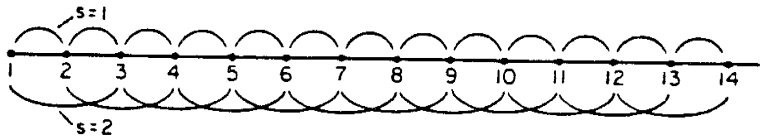

$$2\gamma^*(s) = \frac{1}{N(s)} \sum_{i=1}^{N(s)} \left[Y(X_i) - Y(X_i + s) \right]^2$$

Figure 2. Illustration of the experimental variogram and associated terms. (from Fogg, 1986)

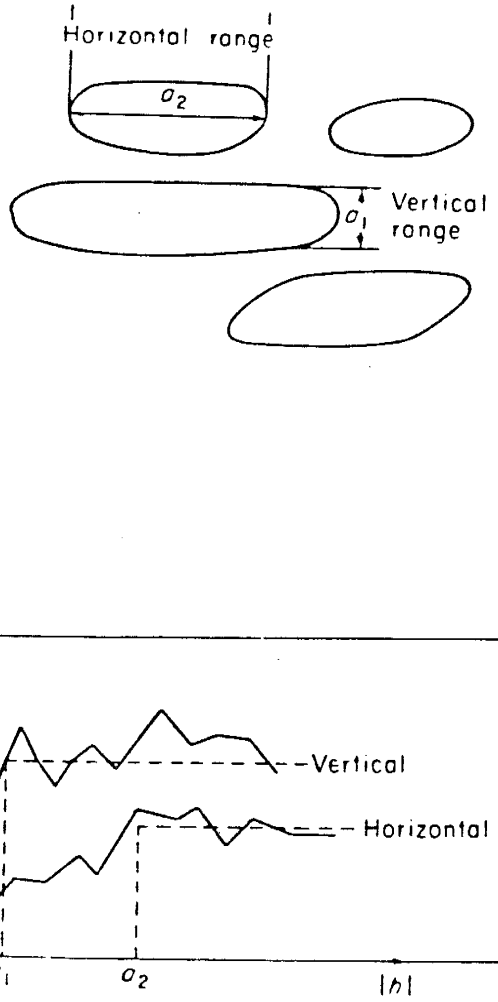

Figure 3. Illustration of statistical anisotropy. The horizontal variogram has a larger range (a_2) than the vertical variogram (a_2) due to the larger dimension of the ore bodies in the horizontal direction. (from Journel and Huijbregts, 1978)

ity density function. Bakr et al. [1978] and Journel and Huijbregts [1978] have stated that a continuum can be adequately represented by the first two moments of this joint probability density function. The first moment is the mean of the field and the second moment is the correlation structure as represented by the variogram.

As stated above, on the order of a hundred measurements are required to construct meaningful variograms for a given spatial scale of variability. Not only does this generally exceed the amount of measurements available at a given site, the information available is usually constrained to a given spatial class based on the source of the information. For example, if all the data is derived from wells (pump test and/or well logs), then the well spacing dictates what scale of variability can be studies with "hard" data alone. In order to supplement the available "hard" permeability data and analyze a variety of spatial scales, we wish to employ the techniques of basin analysis to provide additional "soft" geologic information.

2.1.2 Stochastic hydrology

With the first two moments of the system defined, it is possible to solve the partial differential equations of flow and transport through the field. The details of the methods of solving the equations will not be addressed here in detail. For one approach, the reader is referred to the works of Gutjahr et al. [1978], Bakr et al. [1978], Gelhar et al. [1979], and Gelhar and Axness [1983].

Most solutions of the equations of flow and transport through the continuum representation require two fundamental assumptions regarding the hydraulic conductivity field. These are the assumptions of second order stationarity and the ergodicity.

The condition of second order stationarity states that the first two mo-

ments of the joint probability density function (the mean and covariance) are invariant with respect to location. This condition implies, among other things, that the field exhibits a finite variance. An alternative to second order stationarity is to hypothesize that the field is an an intrinsic random field. This condition requires only that the mean and variogram are spatially invariant [Journel and Huijbregts, 1978]. The intrinsic hypothesis, or the assumption that the field is an intrinsic random field, is usually sufficient for geostatistical operations when dealing with the variogram [Delhomme; 1978]. When regional variations in the mean and variogram occur, it may be possible to use a moving neighborhood approach where each neighborhood is relatively statistically homogeneous [Journel and Rossi, 1989].

The second assumption employed in these studies is that the ergodic condition holds. Stochastic process theory deals with ensemble averages. In other words, the solution to the partial differential equation yields a statistical representation of the state variable (e.g. head or concentration). The statistical properties (mean and variance) of the solution in turn represent the outcome of many aquifers of the same statistical characteristics, when in fact only one aquifer exists. Gelhar [1986] addresses this rather esoteric question:

> In simple terms the ergodic hypothesis presumes that the behavior of a single aquifer, that is, some spatially averaged property of the aquifer, is represented probabalistically by the ensemble average over a large number of realizations of aquifers having the same underlying statistical properties. For the spatial averaging process to be meaningful, the heterogeneities must be relatively small in terms of their spatial scale as compared with the overall scale of observation.

If the spatial scales of correlation change with the scale of observation, the conditions of ergodicity and stationarity are violated.

The statistical assumptions employed are also greatly dependent on the

context in which they are applied. For different regionalized variables and different spatial groupings, the same geologic body may have different statistical behavior. Since the assumptions employed in stochastic hydrology have been neither validated nor invalidated by field investigations, alternative statistical representations of aquifer flow characteristics must be investigated as being equally feasible.

Whereas hydraulic conductivity has traditionally been the variable of study, characterizing aquifer heterogeneity can also be accomplished by analyzing a variety of other parameters. For example, Fogg [1986] performed statistical analysis of sand body thicknesses to arrive at aquifer characteristics. Similarly, Journel and Alabert [1988] proposed a method of indicator kriging which analyzes the connectivity of neighboring values of hydraulic conductivity with respect to a threshold value. They state that this method better simulates the actual continuity that is observed in many geologic deposits than the traditional kriging approach.

These methods of analysis are what we currently have at our disposal. It would be shortsighted to conclude that we must make do with what has been researched and published thus far. In fact, it is hoped that the methodology presented in this thesis will allow, if not force, us to arrive at alternative methods of analysis.

2.2 Basin Analysis

As with the need for understanding the quantitative aspects of characterizing hydraulic conductivity, it is also important to investigate the methods of geological analysis that will aid us in the final characterization. This thesis addresses the problem of characterizing deposits laid down by fluvial processes. However, these methods should be amenable to any type of sedimentary deposit.

Sedimentological facies and their geometric spatial relationship to one another are crucial when analyzing a sedimentary basin. Similarly, the hydrogeologic problem of aquifer characterization is sensitive to spatial relationships and extent of sedimentological facies.

A sedimentological facies is a body of rock which can be defined and distinguished from others by its geometry, lithology, and sedimentary structures [Selley, 1978]. The terms facies associations and lithologic distributions are used here in a similar manner; however, each term stresses a different aspect of the spatial distribution of lithologies. Facies association describes how different sedimentological facies are geometrically and thus genetically related to one another with little emphasis on details of spatial extent. On the other hand, the term lithologic distribution relaxes the facies definition to include a more general class of lithologies and implies a focus on spatial characteristics.

Analysis of clastic depositional systems relies on the use of models in order to reconstruct depositional environments. The term model is used here to mean a simplified version of reality that exhibits useful information in the interpretation and prediction of lithologic distributions and/or facies associations in sedimentary basins. Models of all types have been used to aid sedimentologists in the conceptual understanding of depositional processes and the resulting products of these processes.

Depositional models serve as reference points for comparison. Most depositional models are based on facies associations. By comparing and contrasting observed facies associations to models that represent a relatively well understood process/product relationship, one can draw conclusions about the depositional environment which produced the observed products. A broad range of models exist due to the broad spectrum of both the geologic information available and the objectives of the modeling process. To delineate all types of models

and discuss their advantages and disadvantages is beyond the scope of this thesis. However, all types of models should be considered in the process of studying ancient deposits.

Some models are deemed more useful than others if they are sensitive to the parameters being studied. As will be discussed later, different processes and cycles of processes are manifested differently in the sedimentary deposits. That is, facies associations are unique to the processes that dominated the depositional environment. When conceptual models are developed and actualistic models are distilled into type models, it is necessary to preserve the general character of the deposit as it relates to the processes under study. Limitations on geologic information and the properties of the desired model will influence to what extent the different types of models are used. Facies models have long been the tool of sedimentologists when analyzing depositional environments. Since well logs have been the primary source of geologic information, vertical facies models have dominated sedimentological studies. "A facies model attempts to provide an interpretation of a particular type of facies assemblage in terms of depositional environment " [Miall, 1984]. The utility of the facies models comes from the conceptual understanding of the relationship between depositional processes and products. With a conceptual understanding of a variety of facies models the sedimentologist is then able to deduce the depositional environment based on a comparison of his/her observations with the type model and the processes related to that type model.

Two types of facies models can be delineated. The first are conceptual models which are based on conceptual process/product relations. The other type are actualistic models which consist of distilled versions of a particular studies in which the depositional environments are fairly well understood.

Facies models are usually lumped into a depositional model context in

which an assemblage of facies is interpreted as resulting from a certain type of depositional environment. Often, models representing broad classes of depositional environments are subdivided into sub–environments. Fluvial facies models, for example, concentrate on type models based on modern depositional environments in order to determine ancient depositional environments. Generally, these type models have been categorized according to stream morphology. The stream morphology categorization has resulted from the observation that different facies assemblages result from different stream morphologies. For example, the deposits of a braided stream are generally different from the deposits of meandering, straight, or anastomosing streams. However, when one begins to look in more detail at actual modern streams it becomes apparent that no stream can be categorized as having just one morphology. Similarly one should not expect an actual ancient deposit to fit into a specific stream morphology classification.

Miall [1977] conducted a review of the sedimentologic literature on braided stream deposits. He concluded that facies assemblages and vertical sequences of braided stream deposits fall into four main classes. The basic type models of these four classes are given in Figures 4 and 5. These classes and their associated type models then serve as a basis for the interpretation of braided–river deposits at the surface and in the subsurface. The four type models are: 1) Scott type which is typical of a proximal glacial outwash environment; 2) Donjek type typifying cyclic sedimentation and is the most variable of the four; 3) Platte type representing the deposits of a distal sand dominated braided river; and 4) Bijou Creek type representing an ephemeral braided stream. These models are distilled versions of actual case studies and are intended to serve as end–points on a multi–dimensional continuum.

By comparing and contrasting observed vertical sequences with the type models and associated processes, one can begin to understand the depositional

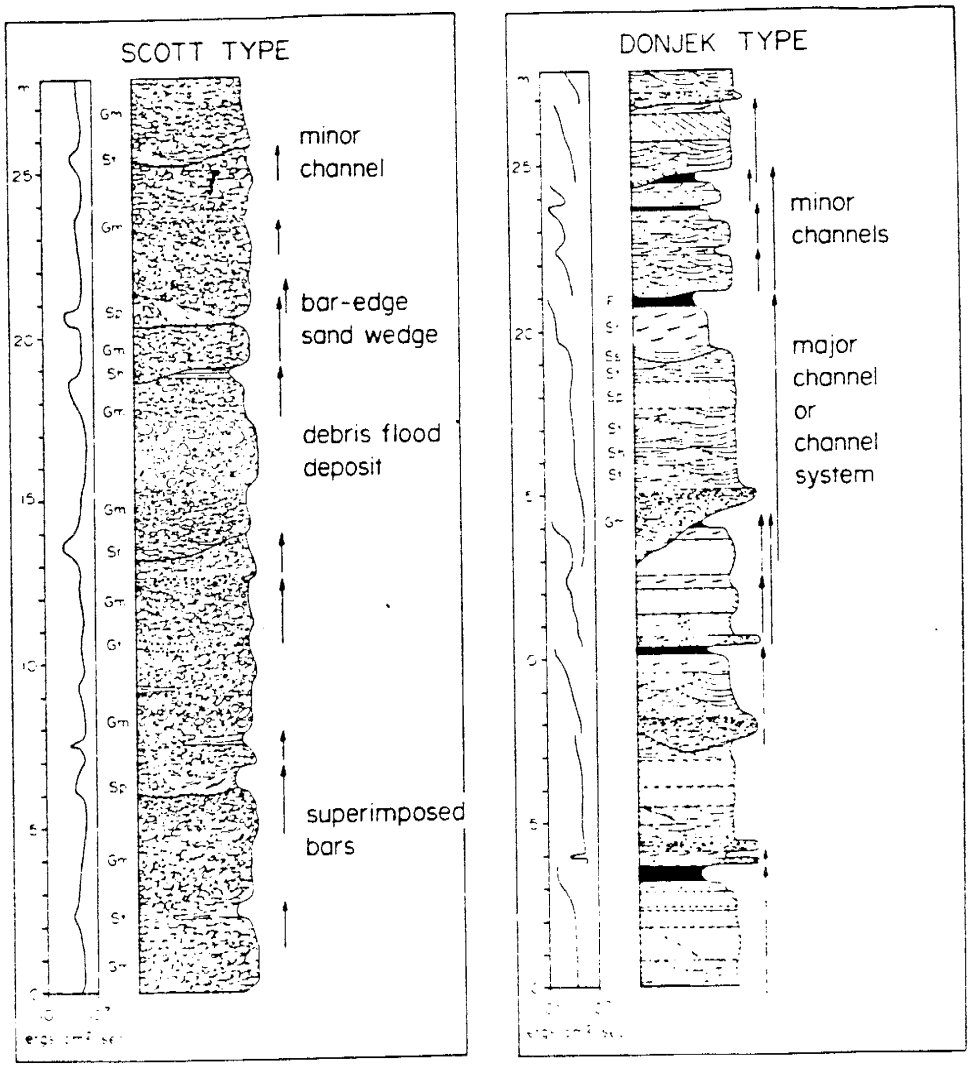

Figure 4. Type models of braided stream depositional environment. Scott type: Named by Miall to suggest a broad similarity with the proximal part of the Scott outwash river, Alaska, studied by Boothyard and Ashley [1975]. Donjek type: Named by Miall to suggest a broad similarity with the deposits of the Donjek River, Yukon Territory, studied by Willians and Rust [1986]. (from Miall, 1977)

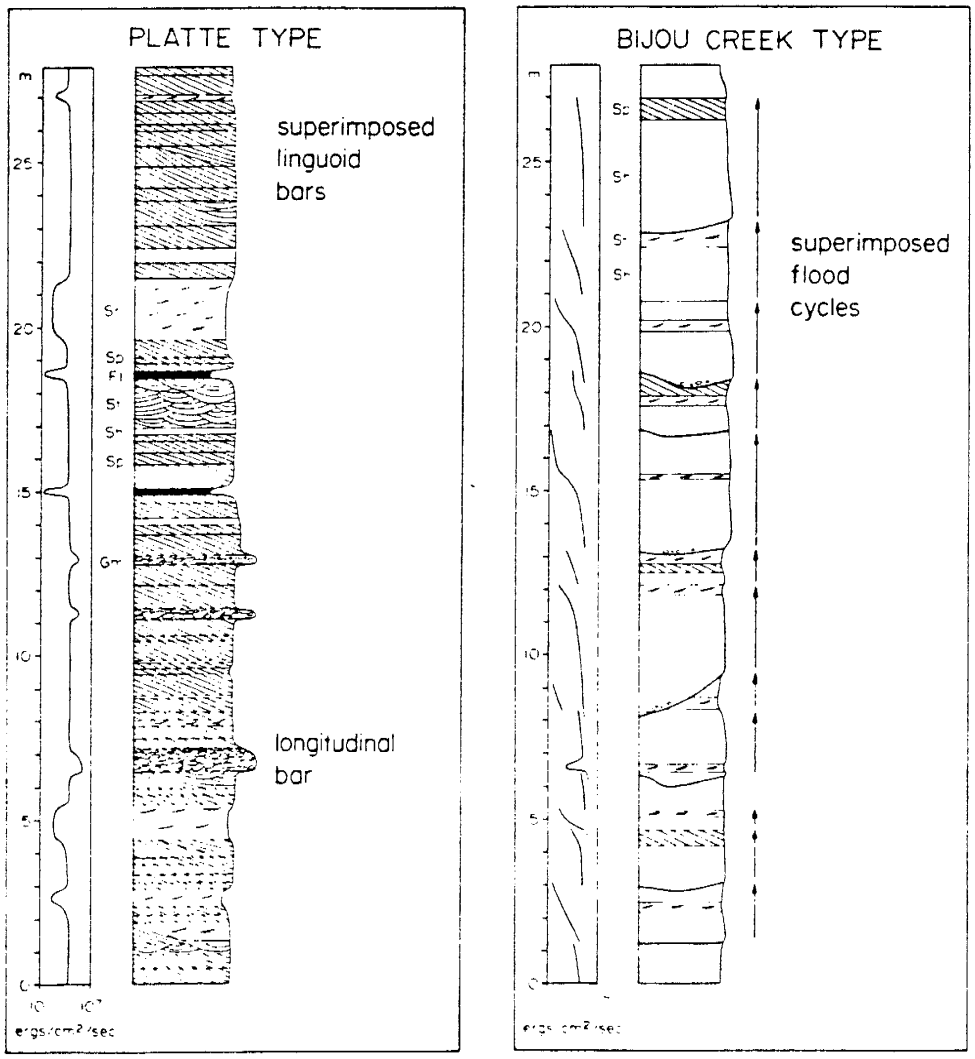

Figure 5. Type models of braided stream depositional evironment. Platte type: Named by Miall after the sediments of the Platte river, Colorado–Nebraska, as studied by Smith [1970]. Bijou Creek type: Named by Miall after the McKee et al. [1967] study of Bijou Creek flood deposits. (from Miall, 1977)

environment of an ancient deposit.

Much effort has been spent on drawing a line between morphologies of braided and meandering streams. Braiding parameters and length of meanders have been used to place modern streams and their associated deposits into a morphological category [Miall, 1977]. Without such a simplifying scheme the field of sedimentology would become exceedingly cumbersome. However, it must be recognized that pigeon–holing observations of an ancient deposit into a morphological category is geologically naive and does little to advance the understanding of the process/product relationship.

Modern streams, as well as ancient ones, consist of a multitude of different morphological components. The ability to distinguish this morphology is geologically useful only if we admit that no stream fits into one morphological category. Braided streams, for instance, often meander to different extents. This meandering component of the stream morphology contributes to the distinctness of the deposit. For example, a point bar deposit may be found in what is otherwise a very characteristic braided deposit.

Once one accepts that the morphological characteristics of fluvial deposits fall on a continuum rather than in a discrete set of pigeon–holes, one may wonder if it is not necessary to then develop a facies model for each deposit on that continuum.

Miall [1985] has addressed the question of classification according to morphology and the limited utility of the vertical facies models. He has suggested that facies models should deal with the third dimension whenever possible and attempt to characterize the environment in which a deposit was laid down instead of the morphology of the ancient stream. He has proposed a method called architectural element analysis in which the geometric relationships of eight basic sedimentological elements are studied in three dimensions. The eight basic ele-

Element	Symbol	Principal lithofacies assemblage	Geometry and relations
Channel	CH	Any combination	Finger, lens, of sheet; concave-upward erosional base; scale and shape highly variable; internal secondary erosion surfaces common.
Gravel bars and bed forms	GB	Gm, Gp, Gt	Lens, blanket; usually tabular bodies; commonly interbedded with SB
Sandy bed forms	SB	St, Sp, Sh, Sl, Sr, Se, Ss	Lens, sheet, blanket, wedge; occurs as channel fill, crevasse splays, bar tops, minor bars
Downstream accreting macroform	DA	St, Sp, Sh, Sl, Sr, Se, Ss	Lens lying on flat or channeled base, with covex upward third order internal upper bounding surfaces.
Lateral accretion deposit	LA	St, Sp, Sh, Sl, Sr, Se, Ss, less commonly G and F	Wedge, sheet, lobe; characterized by internal lateral accretion surfaces.
Sediment gravity flow	SG	Gm, Gms	Lobe, sheet; typically interbedded with GB
Laminated sand sheet	LS	Sh, Sl, minor St, Sp, Sr	Sheet, blanket
Overbank fines	OF	Fm, Fl	Thin to thick blankets; commonly interbedded with SB; may fill abandoned channels.

Table 1. Miall's (1985) classification of the eight basic architectural elements. (from Miall 1988)

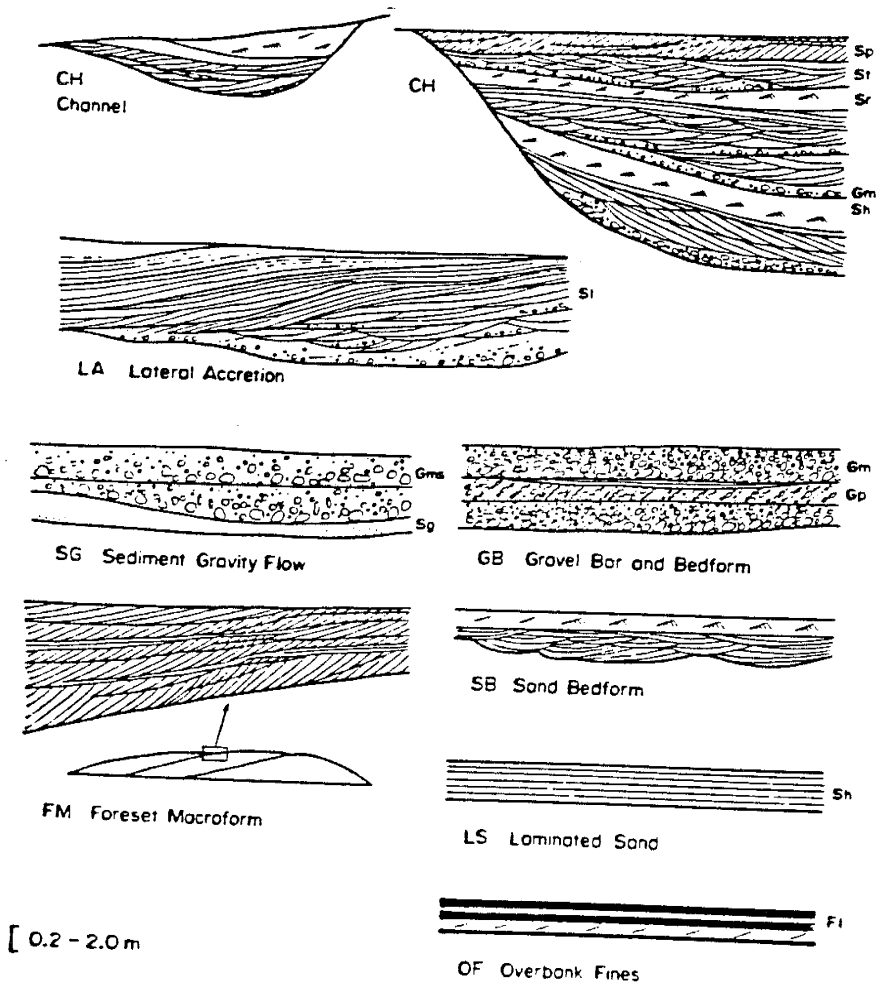

Figure 6. The eight basic architectural elements as defined by Miall [1985]. Note the variable scale. (from Miall, 1985)

ments are summarized in Table 1 and Figure 6 which will not be discussed in great detail here.

The architectural elements represent the different depositional processes acting in a depositional environment. Each element consists of a suite of lithologic facies that are distinctly associated with the depositional processes. In this sense, the specific characteristics of architectural elements are unique to the depositional environment of a deposit.

The advantage of the architectural element approach in the characterization of aquifer heterogeneities is two–fold. First, the three dimensional character of the deposit is preserved. Secondly, on the hypothesis that architectural elements of the same type exhibit similar permeability patterns, then a statistical representation of the spatial distribution of elements would in essence characterize the aquifer heterogeneity. Sedimentological models of architectural elements and their associated permeabiltiy patterns could then be used to compare and contrast against other studies. Similarities in depositional style would result in similar permeability patterns. Likewise, differences between the observed architectural element distributions and architectural element type models would lead to predictable differences in permeability patterns.

Another important concept in fluvial sedimentology is that of cyclicity. Most of the available generalized facies models consist of vertical associations of lithologic facies. Commonly these associations are preserved in vertical sequences which have the same general character but exhibit some variability both within a cycle and between cycles. The cause of this variability is a variability in the depositional processes that produced the deposit.

According to Miall [1980], depositional processes can be broken down into two classes of cyclicity. The first class includes small scale processes in which the distribution of energy within the basin results in a cyclic nature of the deposit.

This class of process is termed autocyclic and includes meander translation and enlargement, meander chute and neck cut–off, crevassing, and avulsion. These processes contribute largely to the variability within a depositional cycle. The second class of cyclic processes is of a larger scale. Depositional processes that originate outside the sedimentary basin are allocyclic. Changes in climate and tectonic activity are examples of allocyclic controls. The within basin manifestation of these large scale controls are changes in the discharge, variability of discharge, and load and slope.

When comparing observed geologic characteristics with type models, the concepts of cyclic processes provide a framework in which to analyze variability within cycles and variability between cycles.

The ideas presented in this section are intended to serve as a brief introduction to the sedimentological concepts and modes of study by which geological information can be incorporated into the characterization of fluvial aquifers. The reader is strongly urged to pursue the references cited to obtain a better understanding of the concepts presented.

2.3 Unification of methods of analysis

The ultimate goal of this research is to arrive at a method of incorporating "soft" geologic information and "hard" permeability data into a representative characterization of the hydraulic conductivity distribution of an aquifer at a variety of spatial scales. There will exist a broad range of data types and associated uncertainty. It is then necessary to incorporate different kinds of information into one mathematically consistent model or set of models.

We have focused our mathematical attention on statistics due to the uncertainty of the hydrologic system, namely the spatial variability of hydraulic conductivity. Geologically, we have adopted the methods of basin analysis in an at-

tempt to establish an analytical framework in which geologic information can be quantified.

Statistics and "quantitative" basin analysis have been studied in the past. Some notable examples that will be discussed in further detail below include: 1) the use of Markov chain analysis in the development of preferred facies sequences, 2) simplified numerical studies on how isolated depositional processes control the geometric relationship of sand bodies, and 3) numerical simulation of basin fill using the Navier–Stokes equations and equations of stream competence and capacity. These are described in more detail below. Each one of these has contributed to a better understanding of how basin fill stratigraphy may be quantified. However, each has restrictions or simply have not been field validated to the extent of acceptance.

One important aspect of aquifer characterization is the ability to predict, even in a purely statistical fashion, the geometric associations of lithologic facies. When working with vertical facies models, many workers employ the method of first order Markov chain analysis in order to establish a "representative" or "preferred" vertical association of facies [e.g. see Cant and Walker, 1976; Miall, 1973]. The general idea is to estimate the probability that one lithologic unit follows another lithologic unit, for all lithologies present. This is done by use of a difference matrix. The reader is referred to Reading [1986] for an example. The problems with this type of approach are many. First of all, only one dimension is taken into account; this neglects the lateral dimensions and associations of the lithologic facies. In addition it is necessary to generalize lithologies into a workable set that contains statistically sufficient populations. This generalization and grouping of lithologic facies often results in the omission of rare yet geologically and hydrologically significant sedimentary features.

From the hydrogeologic perspective however, only a representative real-

ization is needed and it has not been explored how adequate Markov chain analysis could be in generating a hydrologically representative suite of sediments. Furthermore the utility of multi–dimensional Markov analyses has yet to be addressed.

Hydrogeologically, the geologic parameter that is probably the most important is the degree of connectivity of high and low permeability units. A gravel body that is isolated within a clay unit will have very little effect on the overall flow and transport problem but will have profound sedimentological implications. It is then necessary to study not only the dimensions and geometric associations of the lithologic facies but also to pay particular attention to the hydrologically important aspect of connected high and low permeability flow units.

Allen [1978] and Bridge and Leeder [1979] have studied the manner in which certain depositional processes control sand body interconnectedness. Primarily the studies have focused on rates of subsidence, rates of avulsion, and some finer aspects such as differential compaction. Figure 7 illustrates how a slight change in subsidence rates result in much different geometric configurations and degrees of interconnectedness. While these models do not necessarily offer us methods of simulating suites of geologic sediments that honor observed field data, they do offer us insight into how a combined set of depositional processes manifests itself in different geometric patterns.

The most aggressive numerical scheme of studying sedimentary basin analysis in a hydrologic context is the work done by a group at Stanford University. Their goal is to numerically simulate permeability distributions based on basin fill processes and grain size distribution curves. Koltermann [pers. comm.] has modified the SEDSIM numerical model of Tetzlaff and Harbaugh [1989] to estimate spatial distribution of permeability.

How may this understanding of depositional process/product relationships

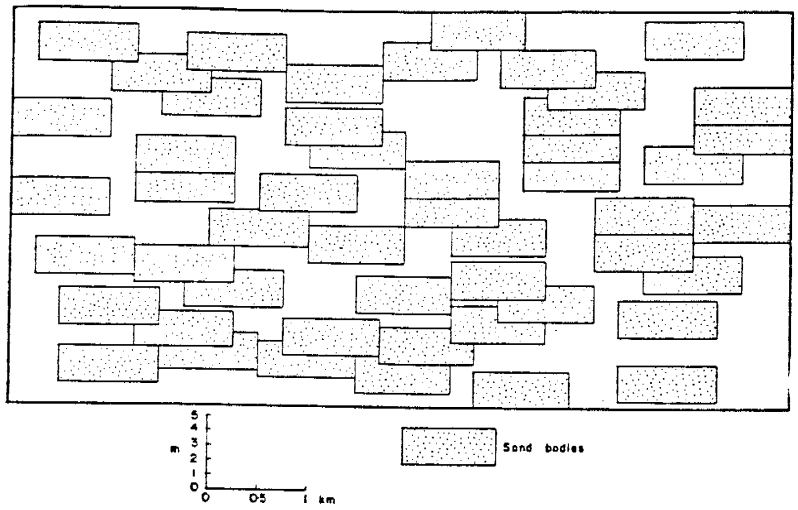

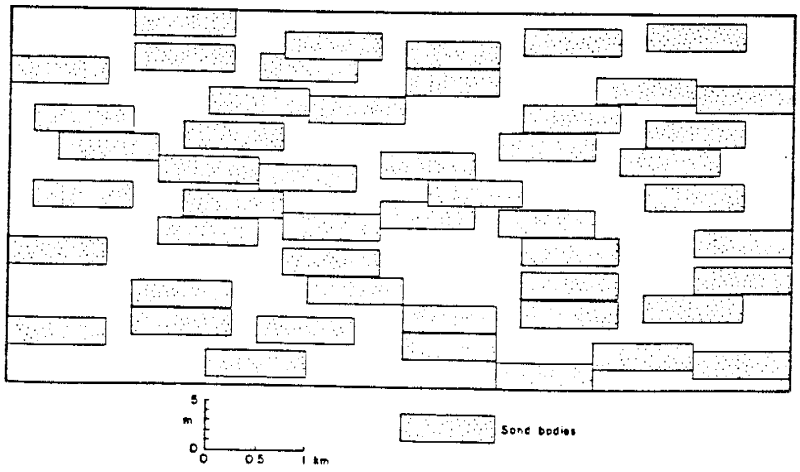

Figure 7. Alluvial suites generated by Allen [1978]. Note the change in amount of interconnected sand bodies. Figure (a) exhibits much more interconnection due to a lower subsidence rate than (b). Also note different thickness scales in (a) and (b). (from Allen, 1978)

aid us in the characterization of aquifer hydraulic conductivity? By studying the depositional processes that result in hydrologically important sedimentary deposits we can infer the general hydrologic character of an aquifer from a sedimentologic analysis. The scale at which this is to be done depends on the scale of the problem being addressed, and no two geologic characterizations will be the same.

There are numerous possibilities for approaching the problem of aquifer characterization. The important thing to bear in mind is that the characterization must be both geologically reasonable and possess a sufficient level of quantification so the flow and solute transport problems can be addressed at a quantitative level. What has been lacking in the past has been research oriented toward the investigation of how geologic materials are naturally distributed and what mathematical approach best describes the existing structure. In the next chapter we will present one approach to how this type of study may be carried out.

2.4 Heterogeneity and spatial scales

Permeability and hydraulic conductivity are by definition averaged properties of the medium. Bear [1979] illustrates this with the concept of the representative elementary volume (REV). That is, he hypothesizes that there exists a finite range of volumes for which the parameter being studied does not change appreciably (Figure 8). Below the valid range of volumes the parameter oscillates due to microscopic effects that are not sufficiently averaged; above the valid range the value begins to incorporate dissimilar material and the averaging process must begin again.

Permeability and hydraulic conductivity depend on the scale or volume over which they are averaged. Similarly, the geostatistical concepts of ergodicity and stationarity depend on the scale or volume over which the regionalized variable is studied (Figure 9). In the cases of both ergodicity and stationarity the va-

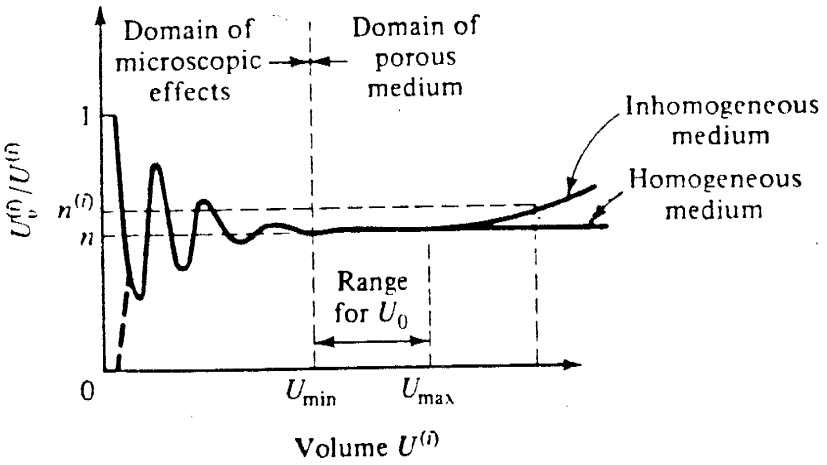

Figure 8. Illustration of the representative elementary volume (REV) concept. (from Bear, 1979)

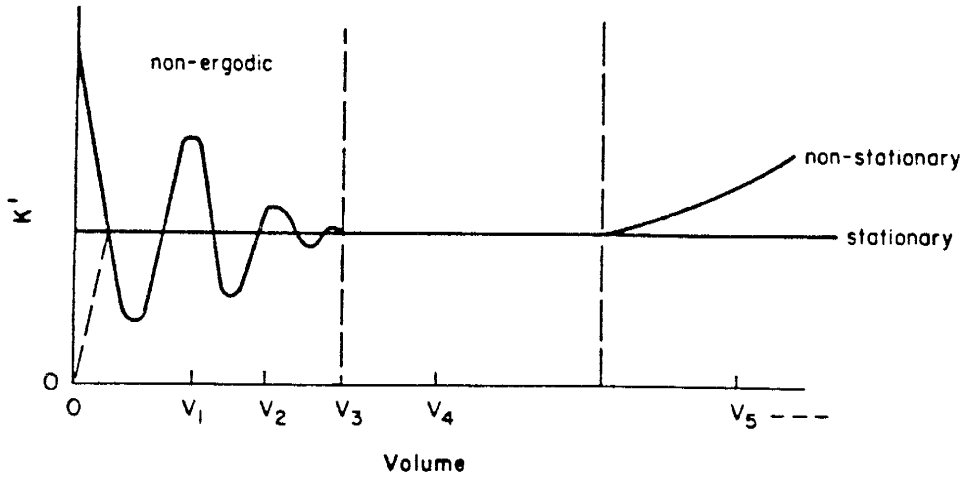

Figure 9. Illustration of the scale dependence of the statistical concepts of stationarity and ergodicity. (from Fogg, 1986)

lidity of the hypotheses can be enhanced by studying the random process at the appropriate scales. In our case the appropriate scales are controlled by the geologic structure.

It is common practice in solving groundwater flow problems to use effective or equivalent values of hydraulic conductivity in order to simplify the heterogeneity. For example, a heterogenous layered system can be represented as an equivalent homogeneous anisotropic system. Provided the phenomenon under study occurs at a significantly greater scale than some characteristic length of geologic heterogeneity, very little attention is paid to this averaging process.

However, when dealing with problems of solute transport and groundwater contamination in heterogenous aquifers, the dispersion of solutes depends on the characteristic scale of the heterogeneity. The study of the controlling factors in solute transport is essentially a study of geologic scales and how hydraulic parameters tie into that structure of scales. Weber [1986] breaks the geologic scales into five classes (Figure 10). The three largest classes will be the focus of the current and pending investigation.

Figure 11 shows a hypothetical progression of valid REV's in a geologic context. The vertical axis represents the variability of hydraulic conductivity and the horizontal axis the scale of the geologic entity. It is hypothesized that geologic entities such as individual lithofacies, architectural elements, and entire fluvial aquifers can be represented by some equivalent or averaged hydraulic conductivity. However, the issue of spatial scale and how these valid representations progress from one to another has received very little attention in the literature and is probably the most important aspect of proper characterization.

It should be noted that this hypothetical nesting of scales of geologic entities is somewhat unrealistic in that lithofacies as well as architectural elements occur over a wide range of spatial scales. While architectural elements are com-

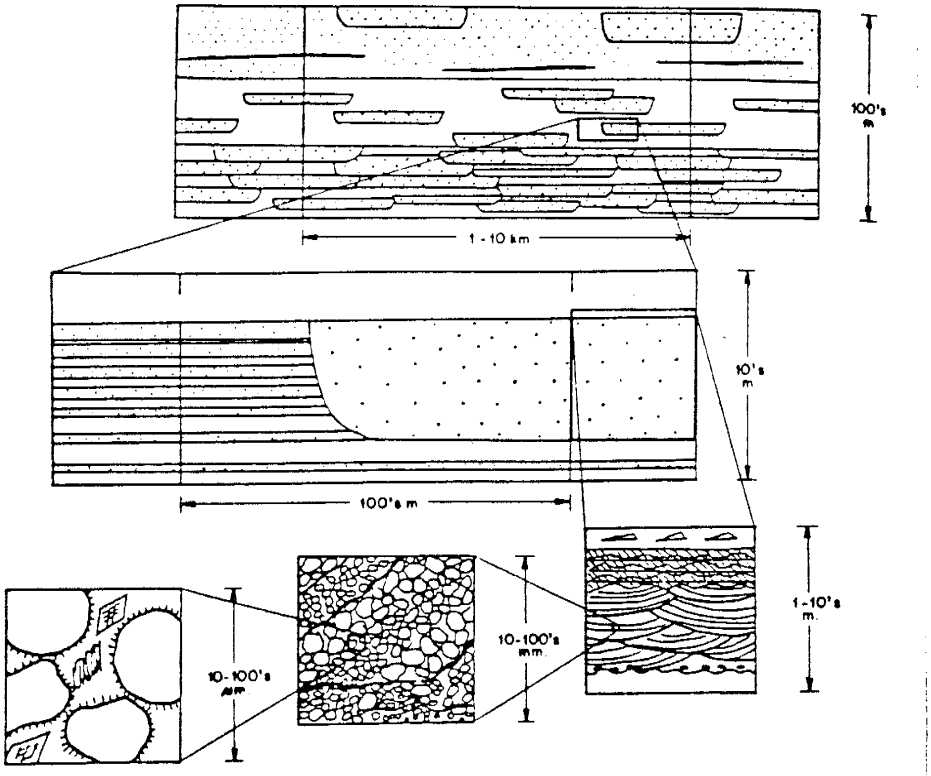

Figure 10. Five–fold breakdown of geologic scale of heterogeneity. (from Weber, 1986)

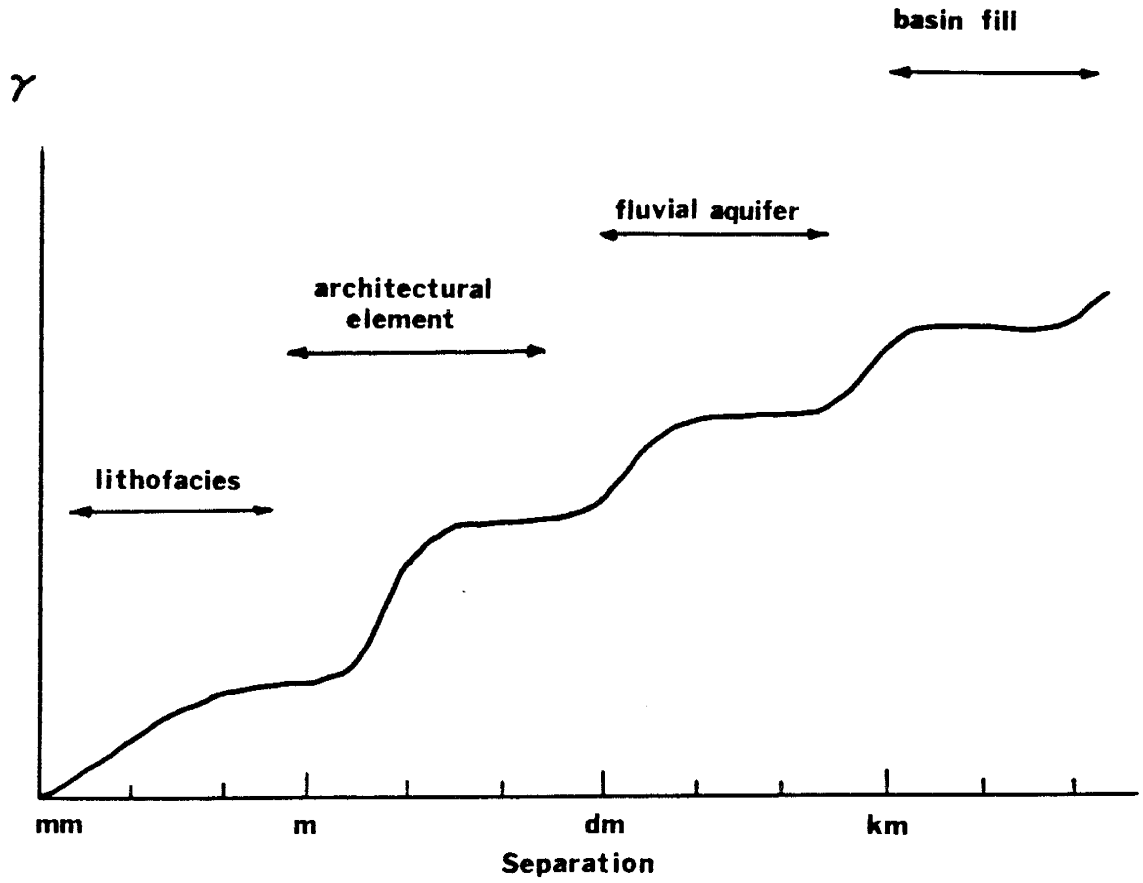

Figure 11. Hypothetical variogram of permeability involving a variety of geologic scales. (modified from Gelhar, 1986)

posed of lithofacies, the elements themselves may cover a broad range of scales for a given deposit.

Further study is necessary in order to better understand and test the hypothetical nesting of scales. It is hypothesized that geologic information and the theory of regionalized variables coexist at the conceptual level of spatial scales. Meaningful geological and geostatistical characterization should be pursued following the concepts of parameter averaging.

CHAPTER 3: Methodology

3.0 Introduction

As discussed above, in order to correlate the geology and the permeability, the two must be studied in parallel. The methodology for such a field study is the topic of this chapter.

While the methodology has been developed for a specific field site, it is believed that the methods presented will be amenable to other sites with little modification. The field site chosen to study permeability patterns and sedimentology is the Sierra Ladrones Formation that crops out extensively along the margin of the Llano de Albuquerque geomorphic surface (Figure 12). The badlands topography provides good three-dimensional exposure and diagenetic effects are minimal. The outcrop extends for approximately 25 kilometers also providing an opportunity to study a variety of spatial scales. The outcrop and field site will be described in further detail in Chapter 4.

The primary goals of the field investigation are to investigate the relationship between observed geology and patterns of permeability, and to investigate how depositional processes result in characteristic styles of heterogeneity. Another main objective is to study how heterogeneity changes with changes in spatial scale, and how these scales progress from one to another. To address these questions quantitatively, it is necessary to obtain spatially located information on both permeability and geology at scales of hydrologic importance.

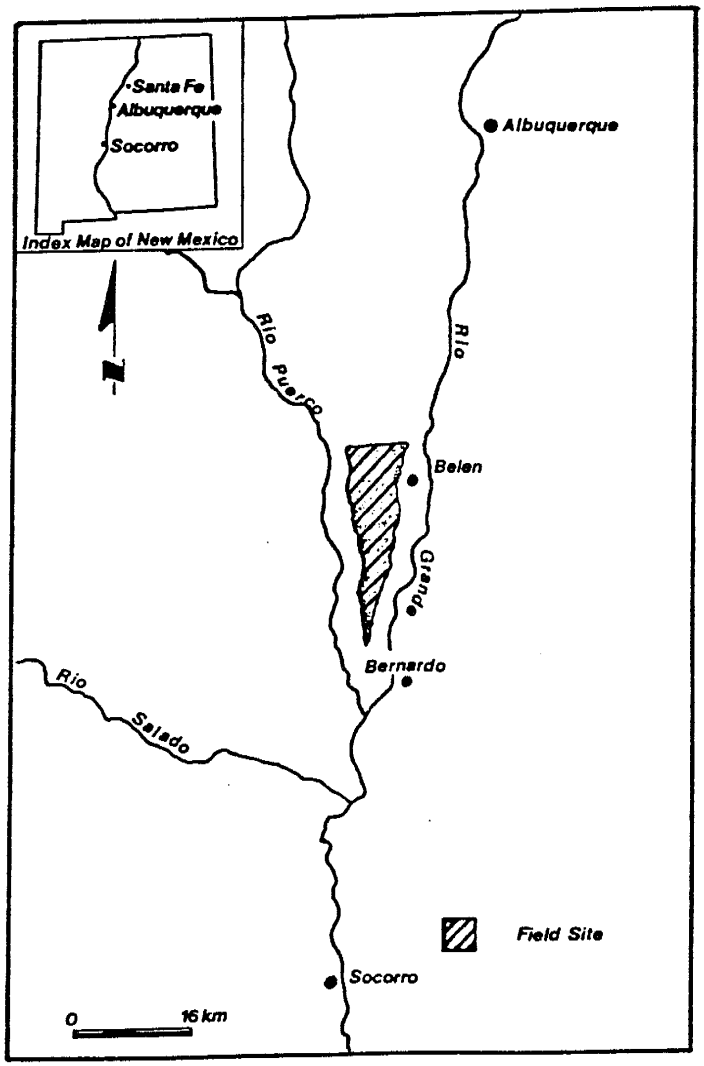

Figure 12. Location map of field site and Plate 1.

Generally the scales of hydrologic importance depend on the scale of the hydrologic problem under study. Since we are concerned with the future development of a generalized approach to the characterization of fluvial aquifers, all scales of hydrologic importance are considered here. Essentially, the heterogeneity must be studied at scales ranging from the hand specimen to that of the regional formation. Our approach is unique in that we address a broad range of scales of heterogeneity.

The desired end result of this study is a sedimentologically based model of permeability distribution developed from depositional process–product relationships. No a priori sampling strategy has been employed here. Rather, the strategy has been to follow the observations and address the questions of interest as the study progresses. The primary purpose of the data is two–fold: first to serve as a basis for geologic interpretation and secondly, to obtain quantitative modeling parameters for the permeability statistics. The uncertainty associated with the geologic information varies according to the scale of observation.

The geology must be studied in sufficient detail so that it is adequate for interpretive purposes. Geologic data must therefore be collected at a variety of scales. While it is important not to get excessively "lost in the details" on the small scale, the details need to be studied so that the research can progress along a directed and geologically reasonable path.

At the interpretive level a clear understanding of geometric associations is more important than actual spatial location in a global coordinate system. However, if the data is to be used in the estimation of statistical parameters, adequate control on the spatial coordinates of the geology will be necessary. Naturally there exists a question of feasibility. It would not be feasible nor would it be necessary to map the entire escarpment in great detail with highly accurate surveying methods. The question is raised: At what level of accuracy must the geol-

ogy and permeability be mapped to obtain a meaningful data set that satisfies the objectives of the study? The process must therefore be a recursive approach.

This chapter describes a field methodology established which economically captures both the geologic and permeability issues. Collection of both geologic and permeability data is performed from a base of control survey points. From the control points, the geologic features are mapped and permeability measurements taken. As mentioned, several scales of variability are of interest. Therefore, the survey methods vary according to scale.

3.1 Geologic Mapping

The geologic information collected serves two purposes. First the information will be used to interpret the geology, and second the information and its spatial structure will be used as a basis for the estimation of statistical parameters. The scales of interest can be broken into three general classes, each of which is slightly different in both the method of establishing spatial control and the goal of the mapping exercise. Each class of scale has an associated geologic entity. Naturally there is a transition between the spatial scales and the geologic entities being mapped. Studying all scales in geologic context will lead to a better understanding of the progression of spatial scales.

3.1.1 Facies Scale

The facies mapping exercises begin with a traditional survey with theodolite and rod. In the survey procedure it is desired to capture the gross geologic features that are apparent from an initial reconnaissance of the area. Prepared outcrops for permeability measurements are also surveyed in (see Section 3.2). The survey data is reduced and translated to a two-dimensional representation of the outcrop being studied.

The second phase consists of a more detailed geologic mapping of the outcrop supplementing the surveyed points with field sketches of the facies relationships. A tape measure is used as a supplemental surveying technique at the larger mapping scale. The field sketches are then transferred to a base map containing the control points. Obviously at this scale some spatial accuracy is forfeited so that an interpretive level of geologic detail can be obtained. It is important however that there be a geologic and hydrologic basis for the defining of the architectural elements.

3.1.2 Major Depositional Cycle Scale

Still another important class of scale is the scale at which depositional cycles vary spatially. Hydrologically this type of variability plays a key role in the large scale interconnection of architectural elements. Based on preliminary mapping exercises, this scale of variability is estimated to be on the order of several kilometers. A 7.5 minute topographic map enlarged two–and–a–half times is used as a base map. It has yet to be determined what "stratigraphic units" are appropriate for mapping at this scale.

The major difficulty lies in the lack of a mappable, laterally persistent transition between two facies. Even though the general trend or package of sediments is laterally continuous there are subtle changes at the boundary. When the outcrop is covered in a thin veneer of colluvium, the mapping process consists of mapping colluvial cover while ocasionally digging through the colluvial cover to confirm the contact.

Figure 13 illustrates how this approach may yield significantly different sedimentological interpretations. First, suppose that the mapping of large scale features is being performed. All that is visible to the geologist is a general contact of a gravelly sand over a clay. In three places the colluvium is removed to

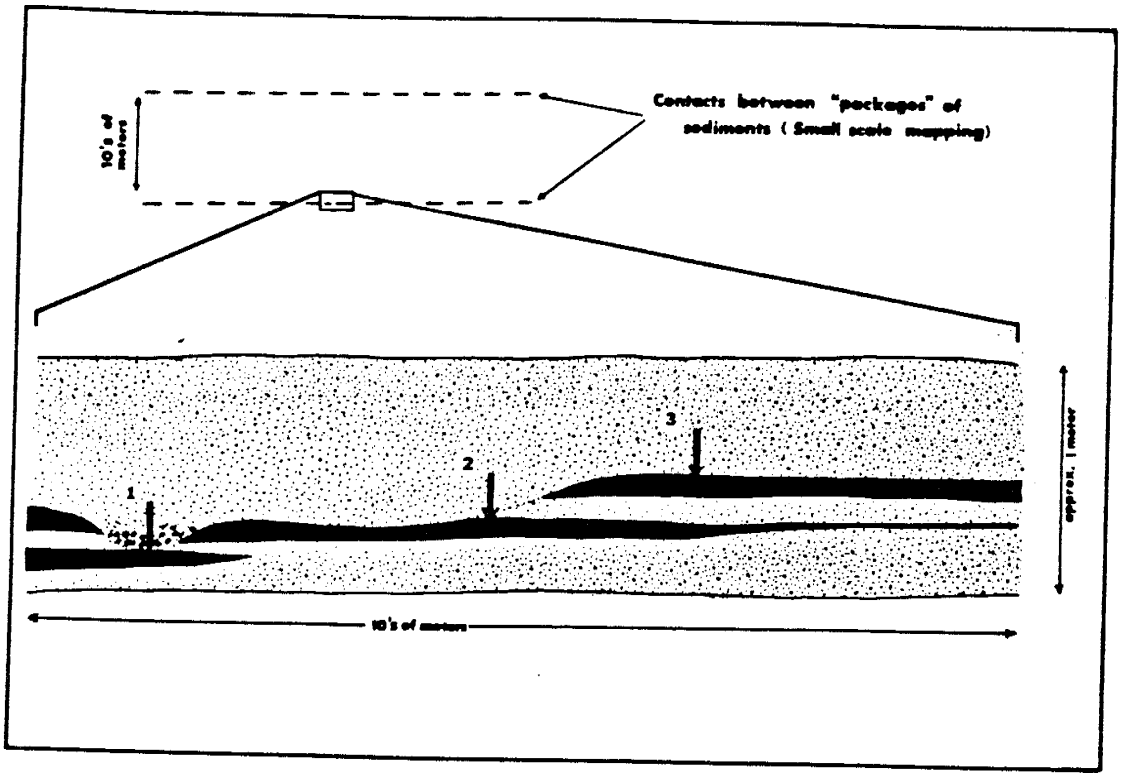

Figure 13. Illustration off contact between major depositional cycles. The three arrows represent the same observed contact of a sand to gravelly–sand over an overbank deposit. When mapping at the scale of major depositional cycles, all three locations are considered one contact. Mapping at the element scale will need to capture depicted level of detail.

observe the hypothesized contact of a gravelly sand over a clay and the mapping continues as the clay being a laterally continuous unit, when in actuality, three different clay layers exist that pinch out and are scoured through by the overlying gravelly sand. The sedimentological as well as hydrological interpretation of the two resulting maps would be quite different.

3.1.3 Element Scale

Once the architectural elements are defined, they can be used to capture the intermediate scale heterogeneity. The intermediate scale mapping provides the link between the facies scale mapping and the mapping of larger scale depositional cycles.

Obtaining geometric relations of architectural elements and the facies within those elements is one of the primary objectives of this study. Provided the statistical properties of hydraulic conductivity within architectural elements are distinct and tractable, the statistical parameters of the entire conductivity field for the scale of particular interest can be estimated. Since we do not have the method in hand that will allow incorporation of geologic information and permeability data into a quantitative model, the level of accuracy required is as of yet unknown.

3.2 Permeability Data

In addition to the geologic information discussed above, spatially located permeability data are necessary for statistical analysis and interpretation. This section will address the issue of obtaining spatially located permeability measurements.

At this stage of the research, we have chosen to neglect effects of diagenesis, such as cementation. The ideal sampling location is an uncemented fresh de-

posit. Much of this methodology is site dependent. The Sierra Ladrones Formation crops out in a badlands topography for approximately 25 kilometers and the vertical extent of the outcrop varies from several meters to approximately 100 meters. Cementation of the formation occurs locally, usually when a permeable layer overlies a fine unit. The majority of the exposure is however uncemented. Colluvial cover of the uncemented portion is again highly variable. Generally only a few inches need be removed before uncemented undisturbed deposits are encountered. The preparation of a permeability measurement site has two primary objectives: 1) remove colluvial cover to expose undisturbed sediment, 2) obtain sampling locations that can be located efficiently.

3.2.1 Air Minipermeameter

In order to obtain a sufficient number of permeability measurements a portable air minipermeameter has been developed. The air permeameter is a modification of a device described by Goggin et al. [1988b] and is described fully in Appendix B . This device allows rapid non–destructive sampling of permeability of the sand facies. In order to measure the permeability of the clay and gravel units, new permeameter designs will have to be developed, or at least a methodology that will enable one to estimate the permeability of the extreme value deposits within a specified degree of certainty.

3.2.2 Spatially located measurements

The methodology developed for obtaining spatially located permeability is still in its infancy. It has resulted from a rather substantial set of constraints and it should be noted that the method described here is somewhat site/project specific. Two issues must be addressed: 1) where the measurements are made and 2) how those measurements are located.

There are several optimization schemes to collect data so that the variogram analysis is able to take advantage of all data [e.g. Warrick and Myers, 1987]. However, we are constrained in sampling by both the physical location of the outcrop, and sampling where the permeameter will work. It will therefore be increasingly important to interpret the data in a geologic context.

The method of locating permeability measurement locations is based on a survey which establishes control points on the ridge. Outcrops are prepared for permeameter sampling by locally digging away the colluvial cover to obtain a vertical face (approximately 3 meters by 1 meter) of undisturbed deposit. The outcrop is then photographed so the location of permeability measurements can be recorded. The photograph serves as a base map on which the location of measurements for the given outcrop can be located. A scale is included in the photograph so that digitizing can be performed. The sampling locations marked on the photograph are then digitized to obtain a set of "local" coordinates. These coordinates are in reference to some arbitrary origin on the photograph. Also digitized from the photograph are the surveyed control points.

The control points on the photograph allow the transformation of the "local" coordinates into the "global" coordinates of the study area. A similar type of locating scheme is employed to supplement the digout type study. In some locations small surfaces, 15 centimeter by 15 centimeter, are prepared and the permeability measurements are performed on a grid of known dimensions. Similarly, these "local" coordinates are then transformed into the "global" system. Figure 14 diagrammatically summarizes the permeability collection scheme.

3.3 On the sampling of extreme values

It has been noted in the literature [Journel and Alabert, 1986] that groundwater flow depends greatly on the spatial distribution and interconnection

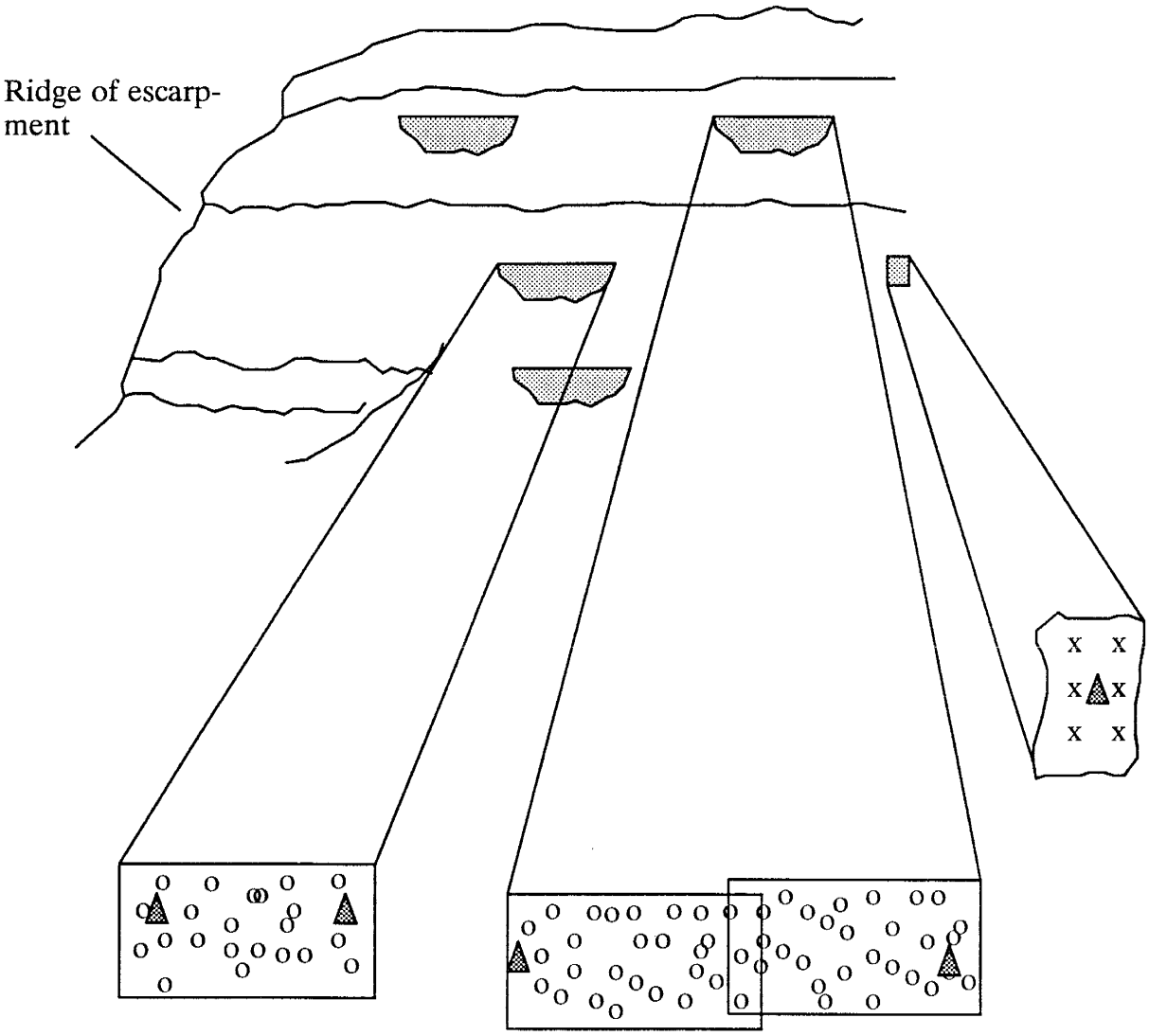

o : permeability locations on 8 1/2 X 12 B&W photo

▲ : survey locations to tie "local" coordinates in with "global" coordinates

: outcrop prepared for air permeameter measurements

x : permeability locations on fixed grid

Figure 14. Diagrammatic sketch of method locating permeability measurements.

of the extreme value permeability units. However the sampling of these extreme values remains as a major stumbling block for experimental hydrologists. Quick and reasonably accurate measurements of clay and gravel permeability has not been a focal point of hydrologic research. Several avenues of investigation are currently being researched on how to overcome this problem as it relates to field scale investigation of permeability distributions.

For example, it may be possible to correlate the compaction variables of the low permeability clay to a permeability value [Harrop–Williams, 1985]. If this can be validated on the specific soils of interest, then permeability may be estimated in the field from a quick consolidation experiment. Another possibility is to perform actual clay permeability tests in the field. A device described by Olson [1966] allows rapid measurements of clay permeability by measuring the pressure response due to a given influx of fluid. The problem of obtaining saturated samples in the field is still the major factor limiting the implementation of such a device.

Similarly, for the gravel units it may be possible to draw an empirical correlation between type of deposit and permeability based on field permeameter tests. It is most likely that these field test would require a bucket permeameter approach to ensure that a sufficient volume (REV) be sampled.

The envisioned bucket permeameter consists of a cylindrical water tank approximately 1 meter in diameter and 0.5 meter tall open at the top. With the tank approximately two–thirds full, a cylindrical sample of gravel (approximately 1 L.) screened at the bottom and open at the top is inserted so that there is small (approximately 1 cm.) difference between the water level in the tank and the water level in the sample cylinder. Once the system reaches steady state, the difference in head and flow rate through the sample can be measured. The permeability can then be estimated based on Darcy's equation.

While some of gravel deposits have undergone diagenetic cementation, the majority of the gravels are uncemented and those will be the focus of hydrologic characterization.

The problem of sampling the extreme values of permeability is an issue that has not been resolved as of the submittal of this thesis. It should be regarded however as a serious deficiency that must be investigated. It should also be borne in mind that it may not be necessary to obtain highly accurate values of permeability for these units of extreme values. It may be sufficient to map out their spatial extent and use some type of "medium (soft–hard)" data approach. The inability to sample clay and gravel permeability need not inhibit the entire effort of studying spatial variability of permeability in fluvial deposits.

CHAPTER 4: Field Site

4.0 Introduction

Development of a successful method for the incorporation of geologic information into the characterization of aquifer heterogeneity will require intensive field investigations. These field studies should be performed on outcrops that have sufficient exposure to obtain information on both the geology and permeability patterns.

Choosing an appropriate field site to study spatial variability of permeability and to develop sedimentological models of that variability is crucial. In the present study our primary objectives are to 1) study heterogeneity at a variety of spatial scales and 2) develop a three–dimensional model of the permeability patterns based on sedimentological models. To somewhat simplify the study, diagenetic effects will not be taken into account. It is therefore desired to choose a study area with extensive three–dimensional exposure over several kilometers and an outcrop that has not experienced a significant amount of cementation. A field site meeting these requirements has been located in the Albuquerque Basin of central New Mexico.

4.1 Sierra Ladrones Formation

The Pliocene/Pleistocene Sierra Ladrones Formation crops out along the Llano de Albuquerque geomorphic surface in a badlands topography (Figure 12). The Albuquerque Basin is one of a series of en echelon rift basins that formed along the Rio Grande Rift during latest Oligocene and early Miocene [Chapin

and Seager, 1975]. The tectonics of the southwest Albuquerque Basin are fairly well understood at the large scale and less precisely in detail. Lozinsky [1988] summarized the tectonic setting for the Albuquerque Basin as a half-graben dipping eastward in the northern part of the basin and to the west in the south basin. The transition is covered by Santa Fe Group basin fill but is believed to occur along a southwest extension of the Tijeras fault just south of Albuquerque.

The structural boundaries of the basin are the San Felipe fault belt in the north, the Joyita uplift in the south, and the Sandia–Manzano–Los Pinos uplift to the east. The western border is less well defined but includes the Lucero and Ladrone uplifts.

The Sierra Ladrones Formation is the uppermost formation of the Santa Fe Group and is reported [Machette, 1978] to be early Pliocene to middle Pleistocene in age. The Sierra Ladrones consists of two main facies: 1) a piedmont slope facies consisting primarily of alluvial fan and coalescing fan deposits, and 2) a basin floor facies consisting mainly of river sands, gravels, and flood plain deposits. The Sierra Ladrones overlies the Popotosa Formation, early to late Miocene in age. The Popotosa Formation also consist of two main facies: 1) a fanglomerate facies which consists of gravelly alluvial fan deposits which grade laterally into 2) a playa facies comprised of fine to medium grained silt, clay and sand with primary and secondary gypsum.

The term facies is used here to delineate between transitional lithologies that resulted from a geographic change in depositional environment. The geologic entities being described are probably better categorized as separate members of the Sierra Ladrones Formation; however, to classify them as members at this time would require that their external geometry and internal lithologic characteristic be documented. The section of the Sierra Ladrones Formation current-

ly under study apparently is located where the two "facies" of the Sierra Ladrones intertongue.

The studies by Young [1982] and Lozinsky [1988] represent the only comprehensive work done on the Sierra Ladrones section in the area of interest. These studies have focused on much broader geologic aspects which involved the Sierra Ladrones Formation.

4.2 Current Geologic Investigation

The geologic investigation of the Sierra Ladrones is one of both sedimentological and hydrological interest. The goal of the current study is to refine the methodologies and concepts described above and a determine how these methods of analysis can serve to study spatial variability of permeability in natural geologic systems. The application of these methods and their geologic as well as hydrologic significance are the topic of this chapter.

Currently, geologic information is being collected for purposes of geologic interpretion. Once a better understanding of the geology is obtained, this information will be used in the estimation of statistical parameters. The geologic analysis is subdivided into the three scale classes; each scale class employs a slightly different method of study as well as a slightly different hydrogeologic and sedimentologic focus.

4.2.1 Mapping of major depositional cycles

The first step in the geologic investigation of the Sierra Ladrones Formation was to become familiar with the general nature of the deposits. The depositional model of Young [1982] was taken as a basis for analysis and modification. Based on size of clasts, lack of fine-grained deposits, thick beds and shape of

channel, Young [1982] interpreted the depositional environment of the Sierra Ladrones Formation as a complex braided stream system.

Initial reconnaissance work revealed that lithologic facies in the northern part of the study area (west of Belen, NM) were laterally continuous on the scale of tens of meters to a few kilometers. To the south (west of Bosque, NM), more lateral variability in deposits was observed. The reason for the change in lateral variability is still unclear but the possibilities include 1) more of a meandering component to the north and/or 2) the confluence of the ancestral Rio Grande and its ancestral tributaries was located to the south.

Similar packages of sediments were observed in both the north and south areas of the field site. Generally, these packages fine upward from coarse sand and gravel to soils and clays. As such, they are believed to represent major cycles of sedimentation. Some are dominated by stacked channels of gravel and coarse sand while others exhibit an abundance of laterally continuous paleosols and overbank material. In an effort to tie the sediments together from north to south, three such packages were noted and mapped on an enlarged topographic map. It is believed that these packages of sediments will serve in the interpretation of the large scale depositional environment which is beyond the scope of this thesis.

It was hypothesized that the sedimentological importance of the mappable contacts would reveal itself as a general understanding of the depositional history evolved. Mapping of major breaks in depositional style will continue in an effort to better understand both the processes responsible and to correlate how these processes have affected the large scale patterns of permeability and interconnectivity.

To aid in the mapping of large scale geologic features, two sections were

measured at the locations shown on Plate 1. These sections are presented in Figure 15 with the descriptions in Appendix C. Additionally, in the large scale investigation it was noted that there are apparently at least three depositional regimes present. By several depositional regimes, it is meant that there was more than one mode of deposition, i.e. a single ancient river was not responsible for the entire suite of sediments observed. The geographic location of the site as well as the deposits studied thus far indicate depositional influences from: 1) the ancestral Rio Grande, 2) the ancestral Rio Puerco/Rio San Jose and, 3) significant debris flows of unknown origin. The ancestral Rio Puerco and Rio San Jose influences are lumped together in this study due to a lack of information regarding that regime. It is not apparent whether or not it is necessary or even possible to distinguish between ancestral Rio Puerco and Rio San Jose deposits. However, it is possible to delineate between the drainage from the western tributaries and that of the ancestral Rio Grande. The presence of Grants obsidian derived from Mt. Taylor (NM) is an idicator of Rio Puerco/San Jose drainage [Young, 1982].

The geographic location of the field site and results of preliminary mapping exercises are evidence of a multiple depositional regime system. Previous work has suggested that the Rio Puerco, Rio San Jose, and Rio Grande were all active in the Albuquerque Basin during Pliocene/Pleistocene time [Young, 1982; Lozinsky, 1988]. The physical locations of the tributaries and axial drainage system during the depositional history of the basin has not yet been studied; however, it is reasonable to assume that the field site (which is located in the south-central part of the basin) was influenced by both the ancestral Rio Grande and the tributaries to the Rio Grande. Results of the mapping exercises also indicate multiple modes of deposition in the area. Mapping on the facies and deposition-

Next page

Figure 15. Measured section of Sierra Ladrones Formation. See Plate 1 for locations.

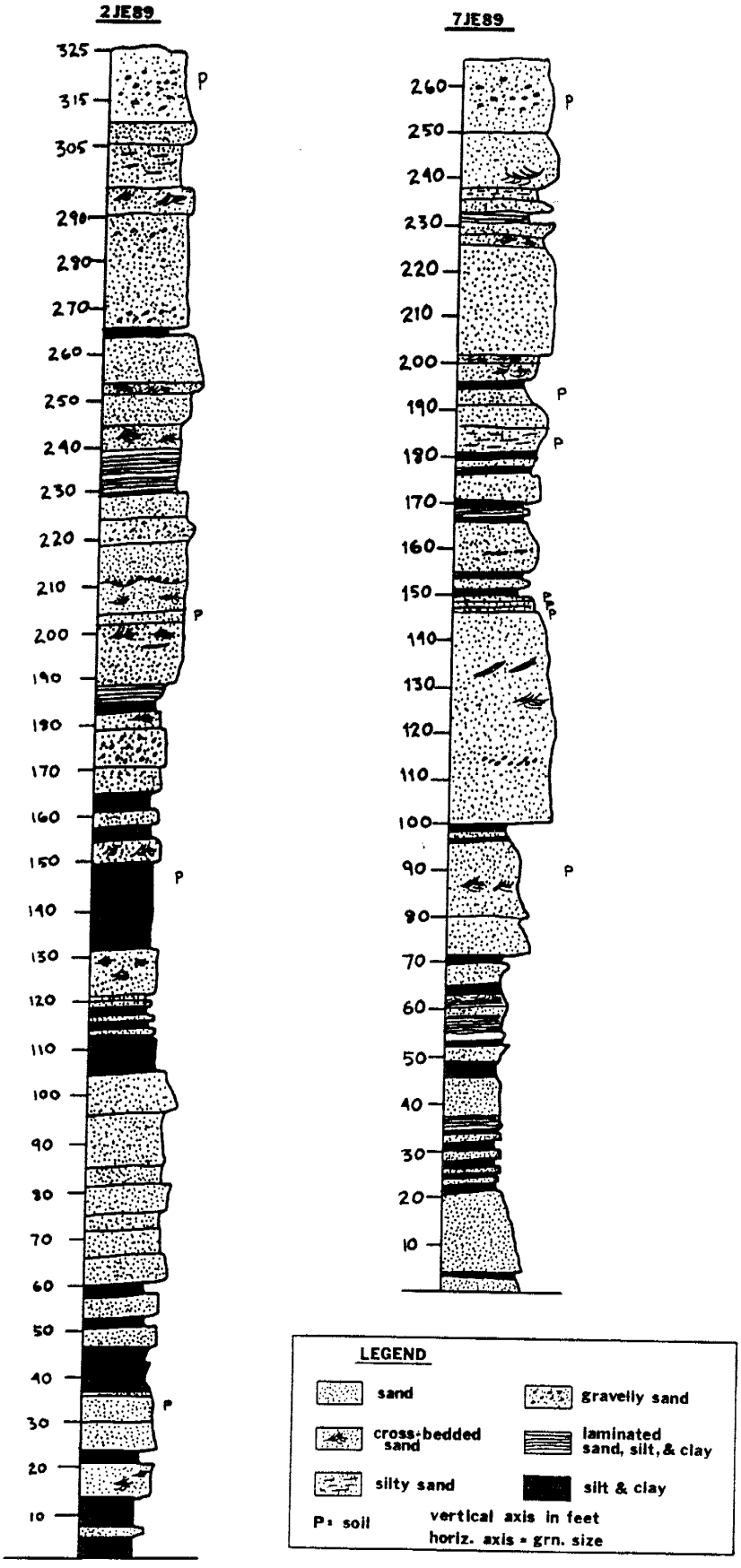
2JE89
325
315
305
290
280
270
260
250
240
230
220
210
200
190
180
170
160
150
140
130
120
110
100
90
80
70
60
50
40
30
20
10
P
7JE89
260
250
240
230
220
210
200
190
180
170
160
150
140
130
120
110
100
90
80
70
60
50
40
30
20
10
P
LEGEND
sand
gravelly sand
cross-bedded sand
laminated sand, silt, & clay
silty sand
silt & clay
P = soil
vertical axis in feet
horiz. axis = grn. size

al–cycle scale both suggest a predominantly fluvial depositional environments, possibly from more than one river channel as discussed above.

Additionally, in the southern part of the field site, just west of Bosque, N.M., a deposit that is several meters thick and extensive laterally for up to a kilometer exhibits features of a large debris flow. Small scale (cm x m) channel structures are preserved. Armored mud balls several centimeters in diameter indicate rapid deposition in a high energy environment. Determination of the origin of this deposit will require mapping of its external geometry as well as clast analysis.

4.2.2 Soils

Another important feature observed during the initial reconnaissance study has been the importance of soils as a depositional unit. In arid climates it is common to observe well developed soils that continue laterally for several kilometers. Aridisols in the southwest have been studied thoroughly by Gile et al. [1981], Walker [1967], Walker et al. [1978], and Machette [1985]. Parent material which may originate from a variety of depositional processes is transformed into soils. Soil development results in three distinctive alterations of the parent material. One of these is the introduction of illuvial clays into the B soil horizon. A second is the destruction of sedimentary structures by roots and soil fauna. Also, calcium carbonate is precipitated in the K horizon [Gile et al. 1981]. The resulting vertical soil profile can be summarized as a relatively thin A horizon lacking significant organic material, a B horizon containing illuvial clays, and K calcic horizon. Gile et al. [1981] recognized five stages of desert soil development. These are discussed in Table 2.

Preliminary observations have indicated that soil development results in a

Stage and general character	Diagnostic carbonate morphology	
	Gravelly sequence	Nongravelly sequence
I Weakest expression of macroscopic carbonate	Thin, discontinuous coatings on gravel clasts	Few filaments or faint coatings on ped surfaces
II Carbonate segregation seperated by low-carbonate fabric	Continuous coatings on clasts some interclast fillings	Few to common nodules
III Carbonate essentially continuous; plugged horizon forms in last part	Many interpebble fillings	Many nodules and internodular fillings
IV Laminar horizon develops over plugged horizon; incipient calcrete formation; forms caprock layer 0.5m thick	Indurated laminar horizon over plugged horizon; thin upper zone of platy structure over zone wiht massive to nodular structure; grades downward into gravelly or nongravelly material with stage III morphology; incipient "caliche profile" of Lovelace (1972) and pedogenic calcrete	
V Multiple laminar horizon develops in upper part of profile; incipient development of degradational features; forms caprock layer up to 2m. thick.	Thick, will-indurated upper horizon; platy to tabular structure with multiple laminar internal fabric; zones of dissolution, brecciation, and recementation locally present; dry bulk densities up to 2.2g/cc.	

Table 2. Stages of carbonate accumulation in gravelly and nongravelly morphogenic sequences. (modified from McGrath and Hawley, 1987)

reduction of permeability. This is believed to be caused by the introduction of illuvial clays, precipitation of calcium carbonate, and the churning caused by roots and soil fauna. Correlating soil type and patterns of permeability within soils may prove insightful. Since the permeability of these units is distinctly different from other depositional units that were not surficially exposed long enough for soil development, the soils are treated as a distinct depositional unit.

The issue of diagenesis versus primary depositional process is treated in this study from a hydrologic perspective. The term diagenesis in this thesis is reserved for physical and chemical alteration that occurs after the sedimentary unit is buried. Soil development is thus treated here as a primary depositional process.

The soils preserved in the Sierra Ladrones Formation may be very useful for two purposes. First, they indicate a long hiatus in fluvial deposition and thus may serve as an indicator of relative quiescence. Second, their general character of being very continuous laterally may serve as a type of marker bed for the mapping of larges scale features.

Generally, thousands to tens of thousands of years of surface stability are necessary for the development of desert soils; however, the soil development process can be highly variable and is considered to be inadequate for absolute dating of the deposits. Other dating possibilities include volcanic ashes and mammal fossils. However, as of this time neither of these have been observed in the field site.

Probably the most useful aspects of the pedogenic facies are their sedimentological implications. These paleosols are indicators of both paleoclimate and paleogeomorphic conditions. When studying the sedimentology of fluvial systems over large distances (km), the paleosols provide a means to correlate

different cycles of sedimentation [Allen, 1974]. The correlation of these cycles of sedimentation is vital in the construction of a depositional environment.

4.2.3 Facies and element scale mapping

The site of the initial detail study is located approximately 15 kilometers west of Bosque, NM (Figure 12, Plate 1). The sudy will include both small scale and intermediate scale analysis of geology and permeability patterns and will subsequently serve as an initial basis for the large scale study. This site was chosen primarily for its accessibility, quality of exposure, and workable terrain. Once the site for facies scale mapping was selected, an initial reconnaissance of the outcrop was performed. The nature and locations of the gross geologic features were noted and surveyed. The goal of the study was to establish "first cut" architectural element definitions and begin to analyze the depositional environment and geologic character of heterogeneity at the element and lithofacies scale.

As discussed above, the large scale reconnaissance effort indicated that major changes in depositional style occur at certain stratigraphic levels. A package of sediments was chosen to be the initial focus of the facies scale mapping. The base of the current package under study is a gravelly channel deposit which lies unconformably on what is possibly an alluvial fan deposit. The upper contact is another large unconformity in which a series of stacked channels cut into the sediments under study. The package under study is approximately 25 meters thick at the location of OUTCROP1. The outcrop of the initial study trends approximately N35E, has an average slope of approximately 45 degrees, and a lateral dimension of approximately 60 meters (Figure 16).

The facies scale mapping exercise was initiated in order to begin to define the architectural elements of this particular package. A lithofacies map is pres-

Next Page

Figure 16. Photograph of OUTCROP1.

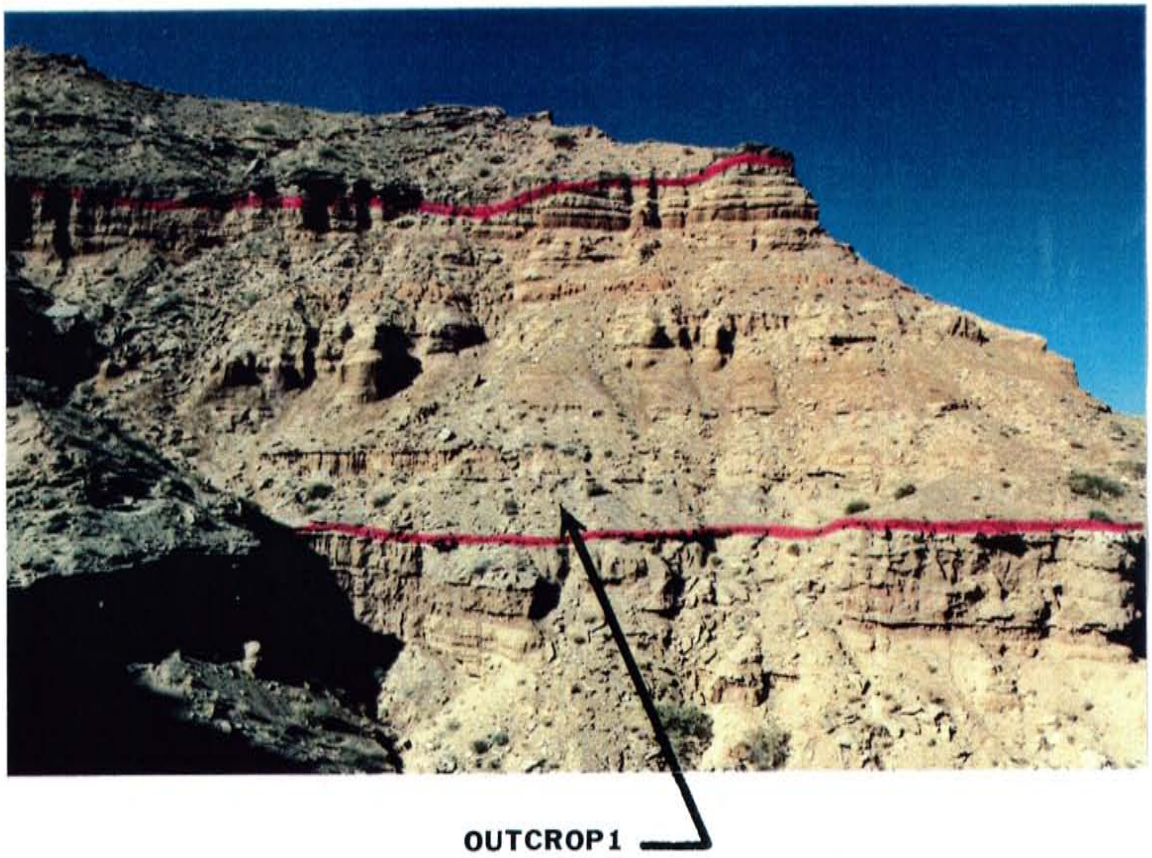
OUTCROP1

ented in Plate 2. Miall's [1978] classification scheme was used as a base for the classification of observed lithofacies. Table 3 summarizes the lithofacies observed during the outcrop study.

Lithofacies Smb, Sfl, and Sm, were added to Miall's [1978] classification. Facies Smb consists of crudely crossbedded sand, sand size clay clasts, and armored mud balls. The basal contact of the Smb facies is commonly erosional. The facies Sfl is a fining upward sand facies. The genesis of the Sfl facies is uncertain; however, their occurrence may represent proximal floodplain deposits. The third addition to Miall's [1978] classification is the facies Sm. The Sm facies is a massive sand in which most or all sedimentary structures have been destroyed. This facies is interpreted as an immature soil.

The amount of spatial detail recorded in the facies scale mapping was restricted principally by the 1:120 scale of the base map. Several lithofacies are actually composites of smaller lithofacies that were lumped together for reasons of feasibility. Those that contain significant sedimentological information have hybrid classifications. For example, the facies denoted Sr/Fm is dominantly a ripple laminated sand facies that contains several laterally continuous mud drapes. Figure 17 shows an example of the Sr/Fm hybrid facies. The mud drapes are not only a distinctive sedimentologic feature, but undoubtedly play a role in the hydraulic characteristics of the unit. This type of small scale heterogeneity currently is being handled with hybrid facies classification.

The paleosol facies occurs commonly in the study area. The paleosols observed in the Sierra Ladrones are generally developed in the non–gravelly type of fabric. They follow the general diagnostic characteristic of having few if any preserved sedimentary structures, a red coloration, and a certain degree of calcium carbonate buildup.

Facies Code	Lithofacies	Sedimentary structure	Interpretation
Gms	massive, matrix supported gravel	none	debris flow deposit
Gm	massive or crudely bedded gravel	horizontal bedding, imbrication	longitudinal bars, lag deposits, seive deposits
Gt	gravel stratified	trough crossbeds	minor channel fills
St	sand, medium to v. coarse, may be pebbly	solitary (theta) or grouped (pi) trough crossbeds	dunes (lower flow regime)
Sp	sand, medium to v. coarse may be pebbl;y	solitary (alpha) or grouped (omikron) planar crossbeds	linguoid, transverse bars, sand waves (lower flow regime
Sr	sand, v. fine to coarse	ripple marks of all types	ripples (lower flow regime)
Sh	sand, v. fine to v. coarse, may be pebbly	horizontal lamination parting or streaming lineation	planar bed flow (l. and u. flow regime
Sl	sand, fine	low angle (< 10) crossbeds	scour fill
Smb	erosional scours with mud balls	crude crossbedding	scour fill
Sfl	sand, v. coarse to fine	fining upward sand sequence	proximal floodplain
Sm	sand, v. fine to v. coarse, may be pebbly	none	immature soil
Sgm	sand, fine to v. coarse, pebbly	none	slumped bank ?
Fl	sand, silt, mud	ffine lamination, very small ripples	overbank or waning flow deposits
Fsc	silt, mud	laminated to massive	overbank deposits
Fm	mud, silt	massive, desiccation cracks	drape deposits
Fr	silt, mud	rootlets	overbank
P	carbonate	pedogenic features	soil

Table 3. Lithofacies observed in OUTCROP1 study

Next Page

Figure 17. (a) Photograph of Sr/Fm hybrid facies. (b) Sketch of mud drapes (Fm) in photograph.

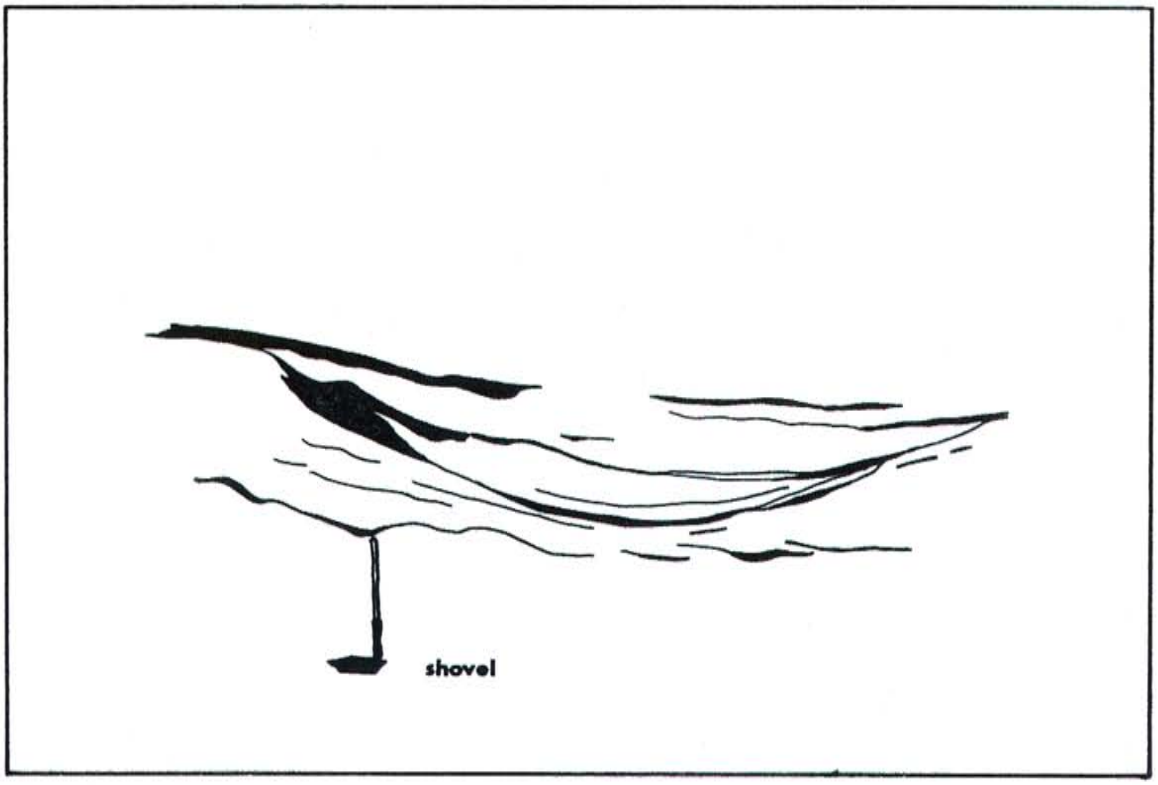
shovel

4.3 Interpretation of Mapping

The geologic interpretation is based on two classes of geologic categorization. The lithologic facies are lumped into architectural elements. The interpretation of the depositional environment is then based on the extent and relationships of the elements. The term element is used rather loosely here since external geometry has yet to be determined. It is likely that more useful elements will be redefined after further data is collected. The facies provide within–element characteristics from which primary processes are inferred.

Four elements have been defined based on the facies map (see Plate 2). These elements are summarized in Table 4 . The channel elements are broken into two types. More elements may be necessary as the study progresses. Additionally, it is likely that the definitions of the four elements observed thus far will be modified as more information is collected regarding their genetic origin. The two distinct types of channel elements preserved in the study area of OUTCROP1 include one that is generally dominated by clean fine–to–coarse grained sandy and gravelly facies, and a second element dominated by sand and sand size clay clasts. The former can be interpreted as the result of a large, distal braided or meandering stream environment. The latter element is dominated by a much finer scale heterogeneity. The common occurrence of sand size clay clasts and armored mud balls indicate that hardened mud drapes were ripped up, broken into sand size clasts, redeposited, and buried in a relatively short distance. The initial mud drapes being the waning flow deposits of the previous flow event indicating an ephemeral flow character. Also small scale (0.1–1 m) scour fill structures have been observed indicating a tributary scale channel.

Element code	Lithofacies present	Description/ Comments
CH–I	Gm, Gt, Sp, St, Sl, Sgm	Channel element consists dominately of gravelly and coarse sand facies. Much of the element is covered by colluvium and will require further study elsewhere.
CH–II	Gms, St, Sp, Sfl, Sh, Sl, Smb, Fl, Fm, Fsc	Sand and sand size clay clasts dominate with local lag gravel deposits.
P	P, Sm, Fsc	Soils and stacked soils
OF	Fr, Fm, Fsc, P	Overbank fines

Table 4. Architectural elements of OUTCROP1

The lowermost occurrence of the CH type–II is probably the most difficult to interpret genetically. Two distinct possibilities exist: 1) a preserved bar deposit of a major channel or 2) a deposit that resulted from a large scale flood event. This CH–II element is dominated by clean planar crossbedded sand with some climbing ripple structures in the lower part and trough cross lamination and ripple lamination in the upper 10–20 centimeters. The basal contact is erosional, cutting into and locally through an overbank fine deposit. The upper contact is sharp. The uppermost CH–II element is also dominated by planar crossbedded sand, and is here grouped genetically with the lowermost CH–II element.

The other occurrences of CH–II are dominated by small scale changes in lithology. The abundance of sand–size clay clasts and armored mud balls imply deposition close to the source. Similarly, the common occurrence of laterally extensive mud drapes are evidence of several flow events. It is hypothesized that the middle two CH–II elements were deposited by an ephemeral small scale channel.

The overbank fine elements (OF) are composed of several distinct overbank deposits. Some of the elements contain weakly to moderately developed, stage I of McGrath and Hawley [1978] (see Table 2) soil horizons. The paleosol elements (P) consist of soil horizons that are generally Stage I–II.

Reconstruction of the depositional environment entails interpreting the relationships and extents of the elements mapped. The paleosol elements are used here as a basis for that interpretation.

Allen [1974] used pedogenic carbonate units to interpret the depositional environment of the Lower Red Sandstone. He constructed a set of conceptual models based on the observation that soil development requires a "substantial

period when its site was denied significant fresh supplies of river–borne clastic sediment" [Allen, 1974; p.190].

As outlined by Allen [1974], the mechanisms of deprivation in a fluvial system include: 1) the migration of the channel away from a site as to deprive that site of channel–borne sediment, 2) entrenchment of the channels so as to deprive sediment to neighboring regions even during large floods, and 3) a combination of (1) and (2).

The models of Allen [1974] adopted here are those that represent lateral–horizontal migration of the channel. Two such migration patterns are postulated. The first represents a pattern of channel migration in which the channel moves continuously, but not necessarily steadily, perpendicular to its course (Figure 18a). This type of migration is referred to by Allen [1974] as a combing type of migration. The second type of migration involves a more sporadic type of channel movement resulting from avulsion events. The hypothetical arrangement of elements is shown in Figure 18b.

The differentiation between the two relies heavily on adequate mapping of profiles normal to the mean paleocurrent direction. At this time the extent of mapping does not allow this differentiation. Therefore, both models are retained here as equally feasible.

The observed architectural elements and the models of Allen [1974] enable an interpretation of the depositional environment. It is hypothesized that the deposits of at least two types of channels are preserved in the study area. From the models discussed, the occurrence of overbank fines and paleosols between these channel deposits indicate a migration of the channel away from its previous position. It is not clear whether the deposits represent an environment in which two distinct types of channels coexisted throughout the depositional history, or

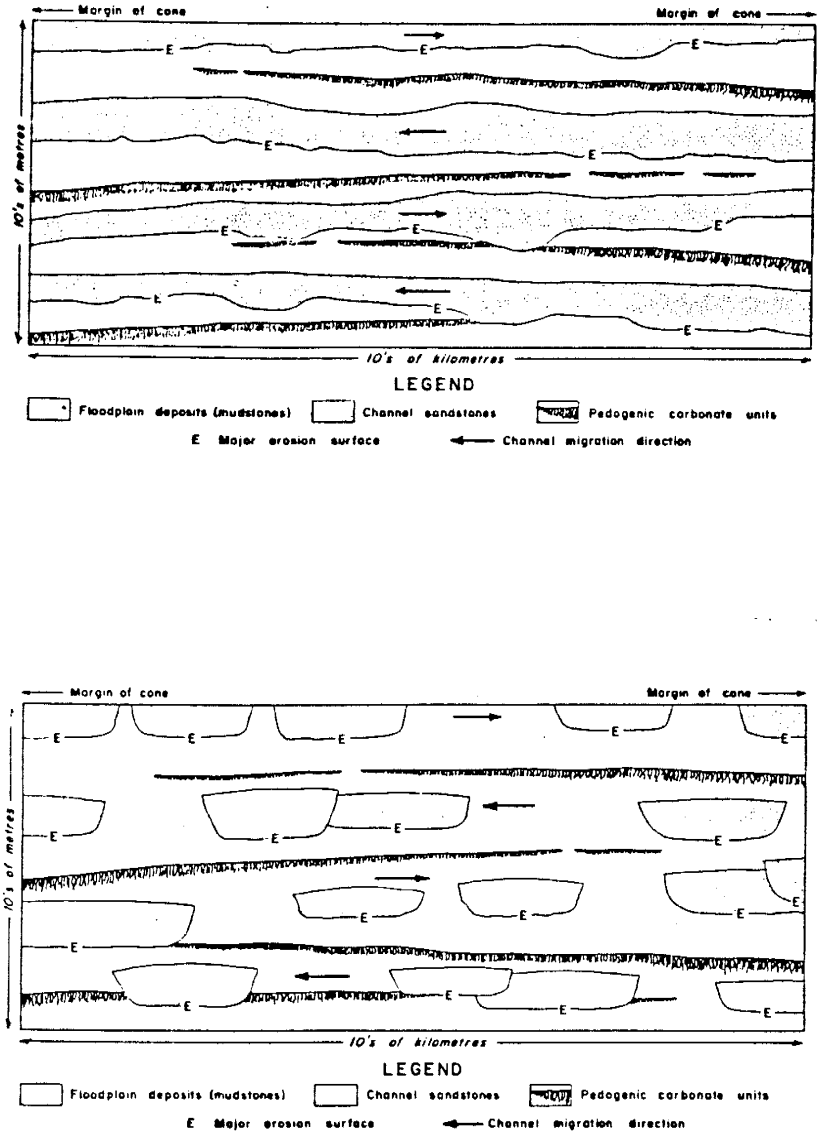

Figure 18. Conceptual depositional models of Allen [1974] based on pedogenic carbonates. (a) Resulting facies association from a steady migration of the channel across alluvial plain (cone). (b) Resulting facies associations from an avulsive type of channel migration across the alluvial plain (from Allen, 1974)

one in which the channel character changed in time.

Continued mapping and interpretation of the architectural elements will be necessary to further determine the depositional environment of this area. The geologic interpretation and reconstruction of a depositional environment is crucial in the description/prediction of lithologic distributions and ultimate characterization of aquifer heterogeneity. It is but a piece of the puzzle in the characterization of large scale heterogeneity; however, it is a first step in the application and subsequent evaluation of the methodology presented above.

CHAPTER 5: Data Analysis and Interpretation

5.1 Introduction

As discussed in Chapter 2, empirical studies of permeability patterns must be pursued in order to better understand and predict heterogeneity of natural geologic material. From the field site in the Sierra Ladrones Formation described in Chapter 4, two small scale studies of permeability distributions have been performed. In addition, a numerical experiment has been performed to evaluate the statistical structure of the facies map of OUTCROP1 (Plate 5).

There are four objectives of the statistical analysis. The first is to empirically estimate the first two moments of the permeability joint probability density function. The second objective is to relate the estimated statistical parameters to the observed geologic features. This is a necessary step in validating the hypothesis that statistical parameters can be estimated via geologic observations. The third objective is to assess the scale dependence of the statistical parameters. That is, to study the problem of heterogeneity and spatial correlation at a variety of scales in order to determine how multiple correlation structures may be estimated based on the dimensions of the geologic entities. Finally, the fourth objective of the analysis is to address the question: "How can geologic information be used to quantitatively predict the spatial statistics of permeability over a broad

range of scales?"

The purpose of statistical analysis is to estimate the statistical properties of a random variable. In our case the random variables are permeability and air flow rate (surrogate to permeability). The methods of estimating the first two moments are those commonly used in geostatistical analysis. Namely, histograms and empirical distribution functions are used to estimate the distribution of a random variable, and variograms are used to estimate the correlation structure.

Three data sets are analyzed in this chapter. The first two data sets are the result of heterogeneity studies at the facies scale. They both consist of air–flow–rate data measured with the air–minipermeameter at small outcrops located at the field site. For each data set, analyses of the distribution statistics and structural statistics are performed. The third data set results from an effort to study the structural statistics of the intermediate scale heterogeneity. The facies map (Plate 2) was used as a basis. Mean permeability was then estimated based primarily on grain size and assigned to each facies present. Variogram analysis of the assigned mean values is presented and discussed.

5.2 Small Scale Permeability Studies

5.2.1 Permeability study 1 (PS1)

The location referred to here as PS1 is located at the Bosque field site (Figure 12). The prepared outcrop is approximately 2 meters wide and 0.5 meters high (figure 19). Plate 3 illustrates the geologic features and sampling locations. The outcrop appears to be a channel bar deposit dominated by a horizontally laminated coarse sand deposit. On top of what appears to be the major bar form, a variety of lithofacies are present. Horizontally laminated fine to medium sands including magnetite and/or illmenite are interbedded with clay drapes,

Next Page

Figure 19. Photograph of PS1 outcrop.

trough cross–laminated sands and ripple–laminated sands. This upper third of the outcrop is interpreted as representing a period of decreased, periodic flow. Two bioturbated zones which destroy the lateral continuity of the primary deposits were also observed and mapped. Each of the disturbed zones terminate upward at different stratigraphic locations indicating at least two periods of relative quiescence.

The outcrop studied represents a small percentage of the overall deposit. That is, the deposit has a larger vertical and a much larger lateral extent than the sample space dimensions. Two–hundred and seventy–seven measurements of air flow rate were obtained from this outcrop.

A histogram of the original data indicates a skewed right distribution (Figure 20a). After performing a natural logarithm transform of the original data, the logarithmic data appear to be normally distributed (Figure 20b). Comparison of the empirical cumulative distribution function of the logarithmic data with the theoretical normal curve and applying the Kolomogorov–Smirnov test further support the log–normality hypothesis. The results of the Kolomogorov–Smirnov test showed a maximum observed difference between the empirical cumulative distribution and the theoretical normal curve of of 0.04. With 277 data points and a 0.20 significance, the Kolomogorov–Smirnov maximum difference tolerance is 0.06 (Figure 21).

Structural analysis via directional variogram estimation was also performed on the logarithmic data set. The horizontal variogram is presented in Figure 22. A common "rule of thumb" in variogram estimation is to use separations (lags) up to approximately half of the sample space dimension [Journel and Huijbregts; 1979]. As such, the variogram estimate was truncated at a lag of 160 centimeters. A sufficient number of pairs for most lag classes (see Figure 22) as

(a) Histogram of original data

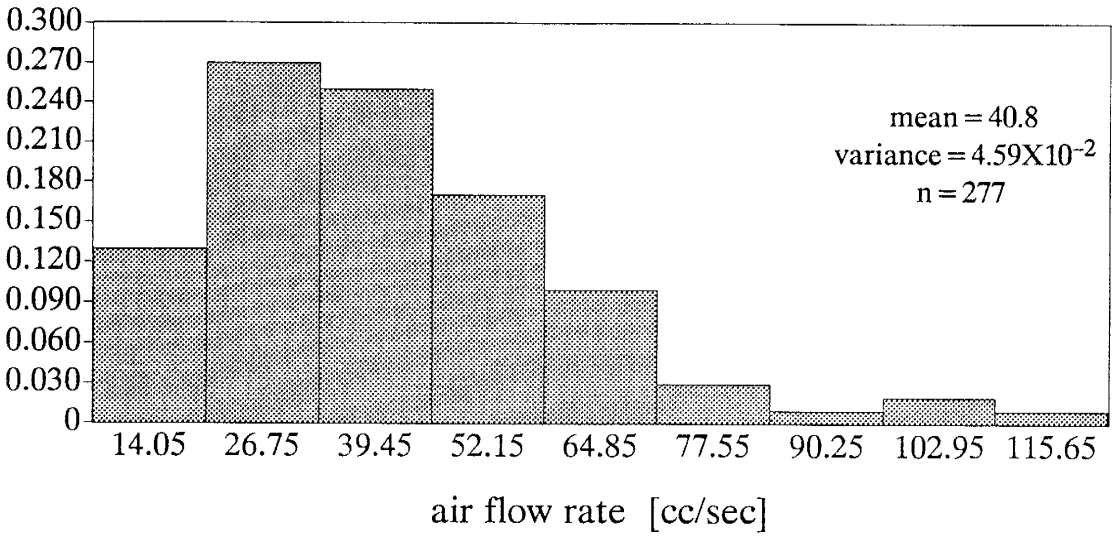

(b) Histogram of logarithm data

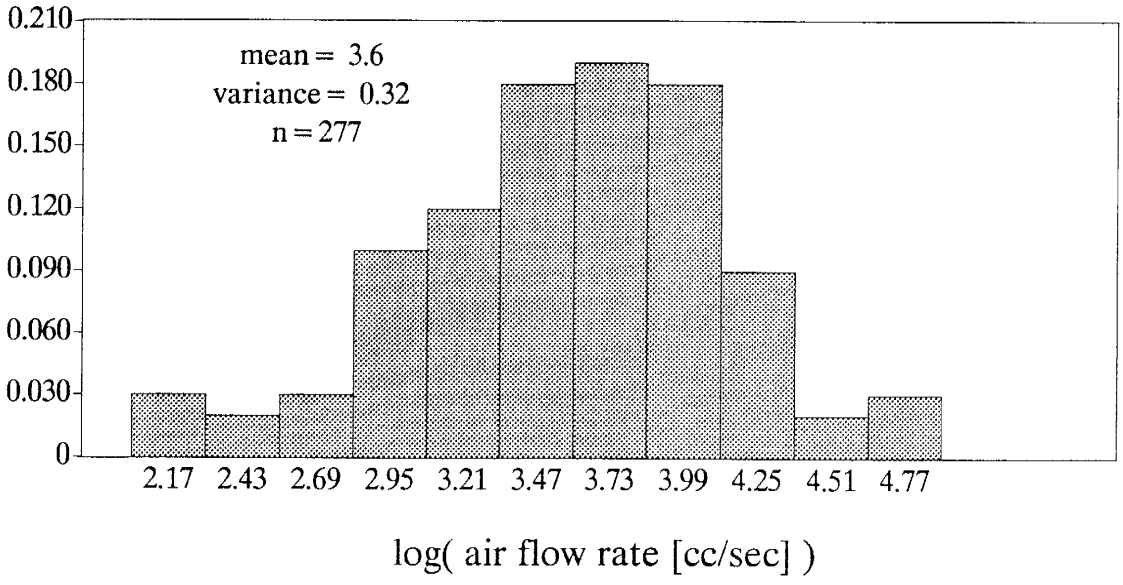

Figure 20. Histograms of PS1 air-flow-rate data.
(a) Histogram of original data.
(b) Histogram of logarithmic data.

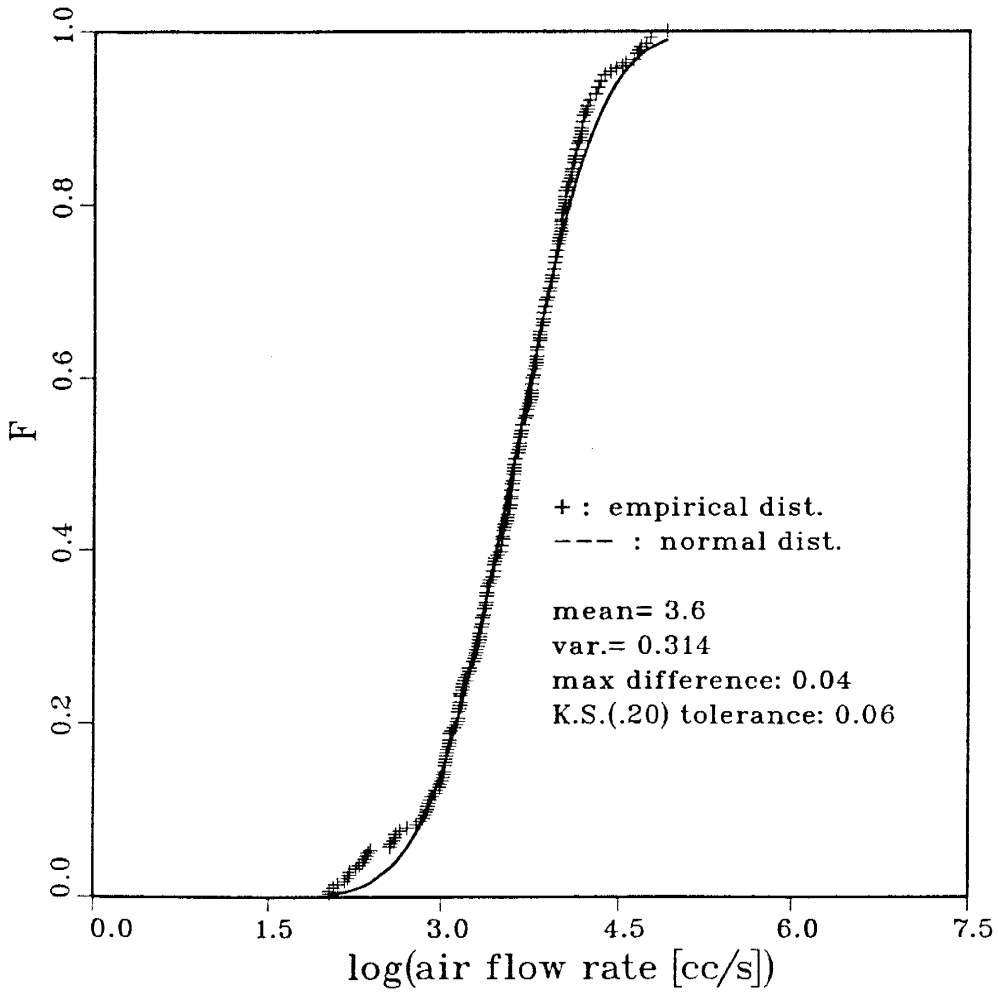

Figure 21. Comparison of cumulative emperical distribution and theoretical normal distribution of PS1 logarithmic data (N=277).

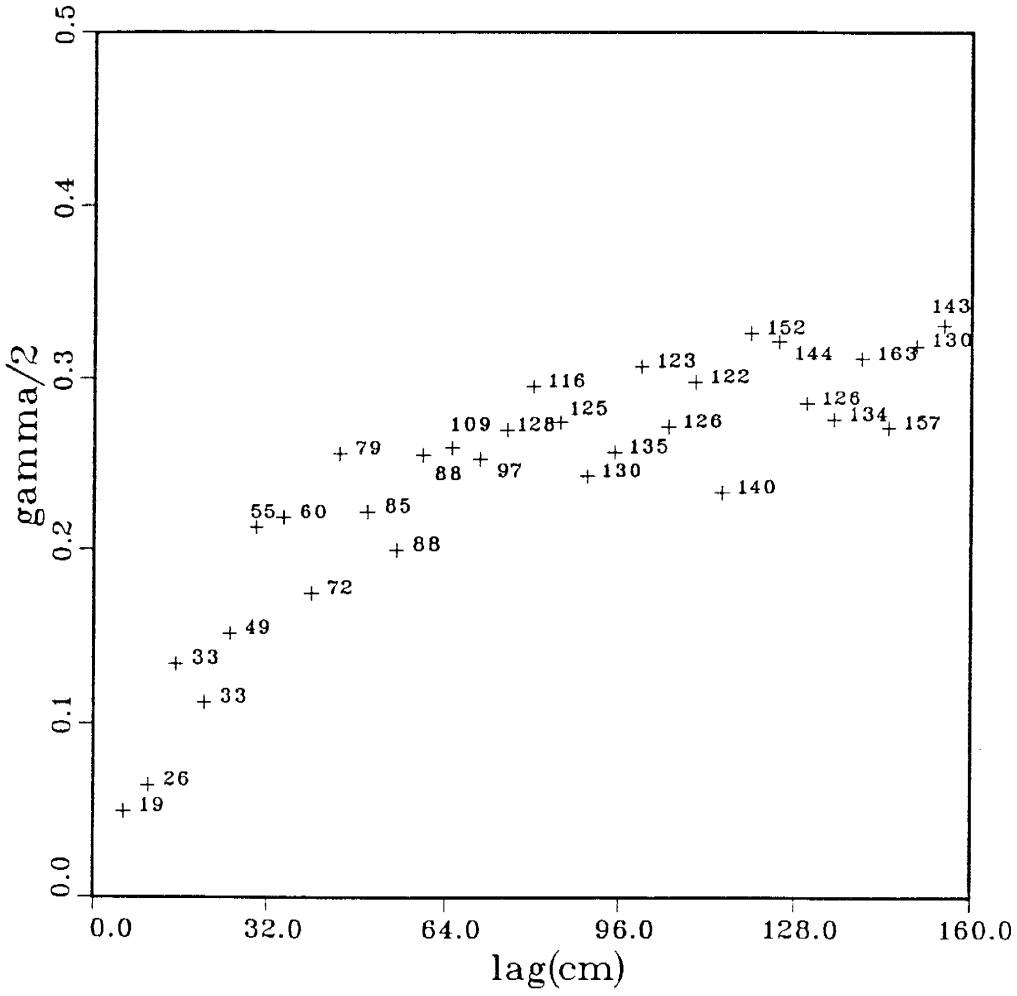

Figure 22. Horizontal variogram estimate of PS1 logarithmic data. Number of pairs for each lag are shown next to plotted variogram estimate. Variogram output is given in Appendix D.

well as a relatively smooth variogram encourages the fitting of a variogram model. An exponential variogram model with a slight nugget is used here to fit the variogram estimate (Figure 23). The fitted model is:

$$\gamma(\xi) = 0.04 + 0.27[1 - e^{(-|\xi|/40)}]$$

The nugget of 0.04 may be attributed to the experiment error associated with the air permeameter. The range of approximately 40 cm. may correspond to the approximate separation of the bioturbation zones; however it will be necessary to conduct many more studies of similar nature to better understand the geology behind the correlation statistics.

The estimated vertical variogram is shown in Figure 24. Unlike the horizontal variogram, it is not feasible to fit a model to the vertical variogram estimate for two primary reasons. The first is that there is not a sufficient vertical sample space dimension to ensure proper estimation. The sampled vertical dimension is approximately 60 centimeters, the vertical variogram model should then be based on values for lags up to approximately 30 centimeters which yields three points each of which contain an insufficient number of pairs. Increasing the lag in the variogram estimation may enhance the number of pairs for each lag, however increasing the lag decreases the total number of points calculated for the variogram estimate. This would result in even fewer points to fit a model to.

The second reason fitting a model is not feasible is that cursory data analysis indicates a possible trend in the mean in the vertical direction which could result in erroneous variogram estimates. The deposit consists of horizontally laminated coarse sands near the base of the outcrop. The sands then tend to fine

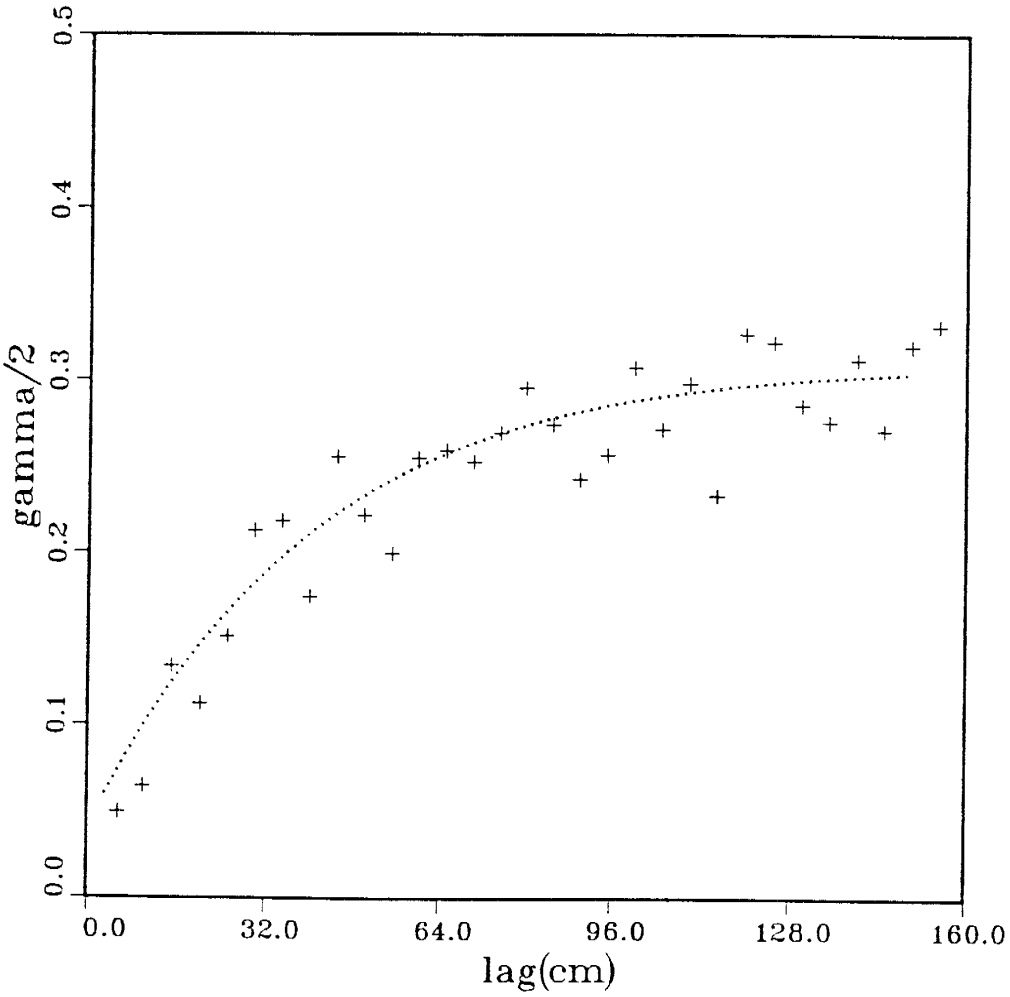

Figure 23. Exponential model fit to the horizontal variogram estimate of PS1 logarithmic data.

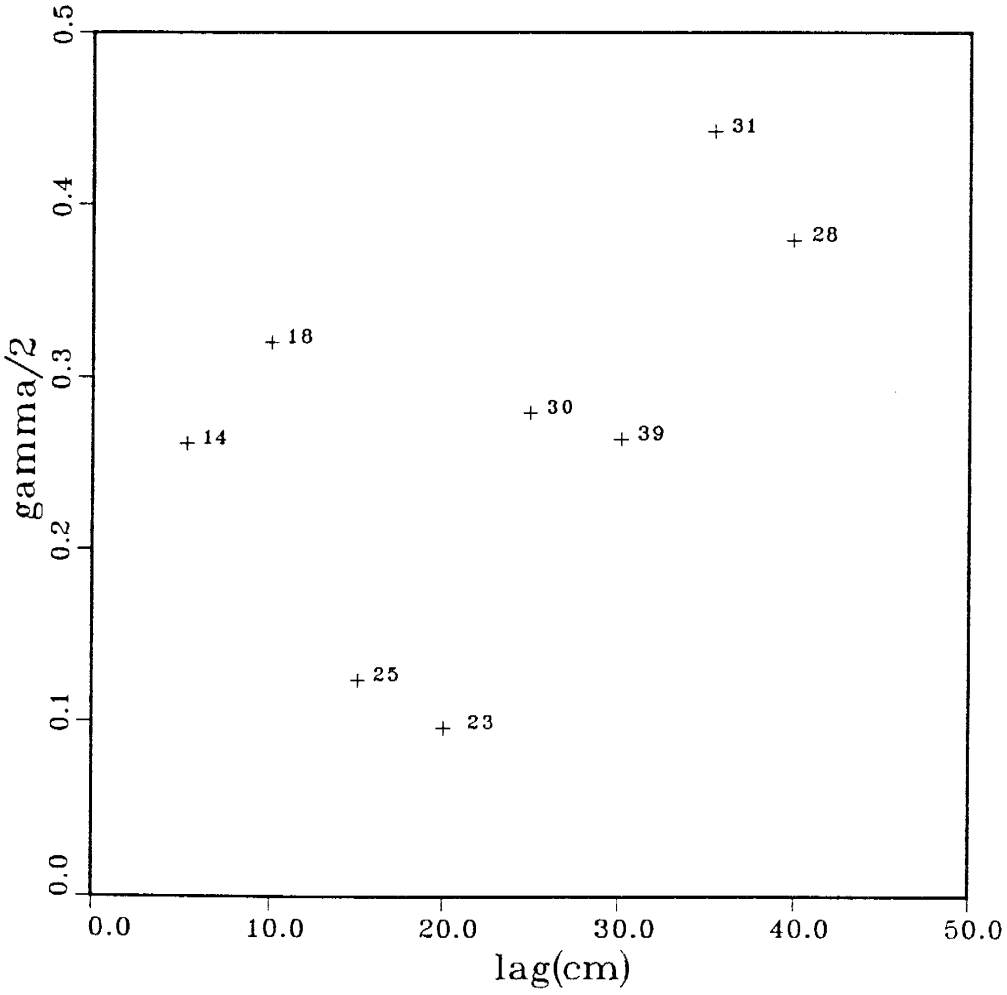

Figure 24. Vertical variogram estimate of PS1 logarithmic data. Number of pairs for each lag are shown next to plotted variogram estimate. Variogram output is given in Appendix D.

upward in the vertical direction into horizontally–laminated, trough–cross–laminated and ripple–laminated medium to fine sands. As will be discussed in Section 5.2.3, the general decrease in grain size warrants concern. Future work with trend analysis as well as increased sampling in the vertical direction will need to be conducted in order to obtain better estimates of the vertical correlation structure.

5.2.2 Permeability study 2 (PS2)

The second outcrop studied (PS2) is located in the lower channel element (type CH–I) of Plate 2. PS2 is approximately 1.5 meters wide and 0.5 meter high (Figure 25). The outcrop can be characterized as a high energy channel deposit with crudely stratified to cross–stratified pebbly gravel interbedded with low angle cross–laminated and trough cross laminated fine to coarse sand (see Plate 4). A zone of ripple laminated sand occurs at the top of the outcrop representing a decrease in flow energy.

As opposed to PS1, PS2 represents approximately 80 percent of a depositional unit. That is, the spatial dimensions of the sample space approximate the spatial dimension of the deposit. Eighty six measurements of air flow rate were obtained from PS2, the locations of which are shown on Plate 4. Again, histogram analysis of the original data indicate a skewed right distribution. The natural logarithm transform was applied resulting in an apparent normal distribution (see Figures 26a and 26b). Applying the Kolomogorov–Smirnov test, the maximum observed difference between the empirical cumulative and the theoretical normal is 0.07. The Kolomogorov–Smirnov 0.20 signigicance tolerance for 86 points is 0.12. Again this implies the data is normal distributed (Figure 27).

Directional variogram analysis was performed on the logarithmic data in

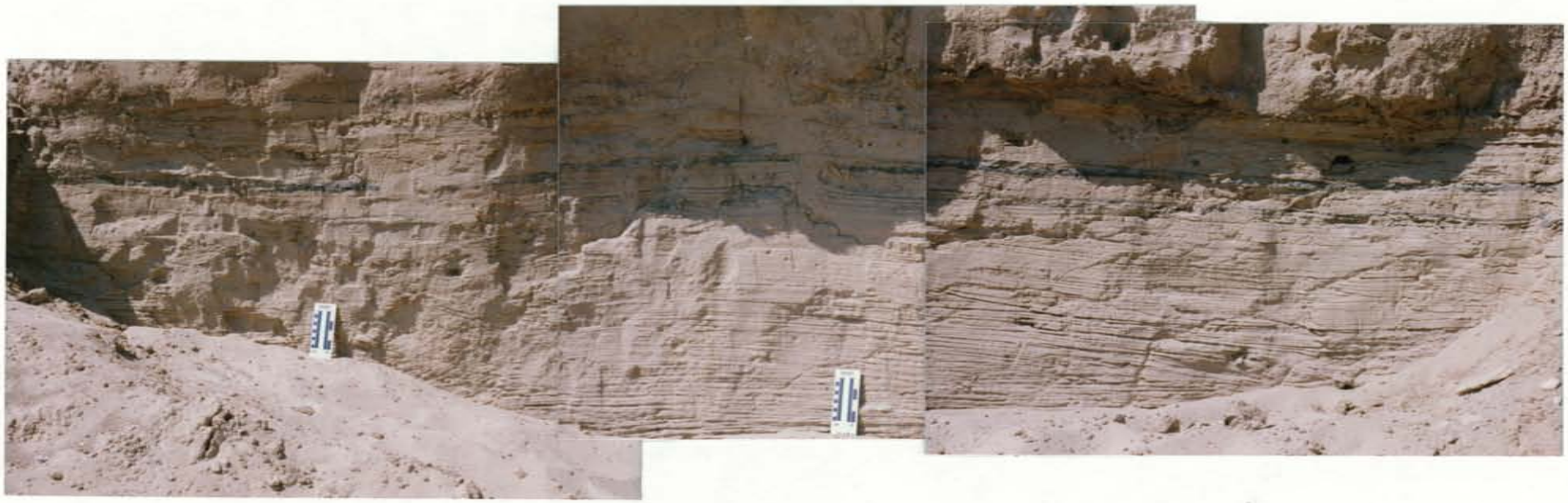

Next Page

Figure 25. Photograph of PS2 outcrop.

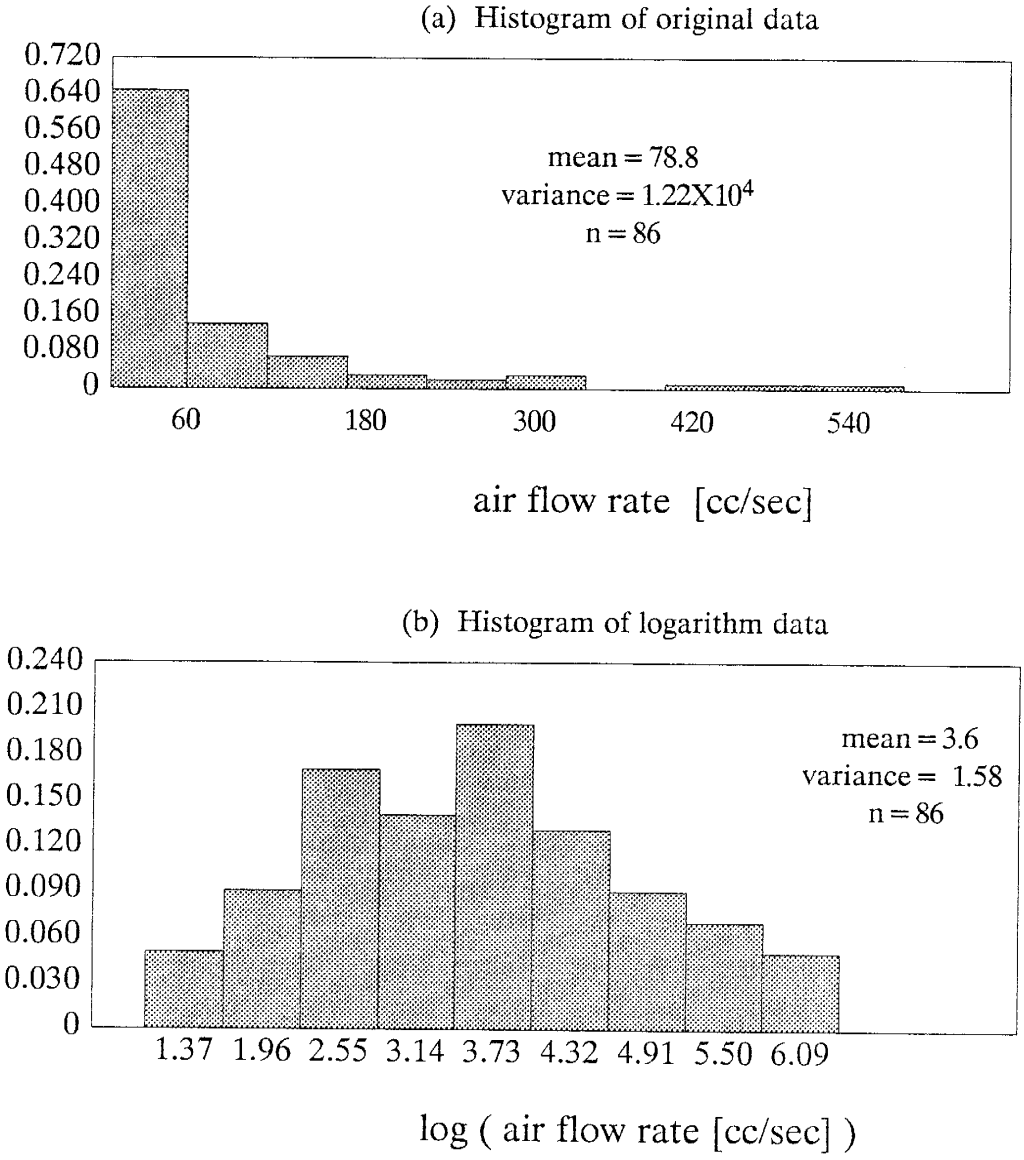

Figure 26. Histogram of PS2 air-flow-rate data.
(a) Histogram of original data.
(b) Histogram of logarithmic data.

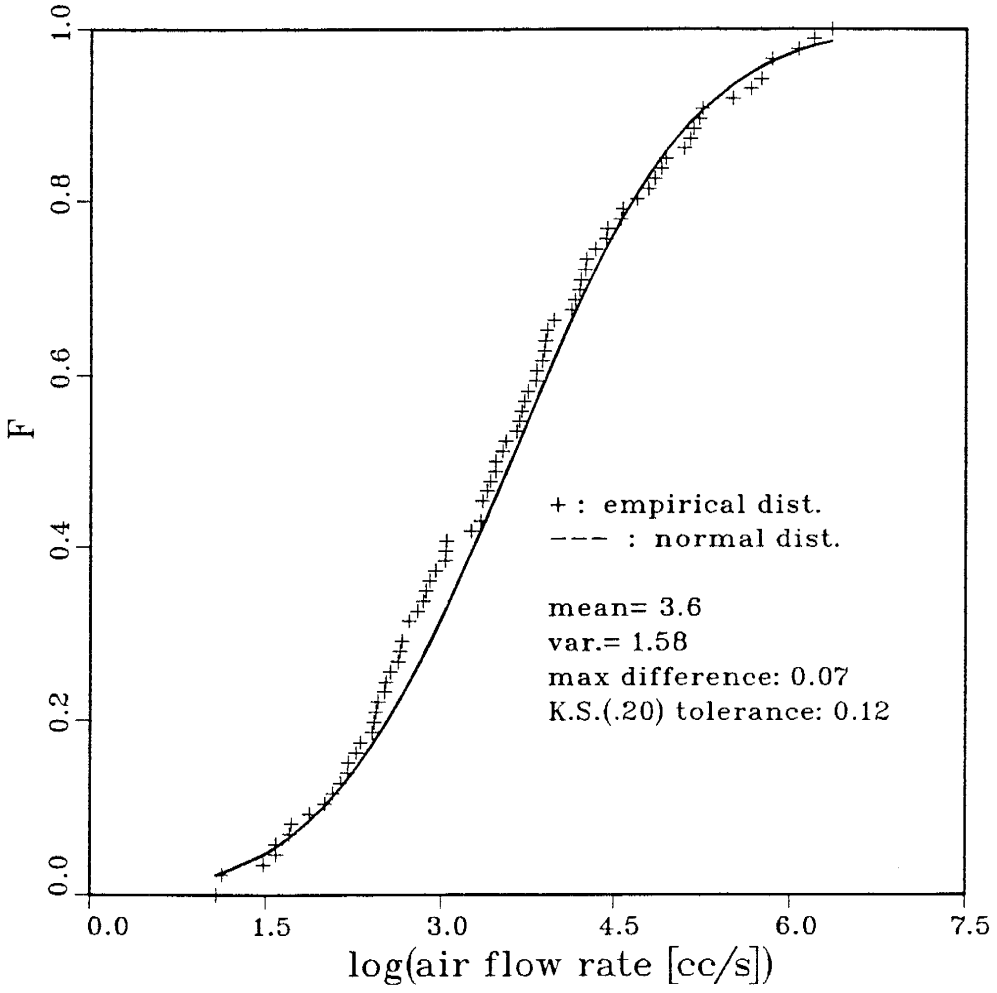

Figure 27. Comparison of cumulative emperical distribution and theoretical normal distributon of PS2 logarithmic data (N = 86).

order to estimate the correlation structure. The horizontal variogram estimate is shown in Figure 28. Initially, the resulting estimate appears to be linear with sufficient numbers of pairs for most lags. However, truncating the variogram for lags greater than approximately 85 centimeters (half of the sample space dimension) results in what appears to be either an exponential or bell-shaped (Gaussian) variogram. Both types of models were fit by eye to the variogram estimate and are presented in Figure 29. Functionally they are given by:

Exponential model:

$$\gamma(\xi) = 1.24[1 - e^{(-|\xi|/60)}]$$

Bell-shaped (Gaussian) model:

$$\gamma(\xi) = 0.07 + 0.90[1 - e^{(-(|\xi|/45)^2)}]$$

Again the nugget in the bell-shaped model may be attributed to the experimental error associated the air permeameter. The fitting of two variogram models to the PS2 horizontal variogram estimate makes interpretation difficult. The correlation lengths of 45 and 60 centimeters both appear to correspond with the average horizontal dimension of the gravelly facies. As with PS1, many more studies of similar nature will need to be conducted in order to better understand the correlation between mappable geologic units and statistical parameters.

The estimate of the vertical variogram is presented in Figure 30. As with the vertical variogram estimate of PS1, geologic observations indicate the possibility of a trend in mean in the vertical direction. The deposit consists of gravels, pebbly sands, and coarse sand near the base. These coarse-grained sediments then tend to fine upward into trough cross-laminated and ripple laminated me-

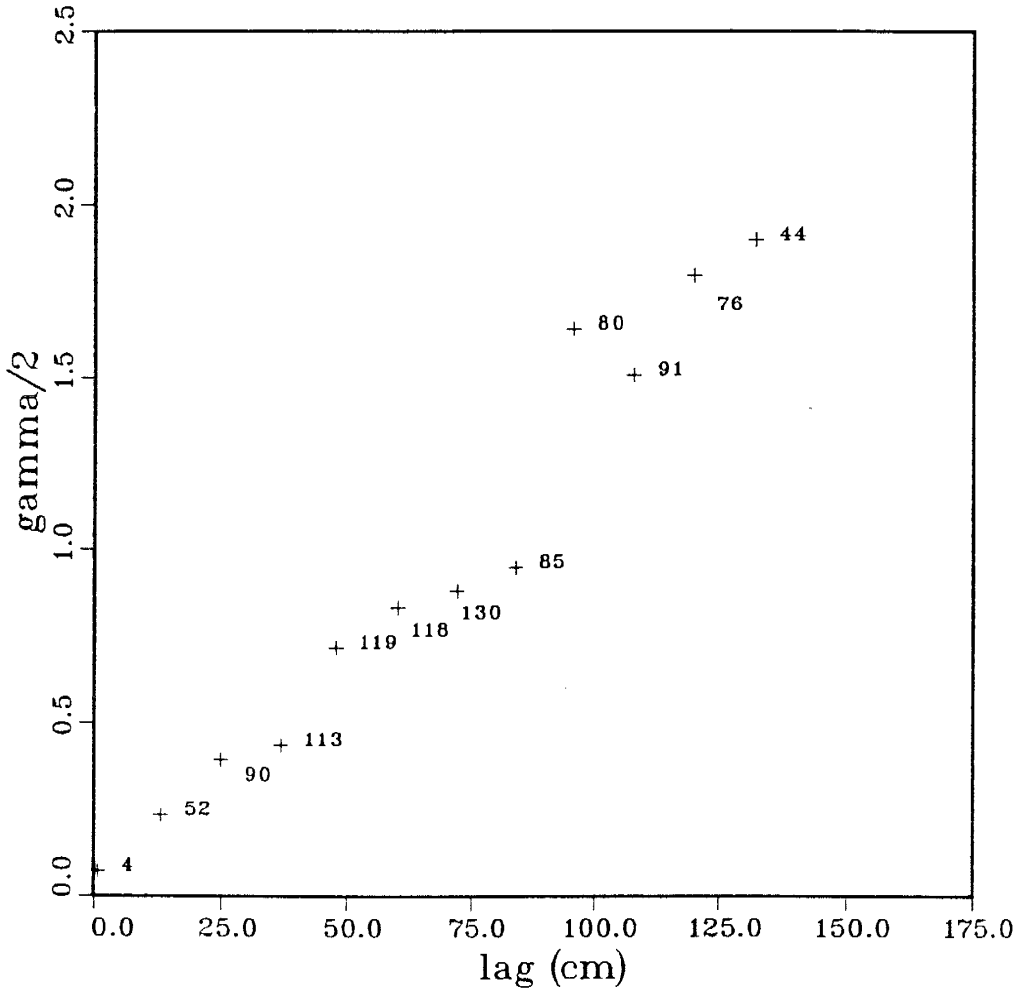

Figure 28. Horizontal variogram estimate of PS2 logarithmic data. Number of pairs for each lag is shown next to plotted variogram estimate. Variogram output is given in Appendix D.

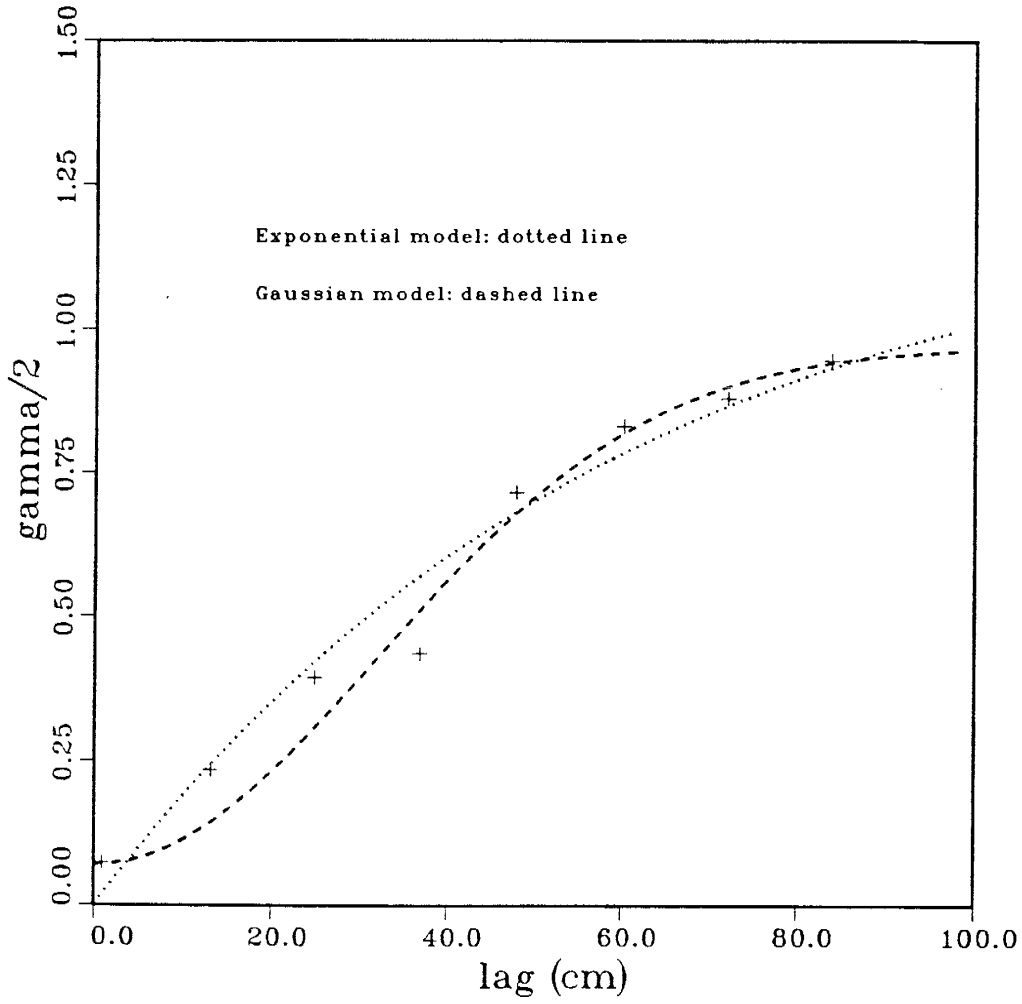

Figure 29. Exponential and Bell-shaped (Gaussian) models fit to the horizontal variogram estimate of PS2 logarithmic data.

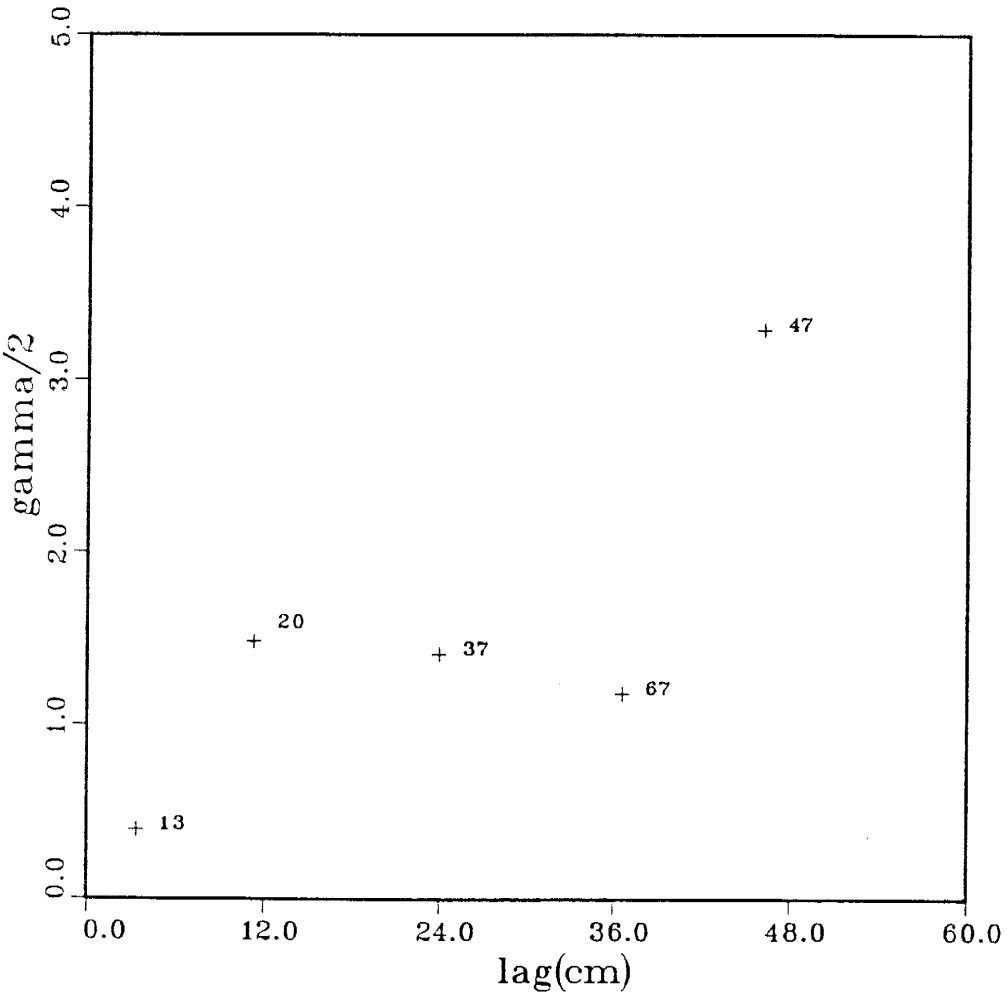

Figure 30. Vertical variogram estimate of PS2 logarithmic data Number of pairs for each lag are shown next to plotted variogram estimate. Variogram output is given in Appendix D.

dium and fine sands. Again, as with PS1, trend analysis is not considered feasible given the insuficient dimension of the vertical sample space dimension.

Comparing the structural statistics of the PS1 and PS2 data, it is interesting to note that it is possible to fit an exponential model to both the data sets even though the underlying geology is vastly different. In both studies of statistical structure of air–flow–rate, the horizontal correlation lengths appear to correspond with the observed mappable geologic features. However, further work will needed to be pursued in order to be able to estimate the correlation structure based on geologic features.

The two studies presented above represent the facies scale heterogeneity resulting from changes in lithology within a depositional unit. Even though the architectural element definitions have yet to be robustly determined, the two outcrops studied thus far can be considered with confidence to each be within a respective architectural element.

5.2.3 Distribution studies

In addition to studying the distributions of each sample set as a whole population, distributional analysis has also been carried out based on grain size classes within sample sets. Each sample set consists of four distinct grain size classes. The PS1 study was conducted in what is believed to be a channel bar deposit; the observed grain size classes are fine, medium, and coarse grained (see Plate 3.). The fourth grain size category which will not be analyzed in detail here is that of the bioturbated sands which is a mixture of several different grain sizes. The PS2 study was conducted in a channel deposit consisting of grain sizes that range from fine to pebbly sands with some gravels (Figure 25 and Plate 4). As eluded to above in Section 3.3, the clast supported gravels cannot be sampled

with the air permeameter. As such, the clast supported gravels were not sampled and therefore are not included in the grain size

The PS1 sample set consists of three principle grain–size classes as well as bioturbated sands which, due to churning by organisms, are a mixture of several grain sizes. Distributional analysis of the air flow rate data for each of the three principle grain size classes reveals that each class is approximately log–normal and exhibit distinctively different means. The results of the distribution analyses are presented in Figure 31 and summarized in Table 5 .

The PS2 data consists of four principle grain–size classes: fine, medium, coarse, and pebbly. Distributional analysis of the air flow rate data for each grain–size class is presented in Figure 32 and summarized in Table 5.

While delineating permeability according to grain size is common in the hydrologic sciences [e.g. see Carmen 1939; Freeze and Cherry, 1979; Milne–Home and Schwartz, 1989], study of the distributions of permeability according to grain–size classification may contribute additional proxy information in the estimation of permeability in natural geologic material. Recall that the primary goal is to supplement "hard" permeability measurements with "soft" geologic information. Grain size is an example of "soft" information.

One possibility for incorporating grain size information into the statistical analysis is using the distribution of permeability based on grain size to supplement "hard" permeability data taken from a region. Using an indicator approach it is possible to incorporate prior information such as cumulative distribution functions into the estimation of permeability [Journel, 1989].

Another possibility may be to incorporate geologic information on how different grain sizes are spatially distributed throughout a deposits in order to better estimate the behavoir of the mean. Knowing the distribution of the per-

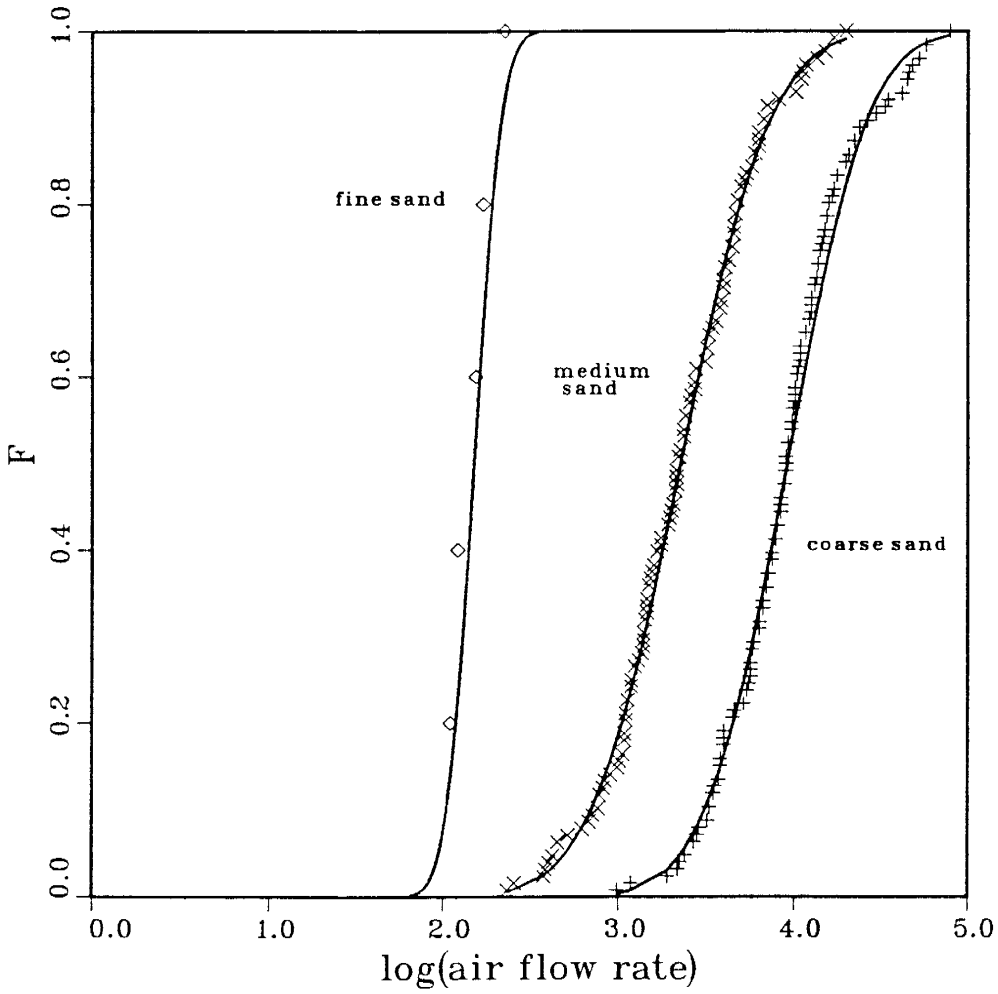

Figure 31. Comparison of empirical distribution functions of air–flow–rate data based on grain size classification for the PS1 logarithmic data.

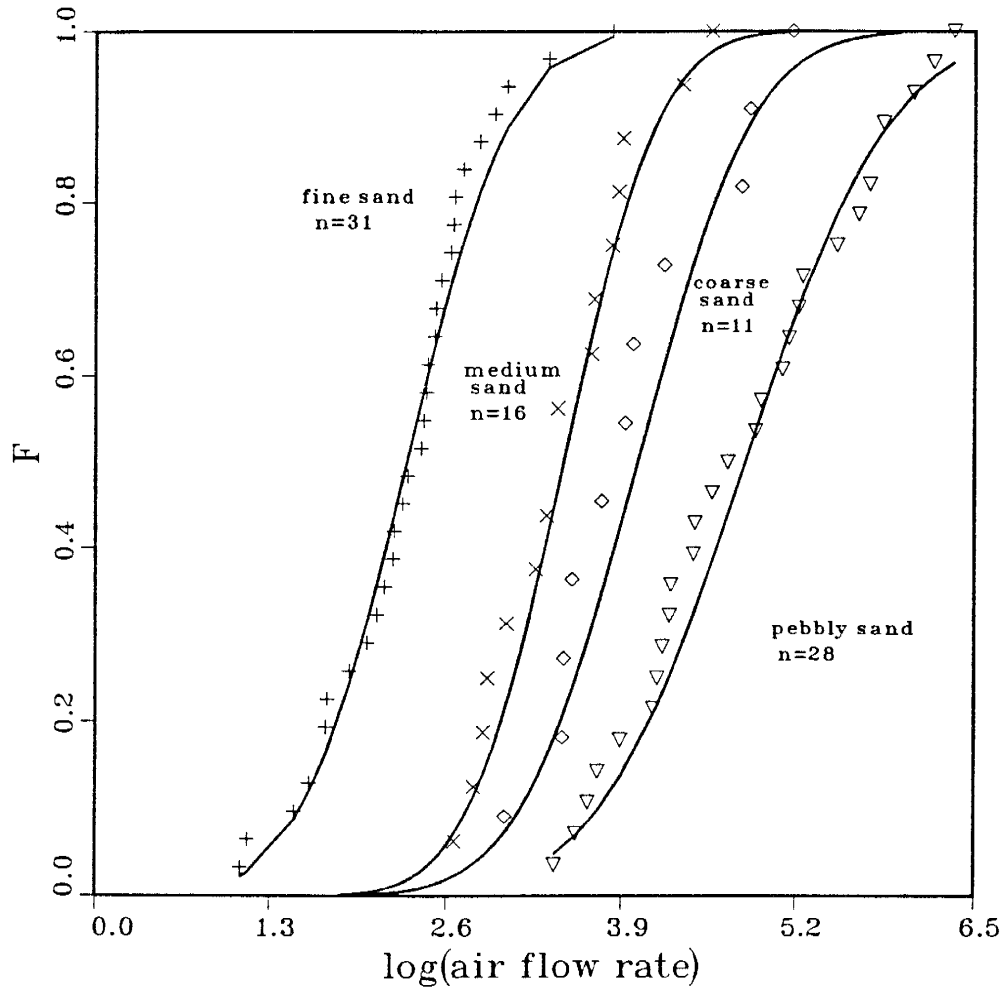

Figure 32. Comparison of empirical distribution functions of air–flow–rate data based on grain size classification for the PS2 logarithmic data.

PS1		Statistical Moments				Kolmogorov – Smirnov Stats	
Grain size	n	mean	variance	kurtosis	skewness	max|diff|	Tolerance
fine	5	2..172	$1.41X10^{-1}$	-1.820	0.2015	0.1806	0.6082
medium	128	3.351	0.1574	-0.240	$-1.067X10^{-2}$	$3.71X10^{-2}$	0.1202
coarse	126	3.956	0.1307	0.1511	0.2053	$6.05X10^{-2}$	0.1202
burrowed	18	2.811	0.3451	-1.407	0.2650	0.2029	0.3206

PS2		Statistical Moments				Kolomogorov – Smirnov Stats	
Grain size	n	mean	variance	kurtosis	skewness	max|diff|	Tolerance
fine	31	2.303	0.3675	$-9.33X10^{-3}$	$6.487X10^{-2}$	0.0845	0.2443
medium	16	3.467	0.3037	-0.9840	0.3234	0.09843	0.3400
coarse	11	4.015	0.4561	-1.333	0.3483	0.1567	0.4101
pebbly	28	4.820	0.7258	-1.220	0.1048	0.1022	0.2570

Mean Flow Rate Values for Different Grain Size Classifications

Data Set	fine	burrowed	medium	coarse	pebbly
PS1	2..172	2.811	3.351	3.956	
PS2	2.303		3.467	4.015	4.820
PS1 & PS2	2.285	2.811	3.365	3.961	4.820

Table 5. Summary of permeability distribution statistics for populations based on grain size classifications.

meability for a given grain size, may enable us to delineate between a trend of a mean and random fluctuation about a mean. Say for instance, a variogram estimate is desired for a fining upward sequence as we encountered with PS1 and PS2. Knowledge of the spatial distribution of grain sizes in a deposit will enhance our understanding the spatial distribution of mean. When performing trend analysis on data, it is always important to have a physical justification for the fitted trend model. Further study of permeability according to grain size and how the spatial patterns of grain size in sedimentary deposits may enhance our ability to predict trend patterns in sedimentary deposits.

5.3 Intermediate Scale Permeability Studies

A study was conducted to estimate the spatial statistics of the permeability at a larger scale. The study maintains the lithofacies distinction as a basis of analysis. Conceptually, this study is a numerical experiment studying the spatial distribution of the mean values of different regions. The utility in such an experiment lies in the ability to obtain large numbers of "measurements" so a structural analysis can be performed. This study is not intended to replace a study using actual measured values, rather to help direct the study and give a preview of what we may expect to see at the larger scale.

The lithofacies observed at OUTCROP1 were broken into four classes based on lithology and approximate permeability. The permeability estimates of Freeze and Cherry [1979; p.29] were used to estimate log–permeability of the observed lithologies. The resulting categories are shown in Table 6.

The facies map presented in Chapter 4 was analyzed on a 60 centimeter by 60 centimeter grid (map scale). For each digitized location (2159 total), the facies at that location was recorded and an approximate log permeability value

Lithofacies	Approxiamte mean permeability [darcy]	log(k)
Gms Gm Sgm	10^3	3
Sp Sl St Sh	10	1
Sr Sr/Fm Sm P	10^{-1}	–1
P(clay) Fl Fsc Fr Fm	10^{-3}	–3

Table 6. Mean log permeability estimates used in intermediate scale study

(from Table 6) assigned. Plate 5 shows the distribution of assigned mean log permeabilites. Variogram analysis of the location and approximate ln(k) values was performed.

With 2159 samples, the variograms can be considered exhaustive and attempts at modelling the variability should be pursued. The results of the vertical and horizontal directional variograms are presented in Figures 33 and 34. It was found that both directional variograms exhibit a hole effect, which represents a positive correlation at some finite distance.

The vertical variogram appears to be strongly periodic. As such, a sine function was used to model the variogram. The fitted function is:

$$\gamma(\xi) = \begin{cases} a|\xi| & \text{for } \xi < 2.45 \text{ meters} \\ 2.5 + 0.65cos(\pi + \xi) & \text{for } \xi \geq 2.45 \text{ meters} \end{cases}$$

The wavelength of the variogram model is 2π (6.28) meters which appears to corresponds to the average repeatability of the facies.

The shape of the horizontal variogram while exhibiting a slight hole effect also exhibits properties of an exponential model. After Journel and Huijbreghts [1979], the variogram model for the horizontal variogram is based on the product of the exponential and cosine covariance functions. A nested structure is also apparent in the horizontal variogram. This is modeled by adding an additional variogram model to the original one for all lags greater than the break (h = 17.5 meters). The resulting model is:

$$\gamma(\xi) = \begin{cases} \gamma_1(\xi) & \text{for } \xi < 17.5 \text{ meters} \\ \gamma_2(\xi) & \text{for } \xi \geq 17.5 \text{ meters} \end{cases}$$

where

$$\gamma_1(\xi) = 1.5[1 - e^{-\xi/3.3}\cos(0.3\xi)]$$
$$\gamma_2(\xi) = \gamma_1 + 0.7\gamma_1(\xi - 17.5)$$

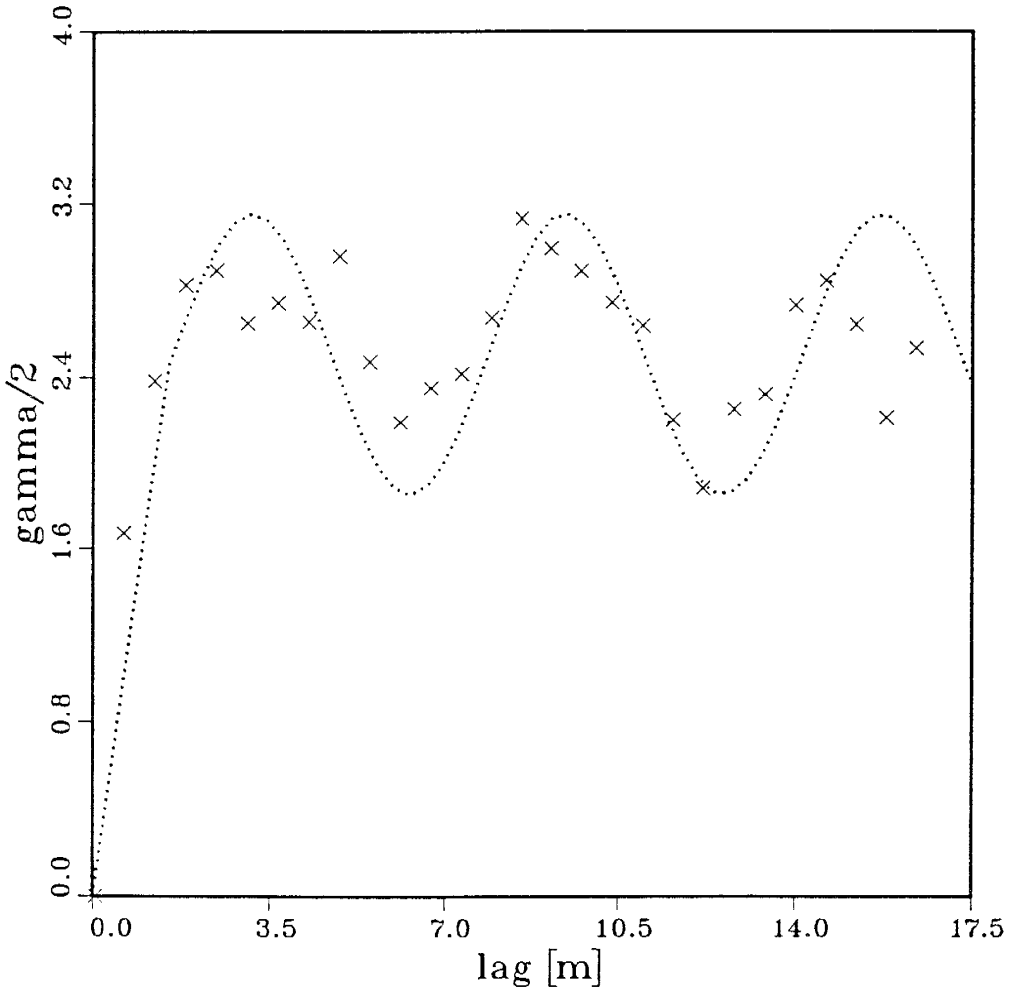

Figure 33. Intermediate scale study vertical variogram estimate (x's) fitted with a linear/cosine variogram model (dotted line). See text for variogram function.

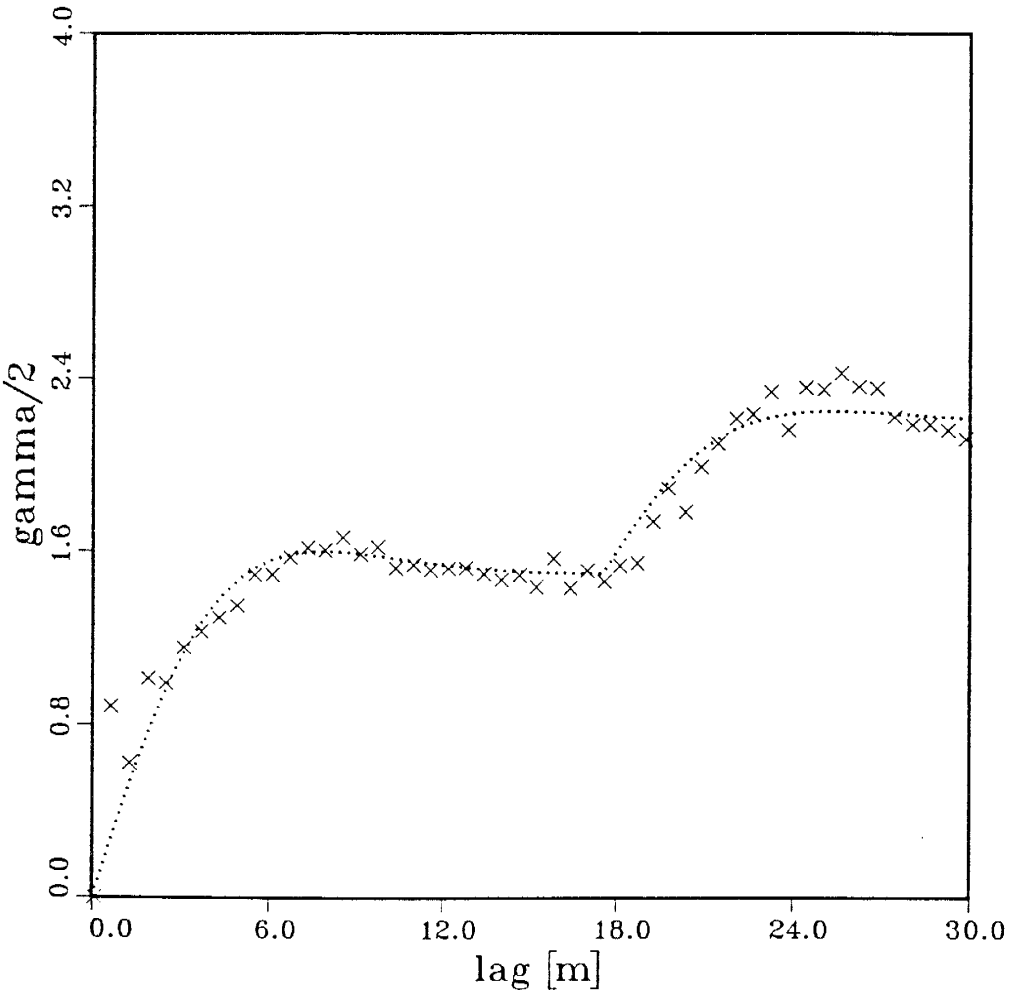

Figure 34. Intermediate scale study horizontal variogram estimate (x's) fitted with exponential/cosine variogram models (dotted line). Note nested structure. See text for variogram function.

The ranges associated with the horizontal variogram models are approximately 3.3 meters for the first (gamma1) structure and 21 meters for the second (gamma2) structure. The first range is can be related to the smallest average lateral dimension of the facies. While there is no compelling geologic evidence for the second range, it is most likely the result of subtle changes in bed thickness.

Both directional variogram models were fitted by trial and error to the experimental variograms. While more sophisticated fitting techniques may be pursued in the future, the trial and error method was preferred with the limited amount of data thus far obtained. Discussion of the analysis will be presented in the next chapter.

CHAPTER 6: Discussion & Conclusions

6.1 Discussion

In order to arrive at more realistic quantifiable characterizations of aquifer heterogeneities, it has been suggested that a variety of information be incorporated into the characterization process. On the hypothesis that there exists a quantifiable correlation between permeability patterns and geology, it has been suggested that realistic characterization may be accomplished by incorporating "soft" geologic information. In light of the fact that aquifer characteristics can never be entirely determined, the probabalistic interpretation of aquifer properties has been proposed.

Concepts of basin analysis and geostatistics have been discussed in hope that they provide us quantifiable parameters. The method of variogram analysis has been discussed and employed as a means to estimate correlation structure of specific permeability fields. Preliminary analysis of the methods used and data collected has highlighted the strengths and weaknesses of the current approach.

Among the strengths is the air permeameter which enables rapid, inexpensive measurements of air flow rate. Also, the method of locating measurements for analysis of structural statistics that has been developed has proven to be efficient and economical. The mapping of lithofacies has enabled us to define architectural elements and begin to interpret the depositional environment of the Sier-

ra Ladrones Formation.

Shortcomings of the current approach includes the inability to sample permeability in the extreme value deposits (clays and gravels). Methods of estimating permeability of these units needs to be pursued since extreme value units play a key role in groundwater flow paths.

While the data analysis cannot be considered final, it has served two purposes. First, from the analysis of results we can address our original hypothesis that there exists a quantifiable correlation between observed geologic structure and the statistical parameters. Secondly, the data analysis can aid in the development of new directions of investigation.

The most fundamental implication of the statistical analysis of the air–flow–rate data is that the distribution of air flow rate (surrogate to permeability) in the deposits studied thus far approximate a log–normal distribution. While apparently fundamental, this assumption has been made time and time again in studies of stochastic hydrology but in most cases has not yet received proper field validation. Further work is necessary to see if this holds for element and formation scale heterogeneities.

The second implication of the statistical analysis of the data is that the observed geologic features (cross–bedding, lateral and vertical changes in lithofacies, changes in grain size) appear to correspond to the estimated statistical parameters of a particular deposit. Again, while geostatisticians may deem this result trivial, it verifies a critically important hypothesis that will enable us to estimate spatial statistical parameters from geologic observations with relatively little hard data.

The results of the data analysis also indicate that the statistical structure of permeability in natural geologic material is a nested structure. That is to say the

geologic entities as described are hierarchical in nature, and each geologic entity may be characterized as a separate region.

6.1.2 Nested Structure

A nested or hierarchical structure is one in which the data can be distinguished according to regions or sub–regions, or even sub–regions of the sub–regions, and so on. That is if Regions I, II, and III are all separate spatial regions and each contain smaller subregions, then the subregions can be defined according to largest region they occur in.

Several researchers in the petroleum industry have suggested that heterogeneity can be broken into classes according to spatial dimensions. Van de Graff and Ealey [1989] delineated heterogeneity at the field scale (1–10 km.), reservoir scale (0.1–1 km.) and sub reservoir scale ($<$ 0.1 km.). Weber's [1986] hierarchy consists of a five–fold breakdown ranging from 10's of micrometers to hundreds of meters.

In chapter 2 we discussed a hypothetical variogram with sills representing different geologic scales of interest. This hypothetical analysis is based on the assumption that the geologic entities can be classified according to spatial scales. Observations from the field site indicate that this may not be a valid hypothesis, as discussed below.

Sedimentary formations are composed of deposits laid down through several cycles of deposition. The major depositional cycles cover lateral distances of kilometers, and are composed internally of architectural elements. The architectural elements, while highly variable in spatial dimension, are by definition composed of lithologic facies as building blocks. The lithologic facies are composed of a distinct lithologic type exhibiting specific structures. For our purposes it can

be viewed as the fundamental building block of a fluvial sedimentary deposit.

Lithofacies, in general, transcend spatial classes. This fact is most pronounced when observing the fine facies. Fine deposits occur from the scale of thin (mm. to cm.) laterally discontinuous (cm. to m.) clay drapes resulting from waning flow in an ephemeral channel to thick (m.'s) sequences of overbank deposits which can extend laterally for several kilometers.

Similar problems with assigning spatial hierarchy occur with the gravelly channel deposits. Generally, the dimensions of the gravel facies depend on the dimensions of the paleo-channel. The disparity in scale naturally is not as significant as with the fines but to restrict oneself to a classification based on rigid spatial scales is believed to be useful only conceptually.

An alternative approach to handling such a hierarchical scheme has been proposed by Miall [1988]. A hierarchy of bedding surfaces is constructed that represent heterogeneity but are not restricted spatially. This method of analysis is the foundation of architectural element analysis. the current problem facing the quantification of such a hierarchical scheme is how to incorporate and study the spatial statistics of a system that defies a classification scheme based simply on spatial scale. Further research needs to be conducted on nested structures and alternative approaches to defining regions.

6.1.3 Estimation vs. Simulation

Development of a method of determining the statistical characteristics of an aquifer is but half the battle. Quantitative description of heterogeneity is necessary so that quantitative studies of flow and transport can be conducted. The statistical representation of hydraulic conductivity is one approach to realistically quantifying heterogeneity. With the statistical representation, two approaches to

solving flow and transport equations are available.

The first, which is here referred to as the stochastic analytic approach, uses the perturbation method to analytically solve the governing equations of flow and transport [e.g. see Bakr et al.,1978; Gutjahr et al., 1978; and Gelhar et al., 1979]. Often the random hydraulic conductivity field exhibits properties that prevent solving the partial differential equations governing flow and transport. Numerical solutions of the flow and transport equations are often employed under such complex conditions. The problem then lies in how to numerically generate a realistic field through which to analyze and simulate flow.

Traditionally, geostatistics offers two methods of generating realizations of fields that exhibit certain statistical characteristics.

The first of these methods is determination of a best linear unbiased estimator (BLUE). The field is then estimated with the linear interpolator from the known information. Commonly referred to as kriging, this method greatly smooths the fluctuations that actually exist. Contouring of data values is a common example of kriging. Non–linear estimators are also possible but less widely used.

The second method of producing a realization of a random function is the method of simulation. The estimation of a field differ from kriging in that the small scale fluctuation about the mean are preserved in accordance with the correlation structure. Two classes of simulation are possible. Unconditional simulation involves only the distribution function and covariance or variogram. The result is a field that honors the statistical properties . Alternatively, known data can be used in addition to the statistical properties of a field. This method of conditional simulation honors not only the statistical properties of the field but also the known values of the random field.

Conditioning on known data restricts the realizations of the random function to those that honor the data. In the cases of both kriging and conditional simulation, additional data provide narrower confidence intervals by reducing the estimation variance.

Journel and Huijbregts [1978] in a discussion of mining applications state: "The estimation curve is preferable to locate and estimate reserves, while the simulation curve is preferred for studying the dispersion of the characteristics of these reserves" [Journel and Huijbregts; 1978]. Given the two methods of producing realizations of random functions and assessing what we know regarding geologic heterogeneity, it seems feasible that a hybrid method of simulation be investigated. Such a method would use kriging to estimate location, extent, and/or interconnection of architectural elements. Subsequently, the within-element statistical properties of the k field could be simulated, preserving the variability or "dispersion" of the process.

Geologic information in the form of depositional process/product relations has been suggested as a quantifiable form of "soft" information. This includes information on both the spatial association and distribution of architectural elements.

In addition, statistical characteristics and patterns of permeability distributions within facies and elements can be arrived at through variogram analysis of measured and possibly estimated k's. There are essentially an infinite number of regionalized variables that can be used in the characterization process. The goal now is to study a variety of them and choose those that best estimate the hydraulic properties of an aquifer.

6.2 Conclusions

While it is not the purpose of this thesis to draw final conclusions on the research described, several fundamentally important conclusions can be made at this time. It has been shown that geostatistical parameters are correlated with geologic observations. The extent of the correlation has yet to be determined rigorously. However, it is felt that pursuing the study of geologic features in parallel with structural statistics is warranted and necessary. Also a hierarchical structure is apparent from the intermediate scale numerical experiment. Finally, much more research needs to be devoted to 1) developing methods to obtain field permeability measurements/estimates of the gravels and clays; 2) experiments with various structural estimator on how information obtained from the data collected may be optimized; and 3) the question of how the geostatistics of nested structures and the rather evasive hierarchy of sedimentary bedding surfaces are interrelated.

This thesis has presented some of the fundamental concepts of geostatistics and sedimentary basin analysis. Some preliminary data analysis has lead us to refine and to some degree validate our hypotheses. The work presented here is not intended to be the final chapter on the incorporation of geologic information into the characterization of aquifer heterogeneity. The purpose has been to evaluate the methods and delineate the major issues facing the final characterization process.

REFERENCES

Allen, J.R.L., 1974, Studies in fluviatile sedimentation: implications of pedogenic carbonate units, Lower Old Red Sandstone, Anglo–Welsh outcrop, *Geol. J., 9, pt. 2,* 181–208.

Allen, J.R.L., 1978, Studies in fluviatile sedimentation: an exploratory quantitative model for the architecture of avulsion–controlled suites, *Sed. Geol., 21,* 129–147.

Anderson, M.P., 1989, Hydrogeologic facies models to delineate large–scale spatial trends in glacial and glaciofluvial sediments, *Geol. Soc. Am. Bull., 101,* 501–511.

Bakr, A.A., L.W. Gelhar, A.L. Gutjahr, and J.R. MacMillan, 1978, Stochastic analysis of spatial variability in subsurface flows 1. Comparison of one and three–dimensional flow, *Water Resour., Res. 14,* 263–271.

Bates, R.L. and J.A. Jackson, eds., 1984, Dictionary of Geological Terms, 3rd edition , prepared by the Amer. Geological Inst., Anchor Press/Doubleday, New York, 571 pp.

Bear, J., 1979, Hydraulics of Groundwater: McGraw–Hill, New York, 567pp.

Boothyard, J.C. and G.M. Ashley, 1975, Process, bar morphology, and sedimentary structures on braided outwash fans, northeastern Gulf of Alaska; in Glaciofluvial and Glaciolacustrine Sedimentation; A.V. Jopling and B.C. McDonald eds., Soc. Econ. Paleontol. Minearal., Spec. Publ. 23, 193–222

Bridge, J.S. and M.R. Leeder, 1979, A simulation model of alluvial stratigraphy, *Sedimentology, 26,* 617–644.

Cant, D.J. and R.G. Walker, 1976, Development of a braided–fluvial facies model for the Devonian Battery Point Sandstone, Quebec, *Can. J. Earth Sci., 13,* 102–119.

Carmen, P.C., 1939, Permeability of saturated sands, soils, and clays, *J. Agric. Soc.*, 29, 262–273.

Chapin, C.E. and W.R. Seager, 1975, Evolution of the Rio Granderift in the Socorro and Las Cruces areas: New Mexcio Geological Society Guidebook 26, p. 297–321.

Dagan, G., 1986, Statistical theory of groundwater flow and transport: pore to laboratory, laboratory to formtion, and formation to regional scale, *Water Resour. Res., 22,* 120S–134S.

Delhomme, J.P., 1978, Kriging in the hydrosciences, *Advan. Water Resour., 1,* 251–266.

Eijpe, R. and K.J. Weber, 1971, Mini–permeameters for rock and unconsolidated sand, *Am. Assoc. Petr. Geol. Bull. 55*, p. 307–309.

Finley, R.J. and N. Tyler, 1986, Geological characterization of sandstone reservoirs, in eds. L.W. Lake and H.B. Carroll; Reservoir Characterization: Academic Press, New York, p. 1–38.

Fogg, G.E., 1986, Stochastic analysis of aquifer interconnectedness, with a test case in the Wilcox Group, East Texas: PhD. Dissertation, University of Texas, Austin; 216p.

Fogg, G.E., 1989, Emergence of geologic and stochastic approaches for the characterization of heterogeneous aquifers; in Proceedings of New Field Techniques for Quantifying the Physical and Chemical Properties of Heterogeneous Aquifers; ed. F.M. Molz et at., Nat. Water Well Assoc., Dallas, March 20–23. 1–17.

Freeze, R.A. and J.A. Cherry, 1979, Groundwater: Prentice–Hall, Englewood Cliffs, NJ, 604pp.

Galloway, W.E. and D.K. Hobday, 1983, Terrigenous Clastic Depositional Systems: Spinger–Verlag, New York, 423pp.

Gelhar, L.W., 1986, Stochastic subsurface hydrology from theory to applications, *Water Resour. Res.,* 22, 135S–145S.

Gelhar, L.W., A.L. Gutjahr, and R.L. Naff, 1979, Stochastic analysis of macrodispersion in a stratified aquifer, *Water Resour. Res., 15,* 1387–1397.

Gelhar, L.W., and C.L. Axness, 1983, Three–dimensional analysis of macrodispersion in aquifers, *Water Resour. Res., 19*, 161–180.

Gile, L.H., J.W. Hawley, and R.B. Grossman, 1981, Soils and geomorphology in the Basin and Range area of Southern New Mexico -- Guidebook to the Desert Project, New Mexico Bureau of Mines & Mineral Resources Mem. 39, 222p.

Goggin, D.J., M.A. Chandler, G. Kocurek, and L.W. Lake, 1988a, Patterns of permeability in eolian deposits; *Soc. Petrol. Engin. Formation Evaluation, 3,* 297–306.

Goggin, D.J., R. Thrasher, and L.W. Lake, 1988b, A theoretical and experimental analysis of minipermeameter response including gas slippage and high velocity flow effects; *In Situ, 12,* 79–116.

Gutjahr, A.L., L.W. Gelhar, A.A. Bakr, and J.R. MacMillan, 1978, Stochastic analysis of spatial variability in subsurface flows 2. Evaluation and application, *Water Resour. Res., 14,* 953–959.

Guven, O., F.M. Molz, and J.G. Melville, 1984, An analysis of dispersion in a stratified aquifer, *Water Resour. Res., 20,* 1337–1354.

Harrop–Williams, K., 1985, Clay liner permeability: Evaluation andvariation, *J. Geotech. Engineering, ASCE, 111,* 1211–1225.

Heller, J.P., 1988, Petroleum Research Recovery Center, New Mexico Institute of Mining and Technology, Socorro; pers. comm.

Jackson, R.G., 1978, Preliminary evaluation of lithofacies models for meandering alluvial streams, in Fluvial Sedimentology; ed. A.D. Miall, Can. Soc. Petrol. Geol. Mem. 5, 543–576.

Journel, A.G. and F.G. Alabert, 1988, Focusing on spatial connectivity of extreme–value attributes: Stochastic indicator models of reservoir heterogeneities, SPE 18324 presented at the 63rd annual Technical Conference and Exhibition, Houston, October 2–5.

Journel, A.G. and Ch. J. Huijbregts, 1978, Mining Geostatistics: Academic Press, New York, 600 pp.

Journel, A.G., 1989, Fundamentals of Geostatistics in Five Lessons: Short Course in Geology vol. 8, American Geophysical Union, Washington, D.C. 40 pp.

Journel, A.G. and M.E. Rossi, 1989, When do we need a trend model in kriging?, *Math. Geol., 21,* 715–739.

Katz, D.L., D. Cornell, R. Kobayashi, R.H. Poettman, J.A. Vary, J.R. Elenbaas, and C.F. Weinaug, 1959, Handbook of Natural Gas Engineering, McGraw–Hill, New York.

Kelton, F.C., 1950, Analysis of fractured limestone cores, *Petr. Trans. AIME, 189,* 225–234.

Koltermann, C.E., Stanford University, Dept. of Applied Earth Sciences, Stanford, California, pers. comm.

Lovelace, A.D., 1972, Aggregate resources in central New Mexico: New Mexico Geological Society, Guidebook to 23rd Field Conference, pp. 187–191.

Lozinsky, R.P., 1988, Stratigraphy, sedimentology, and sand petrology of the Santa Fe Group and pre–Santa Fe Tertiary deposits in the Albuquerque Basin, Central New Mexico: PhD Dissertation, New Mexico Institute of Mining and Technology, Socorro, New Mexico; 298p.

Machette, M.N., 1978, Geologic map of the San Acacia quadrangle, Socorro County, New Mexico, U.S. Geological Survey Map GQ–1415, scale 1:24,000.

Machette, M.N., 1985, Calcic soils of the southwestern UnitedStates: *Geol. Soc. Am. Spec. Paper 203*, 1–21.

MacMillan, J.R., and A.L. Gutjahr, 1986, Geologic controls on spatial variability for one–dimensional arrays of porosity and permeability normal to layering; in , Reservoir Characterization; eds. L. W. Lake and H.B. Carroll Academic Press, New York, 265–292.

McGrath, D.B. and J.W. Hawley, 1987, Geomorphic evolution and soil–geomorphic relationships in the Socorro area, central New Mexico; in Guidebook to the Socorro area, New Mexico, McLemore, V.T. and M.R. Bowie (compilers), New Mexico Bureau of Mines and Mineral Resources, Socorro, New Mexico, 55–67.

McKee, E.D., E.J. Crosby, and H.L. Berryhill Jr., 1967, Flood deposits, Bijou Creek, Colorado, June 1965, *J. Sed. Pet.; 37,* p. 829–851.

Meinzer, O.E., 1923, The occurrence of ground water in the United States: *U.S. Geol. Surv. Water-Supply Paper 489*, 321pp.

Miall, A.D., 1973, Markov chain analysis applied to an ancient alluvial plain succession, *Sedimentology, 20* 347-364.

Miall, A.D., 1977, A review of the braided-stream depositional environment, *E. Sci. Rev., vol. 13*, p. 1-62.

Miall, A.D., 1978, Lithofacies types and vertical profile models of braided river deposits: a summary, in , Fluvial Sedimentology; A.D. Miall ed., Can. Soc. Petrol. Geol. Mem. 5, p.597-604.

Miall, A.D., 1980, Cyclicity and the facies model concept influvial deposits, *Bull. Can. Petr. Geol., 28*, 59-80.

Miall, A.D., 1985, Architectural-element analysis: A new methodof facies analysis applied to fluvial deposits, *E. Sci. Rev., 22*, 261-308.

Miall, A.D., 1984, Principles of Sedimentary Basin Analysis: Springer-Verlag, New York, 490pp.

Miall, A.D., 1988, Reservoir heterogeneity in fluvial sandstones; *Am. Assoc. Petrol. Geol. Bull., 72,* 682-697.

Milne-Home, W.A. and F.W. Schwartz, 1978, Empirical approaches for estimating flow and transport parameters; in Proceedings of the Conference on New Field Techniques for the Quantifying the Physical and Chemical Properties of Heterogeneous Aquifers; F.M. Molz et al. eds. Nat. Water Well Assoc., Dallas, TX, March 20-23. 77-98.

Naff, R.L. and A.V. Vecchia, 1987, Depth-averaging effects onhydraulic head for media with stochastic hydraulic conductivity, *Water Resour. Res., 23,* 561-570.

Neumann, S.P., C.L. Winter, and C.M. Newman, 1987, Stochastic theory of field-scale Fickian dispersion in anisotropic porous media, *Water Resour. Res., 23,* 453-466.

Olson, H.W., 1966, Darcy's law in saturated kaolinite, *Water Resour. Res., 2*, p. 287-295.

Phillips, F.M. and J.L. Wilson, 1989, An approach to estimating hydraulic conductivity spatial correlation scales using geological characteristics; *Water Resour. Res., 25,* 141–143.

Phillips, F.M., J.L. Wilson, and J.M. Davis, 1989, Statistical analysis of hydraulic conductivity distributions: A quantitative geological approach; in Proceedings of the Conference on New Field Techniques for the Quantifying the Physical and Chemical Properties of Heterogeneous Aquifers; in F.M. Molz et al. eds., Nat. Water Well Assoc., Dallas, March 20–23. 19–31.

Pickens, J.F. and GE. Grisak, 1981a, Scale dependent dispersion in a stratified granular aquifer, *Water Resour. Res. 17,* 1191–1211.

Pickens, J.F. and G.E., Grisak, 1981b, Modeling of scale dependent dispersion in hydrologic systems, *Water Resour. Res 17,* 1701–1711.

Reading, H.G., 1986, Sedimentary Environments and Facies, H.G.Reading ed.: Blackwell Scientific, Palo Alto, California, 615pp.

Schwartz, F.W., 1977, Macroscopic dispersion in porous media: The controlling factors, *Water Resour. Res. 13,* 743–752.

Selley, 1978, Concepts and Methods of Subsurface Facies Analysis, Am. Assoc. Petr. Geol. Education Course Notes Series #9, 86pp.

Shapiro, A.M. and V.D. Cvetkovic, 1988, Stochastic analysisof solute arrival time in heterogeneous porous media, *Water Resour. Res., 24,* 1711–1718.

Silliman, S.E. and E.S. Simpson, 1987, Laboratory evidence of the scale effect in dispersion of solutes in porous media, *Water Resour. Res., 23,* 1667–1673.

Skibitzke, H.E., and G.M. Robertson, 1963, Dispersion in groundwater flowing though heterogeneous materials: *U.S. Geol. Surv. Prof. Paper 386–B.*

Slichter, C.S., 1899, Theoretical investigation of the motion of ground waters: *U.S. Geol. Surv. Water–Supply Paper 596,* 121–176.

Smith, L. and F.W. Schwartz, 1980, Mass transport 1, A stochastic analysis of

macrodispersion, *Water Resour. Res. 16,* 303–313.

Smith, N.D., 1970, The braided stream depositional environment: Comparison of the Platte River with some Silurian clastic rocks, North–Central Appalachians, *Geol. Soc. Amer. Bull., 81,* 2993–3014.

Sposito, G. and W.A. Jury, 1986, Fundamental problems in the stochastic convection–dispersion model of solute transport in aquifers and field soils, *Water Resour. Res., 22,* 77–88.

Stalkup, F.I., and W.J. Ebanks Jr., 1986, Permeability variation in a sandstone barrier island–tidal channel–tidal delta complex, Ferron Sandstone (Lower Cretaceous), Central Utah; SPE 15532 presented at the 61st Annual Technical Conference and Exhibition, New Orleans, October 5–8.

Sudicky, E.A., R.W. Gillham, and E.O. Frind, 1985, Experimental investigation of solute transport in stratified porous media 1: The non–reactive case, *Water Resour. Res., 21,* 1035–1041.

Tetzlaff, D.M. and J.W. Harbaugh, 1989, Simulating Clastic Sedimentation: Van Nostrand Reinhold, New York, 202pp.

van de Graaff, W.J.E., and P.J. Ealey, 1989, Geological modeling for simulation studies, *Amer. Assoc. Petrol. Geol. Bull., 73,* 1436–1444.

Walker, T.R., 1967, Formation of red beds in modern and ancient deserts, *Geol. Soc. Am. Bull., 78,* 353–368.

Walker, T.R., B. Waugh, and A.J. Grone, 1978, Diagenesis in first–cycle desert alluvium of Cenozoic age, southwestern United States and northwestern Mexico, *Geol. Soc. Am. Bull., 89,* p. 19–32.

Warrick, A.W., and D.E. Myers, 1987, Optimization of sampling locations for variogram calculations, *Water Resour. Res., 23,* 496–500.

Weber, K.J., 1980, Influence on fluid flow of common sedimentary structures in sand bodies. SPE paper 9247 presented at the 55th Annual Fall Technical Conference and Exhibition of the SPE, Dallas, Sept 21–24.

Weber, K.J., 1986, How heterogeneity affects oil recover; in eds.L.W. Lake and H.B. Carroll Reservoir Characterization: Academic Press, New York, p. 487–544.

Williams, P.F., and B.R. Rust, 1969, The sedimentology of a braided river, *J. Sed. Pet., 30,* 649–679.

Young, J.D., 1982, Late Cenozoic geology of the lower Rio Puerco, Valencia and Socorro Counties, New Mexico: M.S. Thesis, New Mexico Institute of Mining and Technology, Socorro, 126p.

Appendix A– Glossary of Terms

Actualistic models– Those type models that are based on an actual a study of an actual suite of sediments and geologic interpretation. The facies associations are generally distilled down to the basic essence of the deposit.

Allocyclic depositional controls– Cyclic controls on depositional style resulting from variations in discharge, load and slope, which originate outside the sedimentary basin ultimately through tectonic or climatic changes. [Miall, 1980]

Alluvial– Pertaining to or composed of detritus deposited by streams on river beds, flood plains, and alluvial fans.

Autocyclic depositional controls– Cyclic controls on depositional style which arise from energy distributions within the sedimentary basin, including meander translation and enlargement, meander chute and neck cut–off, crevassing and avulsion. [Miall, 1980]

Bioturbated zones– Regions of a sedimentary deposit that have been churned and stirred by plant and/or animal organisms.

Conceptual models– Those type models that are derived from a conceptualization of how sedimentological facies would be associated for a given set of depositional processes.

Correlation length– A physical length over which data points are correlated.

Covariance– A statistical measure of the similarity of data. In this thesis, the the emphasis is on similarity with respect to physical separation between data points.

Cycle of sedimentation– A sequence of related processes and conditions, repeated in the same order, that is recorded in a sedimentary deposit.

Cyclothem– A generally fining upward sequence of sedimentary deposits. The general character is cyclic and controlled by allocyclic processes.

Diagenesis– The physical and chemical alteration that occurs after a sedimentary deposit is buried. Soil development is not considered here to a diagenetic process.

Illuvial– The accumulation, in a lower soil horizon, of material that was transported by groundwater percolation (esp. colloidal material). [Bates and Jackson, 1984]

Facies– A body of rock which can be defined and distinguised from others by its geometry, lithology, and sedimentary structures. [Selley, 1970]

Facies associations– Similar to lithologic distributions. However, facies associations emphasizes how different sedimentological facies are geometrically and thus genetically related to one another.

Lag– A physical length separating a pair (or pairs) of data points.

Lithologic distribution– Similar to facies associations. However, lithologic distributions emphasizes spatial relationships of general lithologies rather than well defined facies.

Log–normal distribution– A sample set whose logarithmic transform (natural or base 10) is normally distributed.

Model (geologic)– A simplified version of reality that exhibits useful information in the interpretation and prediction of lithologic distributions and/or facies associations.

Model (variogram)– A function fitted to an estimated variogram that is presumed to represent the underlying statistical structure.

Paleosol– A buried soil; soil of the past. [Bates and Jackson, 1984]

Pedogenic– Pertaining to the development of soils.

Type model (depositional)– A simplified version fo facies associations that indicate a certain depositional environment. Type models serve as a basis by which to compare and contrast observed facies associations.

Variogram– Similar to *covariance*, however the variogram is a measure of dissimilarity of values that are separated by a *lag* distance.

Appendix B
Air–permeameter

B.1 Introduction

Obtaining large numbers of permeability measurements has been a goal and area of active research in the petroleum industry for some time. In order to achieve this goal, gas has commonly been used as the fluid due to its low viscosity thus enabling steady state conditions much more quickly than water.

Eijpe and Weber [1971] developed one of the first air–permeameters by which the air permeability of consolidated and unconsolidated sands could be measure quickly and nondestructively either in situ or in the form of samples. Goggin and others [1988], of the University of Texas at Austin, constructed a more portable air–permeameter (hereafter referred to as the UT device) and developed a theoretical framework to calculate permeability based on specific flow geometry. The UT device applies a constant pressure from a tank of compressed nitrogen to the outcrop through a tip seal. Steady state is achieved and the resulting flow is measured with a series of rotameters. With a constant pressure and flow rate, the permeability can be calculated for the resulting flow geometry.

The great utility of the Goggin et al. [1988] analysis is that the theoretical development is valid for any system that utilizes a constant pressure in order to achieve steady flow through a specific flow geometry. The flow geometry is radially symmetric with a vertical component (Figure B–1). For this geometry, permeability can be calculated via the equation:

$$k = \frac{q_1 \mu P_1}{a G_0(b_D^{\infty}) \dfrac{P_1^2 - P_0^2}{2}} \qquad \text{(B1)}$$

where:

P_0 = atmospheric pressure
P_1 = tip–seal injection pressure
q_1 = air–flow–rate
μ = dynamic viscosity of air at atmospheric conditions
a = internal radius of tip–seal
$G(b_D^{\infty})$ = geometric factor determined graphically from Goggin et al [1988b]

The concept of obtaining rapid nondestructive permeability measurements in situ was necessary for our work on the characterization of permeability distributions in fluvial deposits. Our design is based on that of the UT device but with a new set of constraints regarding sampling medium and portability. The field site of the current project consists of primarily unconsolidated material. As such it was necessary to apply a very small yet accurately measurable pressure. In order to honor the pressure constraint and increase portability another type of device was investigated. Heller [1988] had done some preliminary development of an air permeameter which used a piston/cylinder apparatus. The piston applied a constant pressure and a seal was maintained between the piston and cylinder with a prophylactic (referred to here as the HPD). The flow rate is then calculated by timing the rate at which the piston falls. The device presented in this thesis is somewhat of a hybrid between the two. The tip seal, which governs the flow geometry is similar to the UT device while the air supply portion was a modified HPD.

B.2 Permeameter Design

Figure B–2 presents the basic design of the air–permeameter developed in this thesis. A Becton–Dickenson® 100cc ground glass syringe was ground further with fine grit corundum to provide a fairly frictionless contact while maintaining an adequate seal between the piston and the syringe casing. The flow rate is obtained by electronically timing displacement fo a known volume. This is achieved with a stopwatch, a set of photoresistors, and lamps (Figure B–3). The tip seal is the part of the apparatus that governs the flow geometry at the permeameter/outcrop interface. The UT design was modified so the same flow geometry could be obtained on unconsolidated samples. The modification entails an increase in the outer diameter of the tip seal in order to provide structural stability when applied to an unconsolidated outcrop.

B.4 Calibration

Efforts to calibrate the air–permeameter have focused on comparing the intrinsic permeability derived from a constant head device (water) with air permeability calculated from equation B1. Calibration results are shown in Figure B–4. Two difficulties have arisen in calibrating the air–permeameter in this fashion. Figure B–4 shows the presence of several "outliers". These are believed to be the result of leaks in the constant head apparatus. Even though that problem has since been rectified, another difficulty with calibrating the air–permeameter in this fashion is the drastic difference in volumes being sampled. The air–permeameter has a radius of investigation on the order of one centimeter, thus sampling approximately a 1cc. volume. On the other hand, the ring samples being used are 5 centimeters in diameter and 5 centimeters in length, a

volume of approximately 100cc. A one–to–one correlation of permeability measured from two such vastly different volumes should not necessarily be expected. While the calibration thus far has not resulted in a robust relationship between permeability derived from the constant head apparatus and air–permeability, the values are encouraging.

B.5 Discussion

As the calibration process continues, other issues inherent with gas permeability will need to be addressed. For instance, at low pressures, the Klinkenburg effect is commonly observed; at higher pressures non–Darcy flow effects result in the underestimations of permeability [Katz et al., 1959]. These issues as well as soil moisture effects will be investigated as the study of geologic heterogeneity continues.

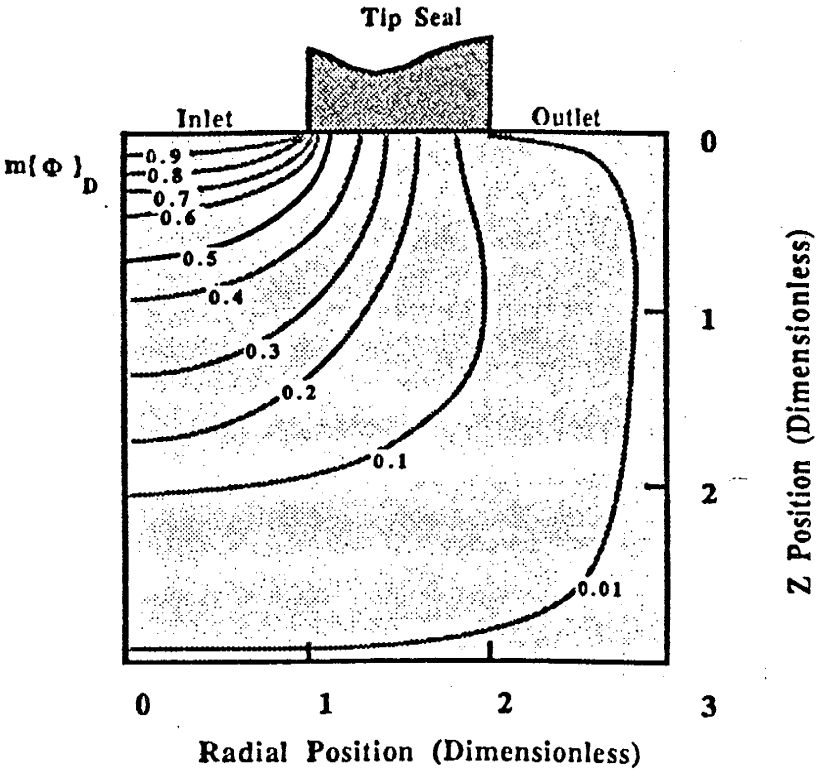

Figure B–1. Pseudo-potential contours illustrating air permeameter flow geometry. (from Goggin et al., 1988b)

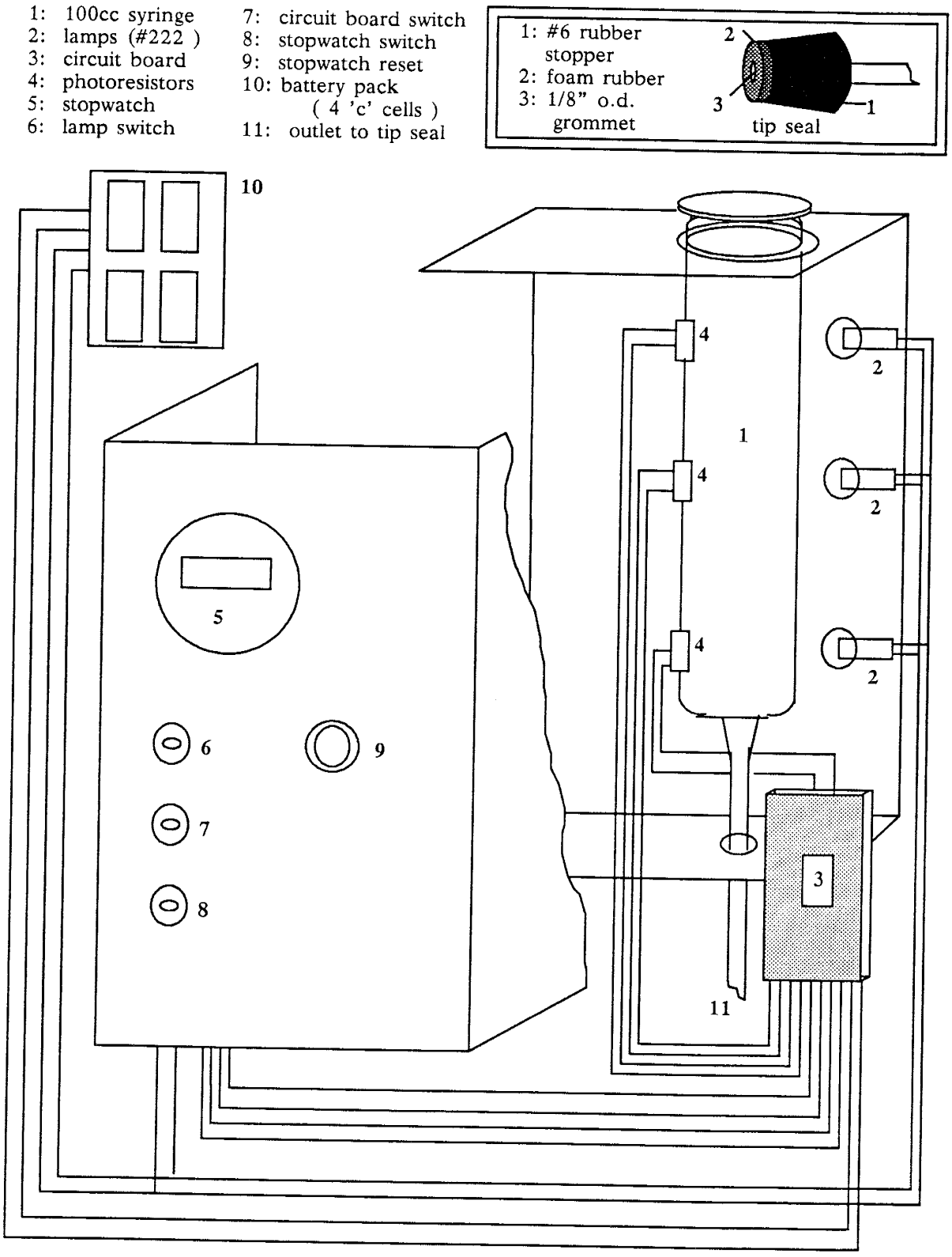

Figure B–2. Schematic diagram of air permeameter

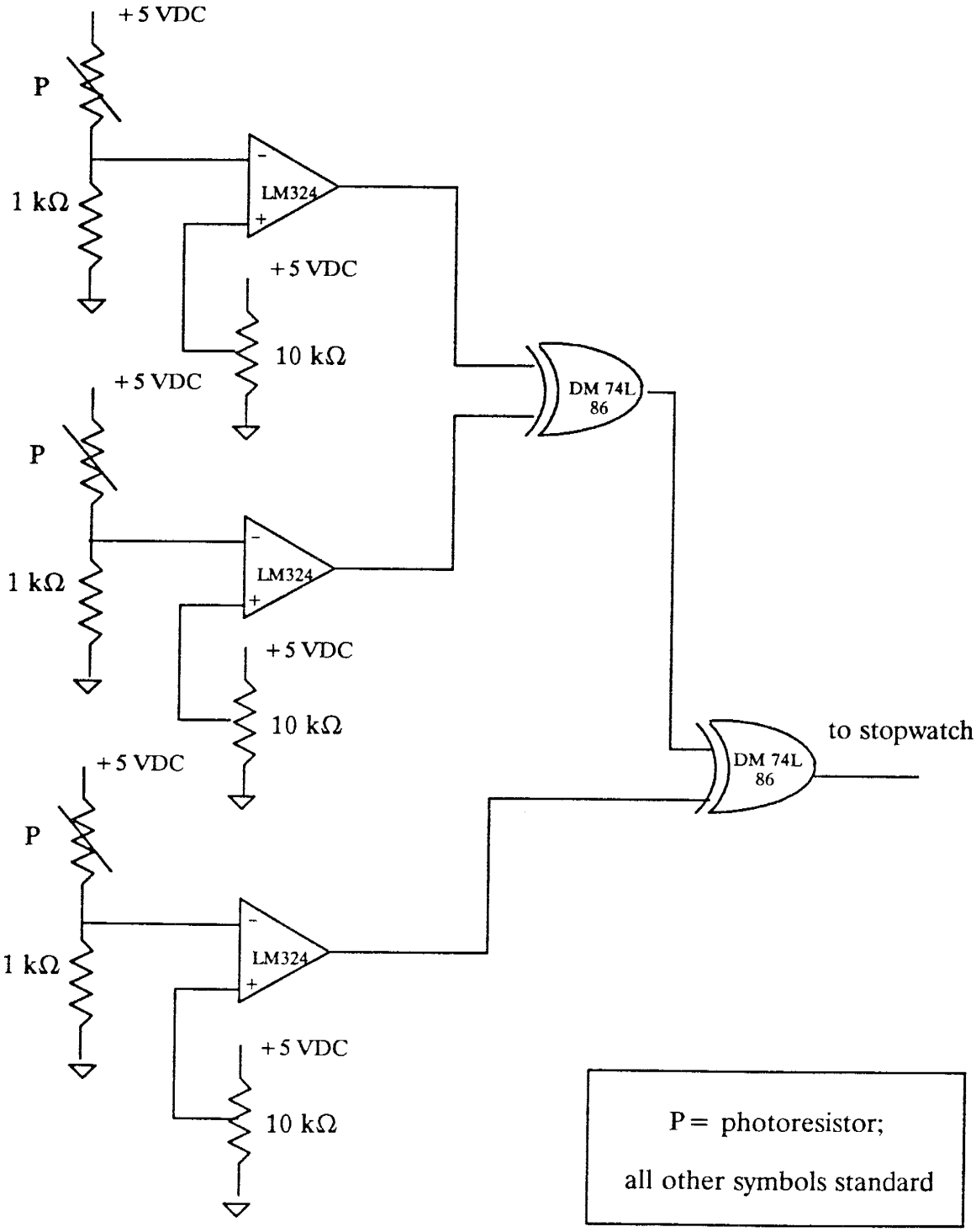

Figure B–3. Wiring diagram of electronic timing device.

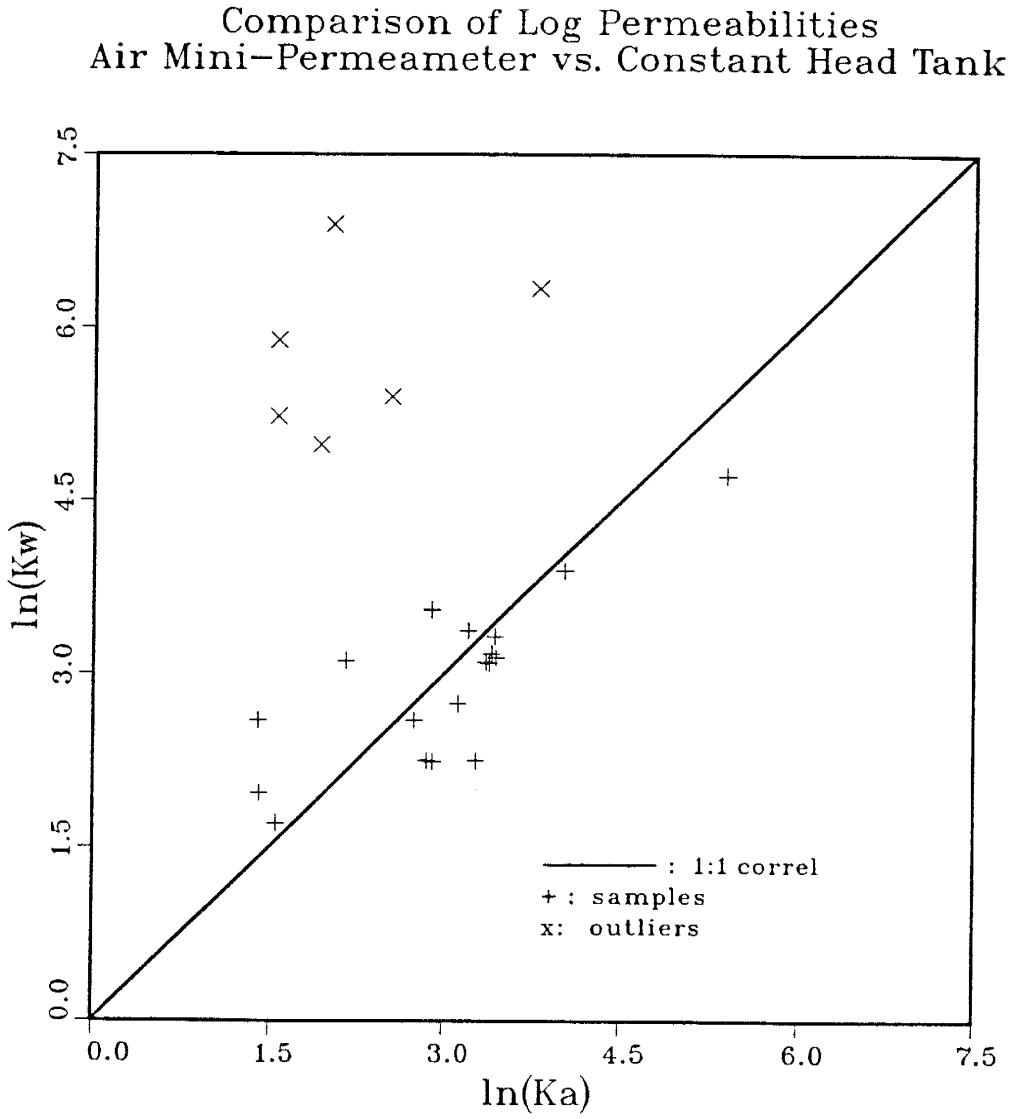

Figure 5-4. Comparison of log-permeabilities derived from air permeameter (Ka) and constant head device (Kw). Coefficient of correlation is 0.79.

APPENDIX C– Measured Sections

Two measured sections of the Sierra Ladrones Formation are presented on the following pages. The locations of the sections are shown on Plate 1. The descriptions are informal and were reproduced directly from field notes.

Measured section #1

The following description is from the notes taken when a section was measured along the transect shown on Plate 1. The accompanying column is shown in figure 15. A jacob staff and Abney level were used to measure veritcally from an arbitrary datum.

From the bottom:

(feet)	Description
0-5	Slope of reddish brown fine sand with loose pebbles from above -- underlain by brown clay.
5-10	six inch thick cream colored sandstone ledge @ 6ft. red-brown clay from 6-10 ft.
10-15	light gray-brown sand with loose pebbles
15-20	continued light grey-brown sand, well cemented @ 20 ft.
20-25	sandstone continues to 21 ft.; S20E troughs 21-25 ft covered with red-brn pebbly colluvium;
25-30	light grey sandstone @ 25 ft.; tan medium sand with red-brown clay (1-2 in. thick). No pebbles.
30-35	paleosol horizon between 30 and 33 ft.; alternating beds of brown silt and red clay between 33 and 35 ft.
35-40	red clayey slope, loose pebbles
40-45	dominately red to red-brown clay; 1 ft. coarse uncemented sand unit at 43 ft.
45-50	ledgey coarse sandstone.
50-55	sand with < 1ft. thick brown clayey unit containing calcium carbonate nodules and armored mud balls
55-60	sand with red clay containing white calcium carbonate nodules, very local infilling, at 59 ft.
60-67	coarse sand with pebbles, ledgey -- well cemented

67-73	slope of red-brown sand, clay, clay balls with loose gravel.
73-75	lenses of reddish cream sandstone in uncemented rusty red-brown sand with calcium carbonate nodules.
75-106	prominant gravelly sand, locally cemented; fine and coarse sand cycles @ 91 ft. S35E troughs
106-110	red brown clay
110-117	alternating beds of silt, clay and sand
117-122	red brown clay
122-140	high angle x-laminated sand grading up into climbing ripples with clay clasts in lee side; medium x-laminated sand fining upward near top.
140-150	silt bands, red-brown clay with calcium carbonate nodules; possibly paleosol
150-157	grey-tan x-laminated fine sand and silt; fine and medium x-laminated sand @ 155 ft.
157-165	unit of tan-grey fine sand in brown clay unit
165-170	tan sand and gravelly sand, locally well cemented, some armored mud balls.
170-175	unsorted gravelly sand; uncertain as to nature debri flow and/or soil.
175-187	sequence of red brown clay, x-laminated grey-tan silt and fine sand, brown clay, and tan silt and clay.
187-197	sand and gravelly sand, gravel and clay rubble near 196 ft.
197-199	paleosol
199-204	low angle x-laminated sand-pebbly sand, partly cemented.
204-207	paleosol
207-212	x-laminated sand scour, gravel; loose gravelly sand.
212-215	pebbly sand w/o sed. structures, sand w/ calcium carbonate nodules (paleosol?)

215-220	ledges of cemented gravelly sand.
220-230	slope of loose grey peebly sand.
230-237	laminated and x-laminated silt and clay.
237-244	sequence of rusty sand, thin brown red clay, x-laminated silt and clay.
244-262	x-bedded gravelly sand, partly conglomeratic, pebbly sand.
262-267	sequence of rusty sand, brown clay, rusty sand, culminating in minor clay.
267-289	slope of pebbly sand, rusty to red coated sand and pebbles.
289-293	well cemented conglomerate of coarse sand and pebbles. S24E trough.
293-297	loose rusty sand.
297-303	alternating units (typically < 1 ft. thick) of brown or red clay and rusty sand
303-310	pebbly gravelly sand with red clay in matrix
310-319	paleosol: Stage V development (see text).
319-320	pebbly sand
320-324	clayey sand

Measured Section #2

The following description is from the notes taken when a section was measured along the transect shown on Plate 1. The accompanying column is shown in figure 15. A jacob staff and Abney level were used to measure veritcally from an arbitrary datum.

From the bottom:

(feet)	Description
0-5	sequence of ledgey sand, reddish soil like sand, red clay, ledgey sand.
5-19	pebbley loose sand, some cemented zones, grading upward into gravelly sand.
19-23	sequence of silt, fine sand, soil
23-38	banded slope consisting of a sequence (from bottom up) of: silt, fine sand, soil, brown clay, tan silt, brown clay, rusty brown sand, brown clay w/ white silt band, rusty tan sand, gray silt and brown clay, brown clay, rusty brown sand, brown clay, grey-tan silt, rusty sand, tan-grey silt, rusty sand. Units are approximately 1 ft. thick
38-43	rusty medium sand, structureless, calcium carbonate nodules. soil-like.
43-72	sequence of brown rubbly clay, gray silt w/ calcium carbonate nodules coarsening upward to medium sand, red clay, grey silt, x-laminated fine-medium sand, rusty-red silt, red brown clay, silt and brown clay, red-rusty fine sand, laminated (white) silt and (red) clay, x-laminated fine grey sand and silt, clay, silt and nodules of cemented silt, sand, red rusty sandy clay
72-80	grey-brown gravel with some sand fining upward into a rusty yellow pebbly sand.
80-90	gravel fining upward into a x-laminated sand.
90-95	stack of palesols.

95-100	sequence of structureless tan-rusty sand, brown clay, sand, brown clay.
100-147	sand and gravelly sand including armored mud balls, local gravel concentrations, x-lamination, and large clay rip ups (as shown on column).
147-150	stacked soils of pebbly clayey sand.
150-155	sequence of red-brown clay, orange rusty sand redding up (may be eolian), red-pink laminated clay and silt.
155-165	grey sand, sand with pebble lenses, rusty red sand.
165-186	sequence of: sand with calcium carbonate nodules, brown clay, laminated fine sand and silt, brown clay, tan slightly rusty x-laminated sand, brown sandy clay, silt, orange sand.
186-189	red brown clayey sand and brown clay (soil-like).
189-190	gravelly sand, locally cemented.
190-194	sequence of gravelly sand with calcium carbonate nodules, clayey sand, rusty-reddish sand. (sequence is soil-like).
194-202	sequence of yellow-brown clay with grey silt, rusty loose x-laminated sand, rusty-yellow sand fine-medium grained x-laminated.
202-225	gravelly sand with armored bud balls.
225-239	sequence of x-laminated sand (locally cemented), gravelly sand, red clay mixed in gravel with soft calcium carbonate nodules, gravelly sand, red clayey sand.
239-250	x-bedded gravelly sand locally cemented.
250-263	paleosol: Stage V development (see text).

APPENDIX D- Data and Variogram Output

The logarithmic air-flow-rate data are presented in the following pages along with the results of the variogram estimation. Each data set has a header which describes the contents of the each column of data. The variogram output is also documented.

column	description
1	Date (yrmody)
2	Facies (numeric code)
3	Grainsize (fine,medium,coarse,burrow)
4	Architectural Element (type)
5	Architectural Element (specific)
6	X - coordinate (centimeters)
7	Y - cooridnate (centimeters)
8	Z - coordinate (centimeters)
9	natural logarithm of air flow rate [cc/sec]

890628	7 m CH2 BQC2.1	-0.116258E+03	0.626669E+02	0.000000E+00	2.83
890628	7 m CH2 BQC2.1	-0.127165E+03	0.647421E+02	0.000000E+00	2.58
890628	4 c CH2 BQC2.1	-0.118623E+03	0.569239E+02	0.000000E+00	4.14
890628	4 c CH2 BQC2.1	-0.128806E+03	0.587578E+02	0.000000E+00	4.22
890628	4 c CH2 BQC2.1	-0.113363E+03	0.566344E+02	0.000000E+00	4.66
890628	7 m CH2 BQC2.1	-0.120891E+03	0.509397E+02	0.000000E+00	3.03
890628	7 m CH2 BQC2.1	-0.115728E+03	0.506019E+02	0.000000E+00	3.16
890628	5 m CH2 BQC2.1	-0.120457E+03	0.462585E+02	0.000000E+00	3.49
890628	5 m CH2 BQC2.1	-0.115728E+03	0.457276E+02	0.000000E+00	3.15
890628	5 m CH2 BQC2.1	-0.126393E+03	0.473685E+02	0.000000E+00	3.51
890628	5 c CH2 BQC2.1	-0.113314E+03	0.397916E+02	0.000000E+00	3.34
890628	5 m CH2 BQC2.1	-0.106558E+03	0.413842E+02	0.000000E+00	3.79
890628	5 m CH2 BQC2.1	-0.987882E+02	0.439420E+02	0.000000E+00	3.75
890628	5 m CH2 BQC2.1	-0.103469E+03	0.451002E+02	0.000000E+00	3.77
890628	5 m CH2 BQC2.1	-0.107379E+03	0.453415E+02	0.000000E+00	3.07
890628	5 m CH2 BQC2.1	-0.111915E+03	0.449072E+02	0.000000E+00	3.40
890628	5 m CH2 BQC2.1	-0.124511E+03	0.388747E+02	0.000000E+00	2.85
890628	5 m CH2 BQC2.1	-0.121712E+03	0.326009E+02	0.000000E+00	3.43
890628	5 m CH2 BQC2.1	-0.108006E+03	0.313461E+02	0.000000E+00	3.59
890628	5 m CH2 BQC2.1	-0.104435E+03	0.321666E+02	0.000000E+00	3.66
890628	5 m CH2 BQC2.1	-0.107041E+03	0.280162E+02	0.000000E+00	3.90
890628	5 m CH2 BQC2.1	-0.103952E+03	0.287401E+02	0.000000E+00	4.00
890628	5 m CH2 BQC2.1	-0.116065E+03	0.316840E+02	0.000000E+00	3.72
890628	5 m CH2 BQC2.1	-0.122822E+03	0.256997E+02	0.000000E+00	4.17
890628	7 m CH2 BQC2.1	-0.129819E+03	0.239624E+02	0.000000E+00	3.11
890628	7 m CH2 BQC2.1	-0.106944E+03	0.206324E+02	0.000000E+00	3.33
890628	5 m CH2 BQC2.1	-0.999947E+02	0.298018E+02	0.000000E+00	3.84
890628	4 c CH2 BQC2.1	-0.106269E+03	0.568757E+02	0.000000E+00	3.84
890628	7 m CH2 BQC2.1	-0.985952E+02	0.600608E+02	0.000000E+00	2.88
890628	7 m CH2 BQC2.1	-0.991260E+02	0.630047E+02	0.000000E+00	3.17
890628	7 m CH2 BQC2.1	-0.939622E+02	0.613156E+02	0.000000E+00	3.37
890628	7 m CH2 BQC2.1	-0.111046E+03	0.621360E+02	0.000000E+00	3.03
890628	18 b CH2 BQC2.1	-0.102263E+03	0.497815E+02	0.000000E+00	3.27
890628	18 b CH2 BQC2.1	-0.992226E+02	0.495884E+02	0.000000E+00	3.45
890628	4 c CH2 BQC2.1	-0.934314E+02	0.532079E+02	0.000000E+00	4.00
890628	4 c CH2 BQC2.1	-0.909701E+02	0.533527E+02	0.000000E+00	4.06
890628	4 c CH2 BQC2.1	-0.867715E+02	0.521462E+02	0.000000E+00	4.13
890628	4 c CH2 BQC2.1	-0.803529E+02	0.517601E+02	0.000000E+00	4.18
890628	4 c CH2 BQC2.1	-0.728243E+02	0.515671E+02	0.000000E+00	3.80
890628	15 m CH2 BQC2.1	-0.898119E+02	0.580822E+02	0.000000E+00	2.88
890628	15 m CH2 BQC2.1	-0.818972E+02	0.562966E+02	0.000000E+00	3.66
890628	4 c CH2 BQC2.1	-0.994156E+02	0.550418E+02	0.000000E+00	3.57
890628	7 m CH2 BQC2.1	-0.882675E+02	0.601091E+02	0.000000E+00	3.04
890628	7 m CH2 BQC2.1	-0.815594E+02	0.602539E+02	0.000000E+00	3.38
890628	7 m CH2 BQC2.1	-0.846963E+02	0.603504E+02	0.000000E+00	3.14
890628	7 m CH2 BQC2.1	-0.786638E+02	0.601091E+02	0.000000E+00	3.13
890628	7 m CH2 BQC2.1	-0.729691E+02	0.598195E+02	0.000000E+00	3.33
890628	5 m CH2 BQC2.1	-0.643306E+02	0.430251E+02	0.000000E+00	3.05
890628	5 m CH2 BQC2.1	-0.683844E+02	0.449072E+02	0.000000E+00	2.40
890628	5 m CH2 BQC2.1	-0.710387E+02	0.450037E+02	0.000000E+00	2.95
890628	5 m CH2 BQC2.1	-0.698322E+02	0.419633E+02	0.000000E+00	3.20
890628	5 m CH2 BQC2.1	-0.770230E+02	0.423012E+02	0.000000E+00	3.24
890628	5 m CH2 BQC2.1	-0.908253E+02	0.423012E+02	0.000000E+00	2.99
890628	5 m CH2 BQC2.1	-0.963752E+02	0.429285E+02	0.000000E+00	3.65

890628	5	m	CH2	BQC2.1	-0.816077E+02	0.313461E+02	0.000000E+00	4.29
890628	5	m	CH2	BQC2.1	-0.870128E+02	0.301879E+02	0.000000E+00	3.55
890628	5	m	CH2	BQC2.1	-0.776021E+02	0.305257E+02	0.000000E+00	4.03
890628	5	m	CH2	BQC2.1	-0.666953E+02	0.274371E+02	0.000000E+00	3.65
890628	5	m	CH2	BQC2.1	-0.665988E+02	0.224180E+02	0.000000E+00	3.38
890628	7	m	CH2	BQC2.1	-0.768782E+02	0.189433E+02	0.000000E+00	3.43
890628	5	m	CH2	BQC2.1	-0.826694E+02	0.241554E+02	0.000000E+00	3.37
890628	7	m	CH2	BQC2.1	-0.920801E+02	0.220802E+02	0.000000E+00	3.58
890628	5	m	CH2	BQC2.1	-0.984504E+02	0.369926E+02	0.000000E+00	3.30
890628	5	c	CH2	BQC2.1	-0.686257E+02	0.377165E+02	0.000000E+00	3.57
890628	7	m	CH2	BQC2.1	-0.557403E+02	0.534010E+02	0.000000E+00	3.18
890628	7	m	CH2	BQC2.1	-0.503834E+02	0.522910E+02	0.000000E+00	3.16
890628	7	m	CH2	BQC2.1	-0.588289E+02	0.596265E+02	0.000000E+00	3.20
890628	7	m	CH2	BQC2.1	-0.464261E+02	0.570687E+02	0.000000E+00	3.33
890628	7	f	CH2	BQC2.1	-0.406349E+02	0.536423E+02	0.000000E+00	2.34
890628	7	f	CH2	BQC2.1	-0.329133E+02	0.526771E+02	0.000000E+00	2.04
890628	18	b	CH2	BQC2.1	-0.557403E+02	0.474650E+02	0.000000E+00	2.22
890628	18	b	CH2	BQC2.1	-0.496595E+02	0.479958E+02	0.000000E+00	2.12
890628	18	b	CH2	BQC2.1	-0.429997E+02	0.408534E+02	0.000000E+00	2.38
890628	7	m	CH2	BQC2.1	-0.410210E+02	0.446659E+02	0.000000E+00	3.50
890628	5	m	CH2	BQC2.1	-0.566090E+02	0.428803E+02	0.000000E+00	3.07
890628	18	b	CH2	BQC2.1	-0.517830E+02	0.427355E+02	0.000000E+00	3.07
890628	5	m	CH2	BQC2.1	-0.550647E+02	0.357378E+02	0.000000E+00	3.65
890628	5	m	CH2	BQC2.1	-0.501421E+02	0.371373E+02	0.000000E+00	3.64
890628	18	b	CH2	BQC2.1	-0.441579E+02	0.366547E+02	0.000000E+00	3.36
890628	18	b	CH2	BQC2.1	-0.373532E+02	0.364617E+02	0.000000E+00	2.95
890628	5	m	CH2	BQC2.1	-0.425653E+02	0.247828E+02	0.000000E+00	3.35
890628	5	m	CH2	BQC2.1	-0.448335E+02	0.245897E+02	0.000000E+00	3.19
890628	5	m	CH2	BQC2.1	-0.434340E+02	0.326974E+02	0.000000E+00	3.33
890628	5	m	CH2	BQC2.1	-0.480187E+02	0.323113E+02	0.000000E+00	3.24
890628	5	m	CH2	BQC2.1	-0.541477E+02	0.314909E+02	0.000000E+00	3.14
890628	5	m	CH2	BQC2.1	-0.517347E+02	0.181229E+02	0.000000E+00	3.64
890628	7	c	CH2	BQC2.1	-0.312725E+02	0.185572E+02	0.000000E+00	3.38
890628	5	m	CH2	BQC2.1	-0.589255E+02	0.232385E+02	0.000000E+00	3.59
890626	7	c	CH2	BQC2.1	-0.320040E+01	0.284480E+02	0.000000E+00	3.98
890626	7	c	CH2	BQC2.1	-0.118364E+02	0.224536E+02	0.000000E+00	3.28
890626	7	c	CH2	BQC2.1	-0.111252E+02	0.284480E+02	0.000000E+00	3.82
890626	7	c	CH2	BQC2.1	-0.162052E+02	0.287528E+02	0.000000E+00	3.73
890626	18	b	CH2	BQC2.1	-0.142240E+02	0.355092E+02	0.000000E+00	2.86
890626	5	m	CH2	BQC2.1	-0.350520E+02	0.287020E+02	0.000000E+00	3.28
890626	7	c	CH2	BQC2.1	-0.318008E+02	0.225044E+02	0.000000E+00	4.16
890626	7	c	CH2	BQC2.1	-0.236220E+02	0.265176E+02	0.000000E+00	3.58
890626	7	m	CH2	BQC2.1	-0.182372E+02	0.459232E+02	0.000000E+00	2.71
890626	7	m	CH2	BQC2.1	-0.238760E+02	0.498348E+02	0.000000E+00	3.00
890626	7	f	CH2	BQC2.1	-0.249428E+02	0.586232E+02	0.000000E+00	2.22
890626	18	b	CH2	BQC2.1	-0.367284E+02	0.400812E+02	0.000000E+00	2.21
890626	7	m	CH2	BQC2.1	-0.311912E+02	0.478028E+02	0.000000E+00	3.41
890626	18	b	CH2	BQC2.1	-0.239268E+02	0.404368E+02	0.000000E+00	2.90
890626	5	m	CH2	BQC2.1	-0.373380E+02	0.230632E+02	0.000000E+00	4.22
890626	7	f	CH2	BQC2.1	-0.348996E+02	0.568452E+02	0.000000E+00	2.08
890626	7	c	CH2	BQC2.1	-0.246888E+02	0.169672E+02	0.000000E+00	3.58
890626	7	c	CH2	BQC2.1	-0.306832E+02	0.170688E+02	0.000000E+00	3.54
890626	7	c	CH2	BQC2.1	-0.365760E+01	0.233680E+02	0.000000E+00	3.60
890626	7	m	CH2	BQC2.1	-0.157480E+02	0.402844E+02	0.000000E+00	3.53
890626	7	c	CH2	BQC2.1	-0.179324E+02	0.533400E+01	0.000000E+00	4.62
890626	7	c	CH2	BQC2.1	-0.142748E+02	0.100076E+02	0.000000E+00	3.80
890626	7	c	CH2	BQC2.1	-0.934720E+01	0.111760E+02	0.000000E+00	4.09
890626	7	c	CH2	BQC2.1	0.614680E+01	0.833120E+01	0.000000E+00	3.77
890626	7	c	CH2	BQC2.1	0.118872E+02	0.104140E+02	0.000000E+00	3.96
890626	7	c	CH2	BQC2.1	0.929640E+01	0.416560E+01	0.000000E+00	4.12
890626	7	c	CH2	BQC2.1	0.249428E+02	0.318516E+02	0.000000E+00	3.07
890626	7	c	CH2	BQC2.1	0.105156E+02	0.320040E+02	0.000000E+00	3.60
890626	7	c	CH2	BQC2.1	0.139192E+02	0.320548E+02	0.000000E+00	3.65
890626	7	c	CH2	BQC2.1	0.200660E+02	0.326136E+02	0.000000E+00	3.71
890626	7	c	CH2	BQC2.1	0.211836E+02	0.298196E+02	0.000000E+00	3.87

890626	7	c	CH2	BQC2.1	0.239776E+02	0.326644E+02	0.000000E+00	2.99
890626	7	c	CH2	BQC2.1	0.134112E+02	0.225044E+02	0.000000E+00	3.46
890626	7	c	CH2	BQC2.1	0.188468E+02	0.188976E+02	0.000000E+00	3.60
890626	7	c	CH2	BQC2.1	0.548640E+01	0.144272E+02	0.000000E+00	3.82
890626	7	m	CH2	BQC2.1	0.198120E+01	0.413004E+02	0.000000E+00	3.35
890626	7	m	CH2	BQC2.1	-0.447040E+01	0.395732E+02	0.000000E+00	3.07
890626	7	c	CH2	BQC2.1	-0.127000E+02	0.574548E+02	0.000000E+00	4.72
890626	7	c	CH2	BQC2.1	-0.179832E+02	0.577596E+02	0.000000E+00	3.38
890626	7	f	CH2	BQC2.1	-0.203708E+02	0.582676E+02	0.000000E+00	2.18
890626	7	c	CH2	BQC2.1	0.313436E+02	0.273812E+02	0.000000E+00	3.89
890626	7	c	CH2	BQC2.1	0.378460E+02	0.264160E+02	0.000000E+00	3.92
890626	7	m	CH2	BQC2.1	0.236220E+02	0.474472E+02	0.000000E+00	2.36
890626	7	m	CH2	BQC2.1	0.244348E+02	0.427736E+02	0.000000E+00	3.75
890626	7	m	CH2	BQC2.1	0.108712E+02	0.374904E+02	0.000000E+00	3.29
890626	7	m	CH2	BQC2.1	0.254000E+00	0.466344E+02	0.000000E+00	3.24
890626	7	m	CH2	BQC2.1	-0.802640E+01	0.510032E+02	0.000000E+00	3.43
890626	7	m	CH2	BQC2.1	0.767080E+01	0.671068E+02	0.000000E+00	3.02
890626	6	m	CH2	BQC2.1	0.452120E+01	0.635508E+02	0.000000E+00	3.04
890626	7	c	CH2	BQC2.1	0.443992E+02	0.675640E+01	0.000000E+00	4.03
890626	7	c	CH2	BQC2.1	0.353568E+02	0.817880E+01	0.000000E+00	4.54
890626	7	m	CH2	BQC2.1	0.376428E+02	0.400304E+02	0.000000E+00	3.14
890626	7	m	CH2	BQC2.1	0.460248E+02	0.484124E+02	0.000000E+00	2.79
890626	18	b	CH2	BQC2.1	0.416052E+02	0.503936E+02	0.000000E+00	3.84
890626	7	m	CH2	BQC2.1	0.464312E+02	0.512572E+02	0.000000E+00	2.57
890626	18	b	CH2	BQC2.1	0.458216E+02	0.555244E+02	0.000000E+00	2.37
890626	7	m	CH2	BQC2.1	0.147828E+02	0.524764E+02	0.000000E+00	3.82
890626	6	m	CH2	BQC2.1	0.194564E+02	0.636016E+02	0.000000E+00	2.92
890626	7	c	CH2	BQC2.1	0.473964E+02	0.222504E+02	0.000000E+00	3.74
890626	7	m	CH2	BQC2.1	-0.130048E+02	0.665988E+02	0.000000E+00	3.50
890626	7	c	CH2	BQC2.1	0.400812E+02	0.192532E+02	0.000000E+00	3.58
890626	7	c	CH2	BQC2.1	0.354076E+02	0.149860E+02	0.000000E+00	3.95
890626	7	c	CH2	BQC2.1	0.513080E+02	0.315468E+02	0.000000E+00	3.51
890626	18	b	CH2	BQC2.1	0.368808E+02	0.682244E+02	0.000000E+00	2.04
890626	18	b	CH2	BQC2.1	0.282956E+02	0.690880E+02	0.000000E+00	2.28
890626	7	c	CH2	BQC2.1	0.196088E+02	0.573532E+02	0.000000E+00	3.94
890626	7	c	CH2	BQC2.1	0.376936E+02	0.328676E+02	0.000000E+00	3.52
890626	7	c	CH2	BQC2.1	0.313436E+02	0.342900E+02	0.000000E+00	3.35
890626	7	m	CH2	BQC2.1	0.371348E+02	0.444500E+02	0.000000E+00	3.22
890702	18	b	CH2	BQC2.1	0.424688E+02	0.496316E+02	0.000000E+00	3.18
890702	6	m	CH2	BQC2.1	0.432308E+02	0.525780E+02	0.000000E+00	2.62
890702	18	b	CH2	BQC2.1	0.424688E+02	0.466852E+02	0.000000E+00	3.79
890702	7	m	CH2	BQC2.1	0.495300E+02	0.492760E+02	0.000000E+00	3.79
890702	7	m	CH2	BQC2.1	0.525272E+02	0.488696E+02	0.000000E+00	4.00
890702	7	m	CH2	BQC2.1	0.560324E+02	0.486156E+02	0.000000E+00	4.17
890702	7	m	CH2	BQC2.1	0.595376E+02	0.483616E+02	0.000000E+00	3.57
890702	6	m	CH2	BQC2.1	0.462788E+02	0.568960E+02	0.000000E+00	4.12
890702	18	b	CH2	BQC2.1	0.392684E+02	0.583184E+02	0.000000E+00	2.31
890702	6	m	CH2	BQC2.1	0.516636E+02	0.559308E+02	0.000000E+00	4.04
890702	6	m	CH2	BQC2.1	0.614680E+02	0.556768E+02	0.000000E+00	4.06
890702	6	m	CH2	BQC2.1	0.686308E+02	0.563372E+02	0.000000E+00	3.79
890702	6	m	CH2	BQC2.1	0.778256E+02	0.584200E+02	0.000000E+00	3.16
890702	6	m	CH2	BQC2.1	0.841248E+02	0.573024E+02	0.000000E+00	3.71
890702	6	m	CH2	BQC2.1	0.885444E+02	0.509524E+02	0.000000E+00	3.31
890702	6	m	CH2	BQC2.1	0.908812E+02	0.509524E+02	0.000000E+00	3.03
890702	7	m	CH2	BQC2.1	0.803656E+02	0.509016E+02	0.000000E+00	3.05
890702	7	m	CH2	BQC2.1	0.751840E+02	0.508508E+02	0.000000E+00	3.04
890702	6	m	CH2	BQC2.1	0.615188E+02	0.524764E+02	0.000000E+00	3.14
890702	7	m	CH2	BQC2.1	0.750824E+02	0.469900E+02	0.000000E+00	3.79
890702	7	m	CH2	BQC2.1	0.577596E+02	0.438912E+02	0.000000E+00	2.60
890702	7	m	CH2	BQC2.1	0.490220E+02	0.447548E+02	0.000000E+00	2.65
890702	7	m	CH2	BQC2.1	0.654304E+02	0.435864E+02	0.000000E+00	2.62
890702	7	m	CH2	BQC2.1	0.741172E+02	0.441960E+02	0.000000E+00	2.91
890702	7	m	CH2	BQC2.1	0.855472E+02	0.468884E+02	0.000000E+00	3.69
890702	7	m	CH2	BQC2.1	0.403352E+02	0.382524E+02	0.000000E+00	2.89

890702	7 c CH2 BQC2.1	0.407924E+02	0.334264E+02	0.000000E+00	3.52
890702	7 c CH2 BQC2.1	0.408432E+02	0.287528E+02	0.000000E+00	3.77
890702	7 c CH2 BQC2.1	0.496316E+02	0.322072E+02	0.000000E+00	4.08
890702	7 c CH2 BQC2.1	0.507492E+02	0.268224E+02	0.000000E+00	3.75
890702	7 c CH2 BQC2.1	0.384048E+02	0.198628E+02	0.000000E+00	3.60
890702	7 m CH2 BQC2.1	0.531368E+02	0.391160E+02	0.000000E+00	3.37
890702	7 m CH2 BQC2.1	0.579120E+02	0.389128E+02	0.000000E+00	3.59
890702	7 m CH2 BQC2.1	0.652780E+02	0.384048E+02	0.000000E+00	3.55
890702	7 m CH2 BQC2.1	0.789940E+02	0.391668E+02	0.000000E+00	3.58
890702	7 m CH2 BQC2.1	0.869696E+02	0.389128E+02	0.000000E+00	3.49
890702	7 c CH2 BQC2.1	0.901192E+02	0.342392E+02	0.000000E+00	3.51
890702	7 c CH2 BQC2.1	0.823976E+02	0.331724E+02	0.000000E+00	3.95
890702	7 c CH2 BQC2.1	0.694436E+02	0.338836E+02	0.000000E+00	3.94
890702	7 c CH2 BQC2.1	0.573024E+02	0.316992E+02	0.000000E+00	3.99
890702	7 c CH2 BQC2.1	0.541020E+02	0.282448E+02	0.000000E+00	3.92
890702	7 c CH2 BQC2.1	0.691388E+02	0.269240E+02	0.000000E+00	3.76
890702	7 c CH2 BQC2.1	0.812800E+02	0.261620E+02	0.000000E+00	4.13
890702	7 c CH2 BQC2.1	0.742188E+02	0.262128E+02	0.000000E+00	3.85
890702	7 c CH2 BQC2.1	0.533908E+02	0.232156E+02	0.000000E+00	3.82
890702	7 c CH2 BQC2.1	0.591312E+02	-0.492760E+01	0.000000E+00	4.03
890702	7 c CH2 BQC2.1	0.472948E+02	-0.462280E+01	0.000000E+00	4.65
890702	7 c CH2 BQC2.1	0.379984E+02	-0.482600E+01	0.000000E+00	4.72
890702	7 c CH2 BQC2.1	0.387096E+02	0.538480E+01	0.000000E+00	4.17
890702	7 c CH2 BQC2.1	0.543560E+02	0.838200E+01	0.000000E+00	3.87
890702	7 c CH2 BQC2.1	0.416052E+02	0.135636E+02	0.000000E+00	4.22
890702	7 c CH2 BQC2.1	0.487172E+02	0.124968E+02	0.000000E+00	3.84
890702	7 c CH2 BQC2.1	0.592836E+02	0.170180E+02	0.000000E+00	3.90
890702	7 c CH2 BQC2.1	0.621792E+02	0.164084E+02	0.000000E+00	4.03
890702	7 c CH2 BQC2.1	0.566928E+02	0.381000E+01	0.000000E+00	4.06
890702	7 c CH2 BQC2.1	0.623824E+02	0.320040E+01	0.000000E+00	3.75
890702	7 c CH2 BQC2.1	0.749300E+02	0.233680E+01	0.000000E+00	3.66
890702	7 c CH2 BQC2.1	0.808228E+02	0.279400E+01	0.000000E+00	4.00
890702	7 c CH2 BQC2.1	0.735076E+02	0.120396E+02	0.000000E+00	3.75
890702	7 c CH2 BQC2.1	0.806196E+02	0.111760E+02	0.000000E+00	3.90
890702	7 c CH2 BQC2.1	0.874776E+02	0.110236E+02	0.000000E+00	3.89
890702	7 c CH2 BQC2.1	0.751840E+02	-0.594360E+01	0.000000E+00	4.34
890702	7 c CH2 BQC2.1	0.857504E+02	-0.609600E+01	0.000000E+00	4.03
890702	7 c CH2 BQC2.1	0.901192E+02	0.381000E+01	0.000000E+00	3.95
890702	7 c CH2 BQC2.1	0.945896E+02	0.406400E+01	0.000000E+00	4.11
890702	7 c CH2 BQC2.1	0.101346E+03	0.462280E+01	0.000000E+00	3.71
890702	7 c CH2 BQC2.1	0.972820E+02	-0.457200E+00	0.000000E+00	4.09
890702	7 c CH2 BQC2.1	0.957072E+02	-0.624840E+01	0.000000E+00	4.34
890702	7 c CH2 BQC2.1	0.113386E+03	-0.533400E+01	0.000000E+00	4.01
890702	7 c CH2 BQC2.1	0.122377E+03	-0.528320E+01	0.000000E+00	4.02
890702	7 c CH2 BQC2.1	0.131572E+03	-0.472440E+01	0.000000E+00	4.15
890702	7 c CH2 BQC2.1	0.131064E+03	-0.187960E+01	0.000000E+00	4.00
890702	7 c CH2 BQC2.1	0.121666E+03	0.172720E+01	0.000000E+00	3.92
890702	7 c CH2 BQC2.1	0.112471E+03	0.848360E+01	0.000000E+00	4.09
890702	7 c CH2 BQC2.1	0.108052E+03	0.143764E+02	0.000000E+00	4.24
890702	7 c CH2 BQC2.1	0.982980E+02	0.162560E+02	0.000000E+00	3.98
890702	7 c CH2 BQC2.1	0.851408E+02	0.171196E+02	0.000000E+00	4.37
890702	7 c CH2 BQC2.1	0.944372E+02	0.271780E+02	0.000000E+00	3.80
890702	7 c CH2 BQC2.1	0.107290E+03	0.293116E+02	0.000000E+00	3.98
890702	7 c CH2 BQC2.1	0.114097E+03	0.230124E+02	0.000000E+00	4.21
890702	7 c CH2 BQC2.1	0.122072E+03	0.230124E+02	0.000000E+00	4.24
890702	7 c CH2 BQC2.1	0.128626E+03	0.128524E+02	0.000000E+00	4.17
890702	7 c CH2 BQC2.1	0.131928E+03	0.248412E+02	0.000000E+00	4.09
890702	7 m CH2 BQC2.1	0.973328E+02	0.394716E+02	0.000000E+00	3.44
890702	7 m CH2 BQC2.1	0.117145E+03	0.362712E+02	0.000000E+00	3.32
890702	7 c CH2 BQC2.1	0.122784E+03	0.319532E+02	0.000000E+00	3.87
890702	7 c CH2 BQC2.1	0.131064E+03	0.323596E+02	0.000000E+00	3.92
890702	6 m CH2 BQC2.1	0.106070E+03	0.553212E+02	0.000000E+00	3.67
890702	6 m CH2 BQC2.1	0.111709E+03	0.548132E+02	0.000000E+00	3.82
890702	6 c CH2 BQC2.1	0.150368E+03	0.391160E+02	0.000000E+00	3.43
890702	6 c CH2 BQC2.1	0.159309E+03	0.428244E+02	0.000000E+00	4.62

890702	6	c	CH2	BQC2.1	0.154686E+03	0.410464E+02	0.000000E+00	4.42
890702	6	c	CH2	BQC2.1	0.172974E+03	0.410972E+02	0.000000E+00	4.18
890702	6	c	CH2	BQC2.1	0.193904E+03	0.384048E+02	0.000000E+00	4.31
890702	6	m	CH2	BQC2.1	0.178613E+03	0.341376E+02	0.000000E+00	3.34
890702	6	m	CH2	BQC2.1	0.166929E+03	0.339852E+02	0.000000E+00	3.62
890702	6	m	CH2	BQC2.1	0.140360E+03	0.343408E+02	0.000000E+00	3.02
890702	7	m	CH2	BQC2.1	0.147320E+03	0.198628E+02	0.000000E+00	3.62
890702	7	m	CH2	BQC2.1	0.139802E+03	0.194564E+02	0.000000E+00	3.67
890702	7	c	CH2	BQC2.1	0.144424E+03	0.130048E+02	0.000000E+00	4.31
890702	7	c	CH2	BQC2.1	0.157226E+03	0.127508E+02	0.000000E+00	4.47
890702	7	m	CH2	BQC2.1	0.159969E+03	0.200152E+02	0.000000E+00	3.60
890702	7	m	CH2	BQC2.1	0.171094E+03	0.205740E+02	0.000000E+00	3.31
890702	7	m	CH2	BQC2.1	0.184760E+03	0.208788E+02	0.000000E+00	3.16
890702	7	m	CH2	BQC2.1	0.193446E+03	0.271272E+02	0.000000E+00	3.09
890702	7	c	CH2	BQC2.1	0.193446E+03	0.152908E+02	0.000000E+00	3.85
890702	7	c	CH2	BQC2.1	0.184861E+03	0.123444E+02	0.000000E+00	3.96
890702	7	c	CH2	BQC2.1	0.175158E+03	0.113284E+02	0.000000E+00	4.29
890702	7	c	CH2	BQC2.1	0.131978E+03	0.751840E+01	0.000000E+00	4.68
890702	7	c	CH2	BQC2.1	0.137262E+03	-0.690880E+01	0.000000E+00	3.95
890702	7	c	CH2	BQC2.1	0.145085E+03	-0.165608E+02	0.000000E+00	4.76
890702	7	c	CH2	BQC2.1	0.152451E+03	-0.132080E+02	0.000000E+00	4.12
890702	7	c	CH2	BQC2.1	0.160833E+03	0.330200E+01	0.000000E+00	4.76
890702	7	c	CH2	BQC2.1	0.175920E+03	0.467360E+01	0.000000E+00	4.19
890702	7	c	CH2	BQC2.1	0.191313E+03	0.558800E+01	0.000000E+00	4.00
890702	7	c	CH2	BQC2.1	0.193497E+03	-0.125476E+02	0.000000E+00	4.52
890702	7	c	CH2	BQC2.1	0.178156E+03	-0.441960E+01	0.000000E+00	3.55
890702	7	c	CH2	BQC2.1	0.186233E+03	-0.365760E+01	0.000000E+00	3.75
890702	7	c	CH2	BQC2.1	0.194666E+03	-0.330200E+01	0.000000E+00	3.45
890702	7	c	CH2	BQC2.1	0.135636E+03	-0.156464E+02	0.000000E+00	4.90

mean= 0.35706E+01
variance= 0.31474E+00
# of data= 277
lag= 5.00
lag tolerance= 1.50

	(horizontal variogram)				(vertical variogram)			
	azimuth = -10.0				azimuth = 90.0			
	plunge = 90.0				plunge = 90.0			
	azim. tol.= 5.0				azim. tol.= 5.0			
	plun. tol.= 5.0				plun. tol.= 5.0			
lag	np	dist	1/2 vario	av/lag	np	dist	1/2 vario	av/lag
1	0	0.00	0.00000E+00	0.000	0	0.00	0.00000E+00	0.000
2	19	5.42	0.49372E-01	3.534	14	5.25	0.26147E+00	3.369
3	26	9.90	0.64352E-01	3.532	18	10.00	0.32010E+00	3.506
4	33	14.99	0.13407E+00	3.494	25	15.00	0.12366E+00	3.533
5	33	20.21	0.11204E+00	3.469	23	20.05	0.96160E-01	3.625
6	49	24.99	0.15143E+00	3.552	30	24.90	0.27920E+00	3.591
7	55	29.92	0.21244E+00	3.479	39	30.08	0.26404E+00	3.643
8	60	34.90	0.21795E+00	3.501	31	35.33	0.44215E+00	3.571
9	72	40.11	0.17431E+00	3.546	28	39.84	0.37909E+00	3.635
10	79	45.06	0.25511E+00	3.511	23	44.99	0.32099E+00	3.770
11	85	50.02	0.22147E+00	3.497	12	49.49	0.90983E+00	3.560
12	88	55.17	0.19943E+00	3.541	12	54.99	0.62330E+00	3.801
13	88	59.95	0.25422E+00	3.484	8	60.20	0.92494E+00	3.767
14	109	65.04	0.25883E+00	3.505	1	64.42	0.69260E+00	3.747
15	97	70.17	0.25203E+00	3.544	0	0.00	0.00000E+00	0.000
16	128	75.06	0.26915E+00	3.477	0	0.00	0.00000E+00	0.000
17	116	79.88	0.29490E+00	3.513	0	0.00	0.00000E+00	0.000
18	125	84.88	0.27366E+00	3.496	0	0.00	0.00000E+00	0.000
19	130	89.93	0.24208E+00	3.553	0	0.00	0.00000E+00	0.000
20	135	94.99	0.25627E+00	3.536	0	0.00	0.00000E+00	0.000
21	123	100.00	0.30692E+00	3.537	0	0.00	0.00000E+00	0.000
22	126	105.00	0.27120E+00	3.534	0	0.00	0.00000E+00	0.000
23	122	109.93	0.29758E+00	3.584	0	0.00	0.00000E+00	0.000
24	140	114.81	0.23265E+00	3.616	0	0.00	0.00000E+00	0.000
25	152	119.96	0.32634E+00	3.579	0	0.00	0.00000E+00	0.000
26	144	124.93	0.32143E+00	3.606	0	0.00	0.00000E+00	0.000
27	126	129.97	0.28510E+00	3.578	0	0.00	0.00000E+00	0.000
28	134	134.96	0.27568E+00	3.625	0	0.00	0.00000E+00	0.000
29	163	140.02	0.31144E+00	3.588	0	0.00	0.00000E+00	0.000
30	157	144.96	0.27082E+00	3.637	0	0.00	0.00000E+00	0.000
31	130	149.99	0.31953E+00	3.609	0	0.00	0.00000E+00	0.000
32	143	154.96	0.33143E+00	3.642	0	0.00	0.00000E+00	0.000
33	121	159.99	0.32670E+00	3.626	0	0.00	0.00000E+00	0.000
34	145	165.02	0.31823E+00	3.668	0	0.00	0.00000E+00	0.000
35	138	169.99	0.28719E+00	3.632	0	0.00	0.00000E+00	0.000
36	118	174.89	0.38960E+00	3.611	0	0.00	0.00000E+00	0.000
37	112	179.83	0.39684E+00	3.710	0	0.00	0.00000E+00	0.000
38	114	185.00	0.39839E+00	3.636	0	0.00	0.00000E+00	0.000
39	102	190.02	0.33323E+00	3.663	0	0.00	0.00000E+00	0.000
40	87	195.12	0.38909E+00	3.651	0	0.00	0.00000E+00	0.000
41	110	200.03	0.44412E+00	3.688	0	0.00	0.00000E+00	0.000
42	102	205.05	0.39362E+00	3.701	0	0.00	0.00000E+00	0.000
43	92	210.05	0.33617E+00	3.691	0	0.00	0.00000E+00	0.000
44	107	214.94	0.48582E+00	3.687	0	0.00	0.00000E+00	0.000
45	86	220.01	0.41211E+00	3.676	0	0.00	0.00000E+00	0.000
46	78	224.99	0.36276E+00	3.628	0	0.00	0.00000E+00	0.000
47	81	230.10	0.44415E+00	3.667	0	0.00	0.00000E+00	0.000
48	77	235.11	0.47647E+00	3.622	0	0.00	0.00000E+00	0.000
49	83	240.04	0.31638E+00	3.716	0	0.00	0.00000E+00	0.000
50	62	245.07	0.35745E+00	3.735	0	0.00	0.00000E+00	0.000

Semi-variogram output for PS2 page: 1

mean= 0.35591E+01
variance= 0.15773E+01
# of data= 86
lag= 12.00
lag tolerance= 6.00

	(horizontal variogram)				(vertical variogram)			
	azimuth = 0.0				azimuth = 90.0			
	plunge = 90.0				plunge = 90.0			
	azim. tol.= 10.0				azim. tol.= 10.0			
	plun. tol.= 10.0				plun. tol.= 10.0			
lag	np	dist	1/2 vario	av/lag	np	dist	1/2 vario	av/lag
1	4	0.87	0.72921E-01	2.882	13	3.35	0.39347E+00	3.078
2	52	13.05	0.23358E+00	3.303	20	11.28	0.14782E+01	3.706
3	90	24.84	0.39342E+00	3.234	37	23.94	0.14052E+01	3.874
4	113	36.84	0.43459E+00	3.301	67	36.58	0.11775E+01	3.051
5	119	47.77	0.71551E+00	3.373	47	46.18	0.32879E+01	3.501
6	118	60.10	0.83087E+00	3.280	4	54.82	0.39077E+01	4.841
7	130	72.01	0.87949E+00	3.458	0	0.00	0.00000E+00	0.000
8	85	83.83	0.94623E+00	3.537	0	0.00	0.00000E+00	0.000
9	80	95.57	0.16412E+01	3.607	0	0.00	0.00000E+00	0.000
10	91	107.79	0.15069E+01	3.812	0	0.00	0.00000E+00	0.000
11	76	119.82	0.17966E+01	3.827	0	0.00	0.00000E+00	0.000
12	44	132.07	0.18989E+01	3.724	0	0.00	0.00000E+00	0.000

51	!	74	250.03	0.47864E+00	3.687!	0	0.00	0.00000E+00	0.000!
52	!	64	255.20	0.46126E+00	3.746!	0	0.00	0.00000E+00	0.000!
53	!	52	260.05	0.41423E+00	3.762!	0	0.00	0.00000E+00	0.000!
54	!	43	264.91	0.50396E+00	3.726!	0	0.00	0.00000E+00	0.000!
55	!	46	270.00	0.39163E+00	3.721!	0	0.00	0.00000E+00	0.000!
56	!	47	274.97	0.32093E+00	3.735!	0	0.00	0.00000E+00	0.000!
57	!	47	279.83	0.28156E+00	3.731!	0	0.00	0.00000E+00	0.000!
58	!	42	285.10	0.28716E+00	3.636!	0	0.00	0.00000E+00	0.000!
59	!	33	290.25	0.29533E+00	3.659!	0	0.00	0.00000E+00	0.000!
60	!	38	294.93	0.26936E+00	3.629!	0	0.00	0.00000E+00	0.000!